2009

Laboratory testing of full-depth precast, prestressed concrete deck panels used in the Boone County IBRC accelerated bridge replacement project

Ryan Paul Bowers
Iowa State University

Laboratory testing of full-depth precast, prestressed concrete deck panels used in the Boone County IBRC accelerated bridge replacement project

by

Ryan Paul Bowers

A thesis submitted to the graduate faculty

in partial fulfillment of the requirements for the degree of

MASTER OF SCIENCE

Major: Civil Engineering (Structural Engineering)

Program of Study Committee:
F. Wayne Klaiber, Co-Major Professor
Terry J. Wipf, Co-Major Professor
Brent Phares, Co-Major Professor
Loren Zachary

Iowa State University

Ames, Iowa

2009

TABLE OF CONTENTS

LIST OF FIGURES

LIST OF TABLES

ACKNOWLEDGEMENTS

The research presented in this thesis was conducted by the Bridge Engineering Center under the auspices of the Engineering Research Institute at Iowa State University. This research was sponsored by the Iowa Highway Research Board, Iowa Department of Transportation, and the Federal Highway Administration.

The author wishes to thank his Program of Study committee members, particularly my co-major professors, Dr. F. Wayne Klaiber, Dr. Terry J. Wipf, and Dr. Brent Phares, for their knowledge and guidance throughout the completion of this work. Also, thanks is extended to James Nelson of the Iowa DOT, along with the other DOT personnel involved in the project, for all of their input and assistance with the laboratory tests.

The author would like to thank Doug Wood, Structures Laboratory Manager, for his assistance with the laboratory testing conducted during the completion of this project. In addition, special thanks is extended to the following undergraduate students for their help in the laboratory: Matt Goliber, Matt Becker, Nathan Hardisty, Tom Lewin, Carl Zeigler, Casey Faber, Ryan Evans, Jacob Wilson, Jill Barada, Greg Cabalka, and Laura Scott. Finally, thanks are given to the following graduate students for their help with the laboratory testing: Vernon Wineland, Mark Currie, Adam Faris, Samantha Kevern, and Jeremy Koskie.

ABSTRACT

As the United States highway infrastructure is in need of rehabilitation due to increasing traffic needs and structural inadequacies, use of precast concrete elements is increasing. Use of precast concrete systems provide various advantages, including minimizing traffic disruption, increasing the quality of the final product, and lowering life-cycle costs. Both the Federal Highway Administration and the Iowa Department of Transportation have recognized the benefits of using precast concrete elements in bridge construction to help reduce the duration of construction projects.

This thesis focuses on the laboratory testing of full-depth precast, prestressed concrete deck panels used in the construction of a continuous four-girder, three span bridge over Squaw Creek on 120th Street in Boone County, Iowa. Various laboratory tests were conducted on a single panel and on two panels connected by a closure pour. These tests ranged from determining physical properties of the panel (compressive strength and prestressing force), to determining the panel's response in various circumstances (moving with a crane, during field leveling, and under loading).

Tests were conducted to determine physical characteristics of a deck panel such as compressive strength and stress in the mild reinforcing due to prestressing. The average compressive strength of the concrete core samples was 7,600 psi, which exceeded the specified compressive strength of 5,000 psi. Prestressing strands in one post-tensioning channel were cut to determine the amount of stress in each strand due to prestressing. Of the six bars instrumented, five were found to have a stress lower than that expected from the initial prestressing force.

Strains in the mild reinforcing bars were monitored in the laboratory while a panel was lifted with a crane. Two different strap configurations were used to lift the panel; the first configuration used four lifting straps, and the second used two lifting straps. Results from these tests showed the strap configuration did not have a significant effect on the strain induced in the mild reinforcing bars. The total strain (measured plus induced due to prestressing) of a bar used during these tests had a maximum value of 70%. Panels were also leveled in the laboratory to monitor the strains in the mild reinforcement. Bars were found to utilize 86% of the yield strain during this process.

Service load tests were performed on both a single panel and two panels connected by a closure pour. Through these tests it was determined that the deck panels had adequate strength under service loads.

Both a single panel and two connected panels were tested to failure. Ultimate load tests included testing a single panel and two connected panels to a flexural failure, and testing the connected panels to a punching shear failure. The connected panels also experienced a combination punching shear and flexure failure during one test. Failures during each test occurred at loads much greater than the service loads the panels are expected to experience in the field.

1. INTRODUCTION

1.1 Background

Due to factors including increasing traffic needs, inadequacies of the structure, and increasing truck weights, the highway infrastructure in the United States (U.S.) is in need of rehabilitation or replacement. In order to ensure the safety of the public, this rehabilitation/replacement must be conducted in a manner that both minimizes congestion and improves safety. A way to meet these goals is through the use of prefabricated concrete systems (Russell *et al*., 2005).

Prefabricated concrete systems provide various advantages over the use of cast-in-place (CIP) systems. Use of prefabricated concrete systems can:

- Minimize traffic disruption
- Improve constructability
- Improve work-zone safety
- Minimize construction impact on the environment
- Increase the quality of the final product
- Lower life-cycle costs

Use of precast bridge elements also allows construction to proceed during cold weather. Bridges can be constructed quicker because of the elimination of cure times from the critical path of the construction schedule (Russell *et al*., 2005).

Both the Federal Highway Administration (FHWA) and Iowa Department of Transportation (DOT) have recognized the need for use of precast concrete elements in bridge construction. This thesis focuses on the use of precast elements in the construction of the

superstructure of a bridge constructed in Boone County, Iowa. The work presented in the thesis was sponsored by the FHWA and Iowa DOT.

The bridge in Boone County, Iowa is located over Squaw Creek on 120th Street. Shown in Figure 1.1 is a map of Boone County with the location of the bridge marked. A continuous, four-girder, three-span bridge design was chosen to replace an existing Marsh Arch bridge at the site. A photograph of the Marsh Arch bridge that was replaced is shown in Figure 1.2a, while the replacement bridge is shown in Figure 1.2b. Dimensions of the replacement bridge are 151 ft - 4 in. long and 33 ft - 2 in wide. Span lengths are 47 ft - 5 in., 56 ft - 6 in., and 47 ft - 5 in. The original Marsh Arch bridge was a single span arch 76 ft in length and 18 ft wide.

Precast elements used for this bridge include abutment caps and pier caps for the substructure and girders and full-depth deck panels for the superstructure. Deck panels were prestressed in the transverse direction of the bridge and had two full-depth channels over the girders for post-tensioning. After all the deck panels were placed, the bridge was post-tensioned in the longitudinal direction. Performance of the deck panels was evaluated in the laboratory and is discussed in this thesis.

1.2 Research Objectives

Objectives of this research were based on input from the Iowa DOT and Iowa State University (ISU) Bridge Engineering Center (BEC) researchers involved with the project. The following objectives were the focus of this research project:

- Determine the strength and behavior of the longitudinal closure joint connecting deck panels
- Monitor the stresses present in the mild reinforcing bars during lifting and leveling of the deck panels

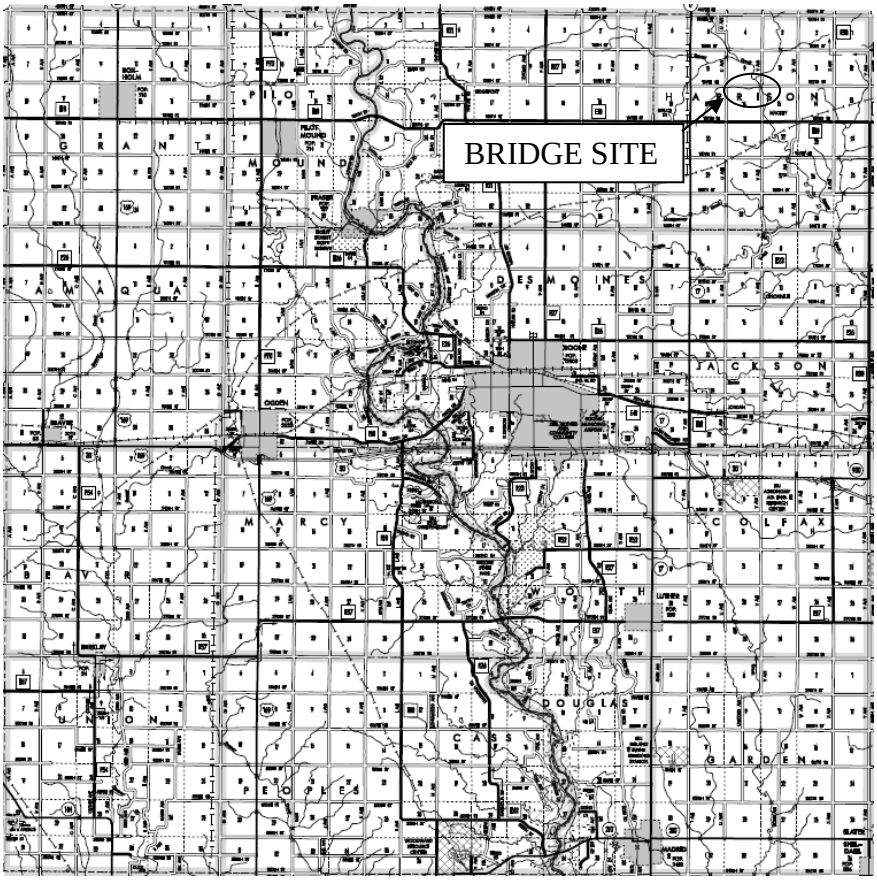

a) map of Boone County

b) location of bridge

Figure 1.1. Location of Boone County bridge.

a) replaced Marsh Arch bridge

b) completed replacement bridge

Figure 1.2. Original and replacement Boone County bridges.

- Observe the flow of concrete in the post-tensioning channels to ensure no void spaces are created

These objectives were met through various laboratory tests performed on specimens; test details and test results will be presented in this thesis.

1.3 Scope of Research

The first task for this project was the completion of a review of literature related to the project. First, literature relating to accelerated precast concrete superstructure elements was reviewed which was followed by a more focused review of projects involving various deck panel systems. A summary of the literature reviewed for this project is presented in Section 1.4.

Once the literature review was completed, laboratory testing of the deck panels was conducted. A variety of tests were executed to meet the previously stated project objectives. An explanation of the various laboratory setups and tests conducted is presented in Chapter 2.

Test results from the various laboratory tests along with a discussion of the results are presented in Chapter 3. Also, a comparison of the results to design standards and material yield strengths is provided. A summary of the research, conclusions, and recommendations based on the laboratory tests are presented in Chapter 4.

1.4 Literature Review

An increase in costs coupled with a decrease in highway revenues have had a serious impact on the highway construction program, leading to the need for economical bridge systems. Because of this, the use of precast bridge elements has become more prevalent in the construction industry (Tokerud, 1979). Using precast bridge elements in place of CIP elements offers various advantages. Precast concrete construction contributes to the practice of sustainability by incorporating integrated design, using materials efficiently, and reducing construction site disturbance, waste, and noise (VanGeem, 2006). Economics also influence the decision to use CIP or precast elements.

By using precast elements, major time-consuming tasks such as the erection and removal of formwork, placement of reinforcing steel and concrete, and concrete curing are not completed

at the job site. Instead, these tasks are completed off-site, and the finished element is delivered to the construction site and placed when needed for the construction to continue. This can significantly compress the project timeline and reduce traffic disruption. Reducing the construction schedule is important in colder climates where a large number of construction projects must be completed in the short period of time when the weather conditions are favorable (Bell III *et al*., 2006).

A second advantage of using precast concrete elements is that fabrication occurs in a controlled environment with stringent quality control. By fabricating at a plant, the fabricator can take as much time as necessary to properly fabricate the elements. This leads to greater durability and uniformity of the elements (Hieber *et al*., 2005). Also, this allows for greater control of the concrete cover over the reinforcing steel, decreasing the likelihood of inadequate cover and surface spalling (VanGeem, 2006).

Work-zone safety is improved by using precast concrete elements. Workers are exposed to high-speed traffic and other on-site construction hazards for a shorter amount of time due to the elimination of constructing formwork and casting concrete on-site (Hieber *et al*., 2005). Safety is also increased because less work is done in close proximity to power lines and over water (Bell III *et al*., 2006).

Precast elements provide some economic advantages. A more durable product typically results from precasting, which in turn can decrease life cycle costs. Another economic benefit is the potential the same precast elements can be used at different projects, resulting in a repeatability of the use of the design (Bell III *et al*., 2006). CIP concrete has seen an increase in cost due to rising labor costs. Labor requirements for CIP concrete include the construction of falsework, forms, placing steel, and casting and finishing the concrete (Tokerud, 1979).

Construction of CIP concrete bridges has a greater impact on the environment than using precast elements. Erection and removal of the formwork required for CIP bridges requires workers and equipment to access the underside of the bridge. This causes a great disturbance to the surrounding environment and increases the probability of materials falling into the waterway (Bell III *et al*., 2006).

CIP concrete decks do provide some advantages over using precast elements. Adjustments can be made to CIP decks in the field, allowing for the production of a smooth roadway profile. Also, CIP concrete decks provide composite action. However, use of CIP decks result in a low construction speed, the need for strict field quality control, and cracking due to shortening of the deck as a result of cooling during cement hydration cycle and differential creep and shrinkage. Because of cracking, CIP concrete decks often will require major repair or replacement within 15 to 25 years of construction (Fallaha *et al*., 2004). CIP decks also have a high cost because of the need to install formwork, require an extensive amount of fieldwork, and are limited in use during cold or inclement weather (Badie *et al*., 1998).

Overall, use of prefabricated elements and systems is increasing. Some of the major problems inhibiting the implementation of broader use of prefabricated systems are the initial cost, lack of standardization, lack of specialized contractors, and problems with the connections between elements (Ehmke, 2006).

1.4.1 Superstructure Types

Four types of precast concrete superstructure systems are prevalent. These systems are partial-depth precast concrete deck panels, full-depth precast concrete deck panels, prestressed concrete multibeam superstructures, and pre-constructed composite units (PCUs) (Hieber *et al*., 2005).

1.4.1.1 Partial-Depth Precast Concrete Deck Panels

Partial-depth precast concrete deck panels typically are 3.5 in. deep, 8 ft long in the longitudinal direction, and wide enough to span between bridge girders. Because the panels are only 3.5 in. deep, a CIP deck is cast once the panels are placed. The panels serve as stay-in-place forms for the CIP deck (Hieber *et al*., 2005).

Reinforcing in the deck panels is provided by pretensioning strands. Panels are pretensioned in the transverse direction. Strands are located at the mid-depth of the panel and serve as the bottom layer of reinforcing steel in the bridge deck. After the panel is placed in the field, the top layer of reinforcing steel is placed, and the CIP concrete portion of the deck is cast. Once completed, the CIP concrete and precast panels act as a composite slab (Hieber *et al*., 2005).

One problem observed with this system is the presence of reflective cracking of the CIP deck at the panel edges (Fallaha *et al*., 2004). This occurs because the deck panels are not connected at the transverse joint. Individual panels therefore can deflect differentially at the transverse joint, resulting in cracking of the CIP deck.

Experimentation has shown another problem with this system is the reduced panel arching action due to a lack of beam support anchorage for the transverse pretensioning strand in the individual panels. This in turn reduces the load capacity of the system compared to full-bridge width CIP or panel systems. Another disadvantage is the cost associated with having to construct conventional formwork for the bridge overhangs (Fallaha *et al*., 2004).

One of the first projects using partial-depth panels was the Illinois Tollway project in the 1950's. Currently partial-depth panels are used by at least 28 states and Canadian provinces. In the state of Washington, previous applications using partial-depth panels had higher construction

costs but overall savings. Savings were a result of the reduced amount of traffic control required (Hieber *et al*., 2005).

The NUDECK system is a variation of the partial-depth panel system. Six inch precast concrete panels pretensioned transversely are used. Prestressing is provided by pairs of ½ in. diameter, Grade 270 low-relaxation strands at a 24 in. spacing. The pretensioning strands have a 1 in. clear spacing vertically. An effective pretensioning stress of 350 psi after losses is achieved. High-strength wire spirals are placed around the final 24 in. of each strand pair to ensure a short transfer length of the prestress force (Fallaha *et al*., 2004).

NUDECK panels contain an opening over the girder lines for running post-tensioning strands. Using an open post-tensioning channel reduces interference between the strands and shear studs and simplifies the process of post-tensioning in the longitudinal direction. Post-tensioning is executed after a strength of approximately 1500 psi is reached in the transverse joints and prior to composite action developing. If post-tensioning is done at this time, the post-tensioning force is applied to only the deck, with none of the force distributed to the stiffer beams. Once post-tensioned, the deck is highly resistant to transverse cracking (Fallaha *et al*., 2004)

To preserve the tension in the prestressing strands through the open longitudinal channel, four #7 reinforcing bars are grouped with each pair of strands. Number 7 bars were used because of the need to resist buckling in the reinforcement during the release of the prestress and bending during handling and erection. Longitudinal reinforcement for NUDECK panels is provided by #5 steel bars spaced on 12 in. centers (Fallaha *et al*., 2004).

Conclusions based on the use of the NUDECK system are: 1) use results in control of the transverse cracking of the deck frequently observed in CIP decks due to shrinkage; 2) the

continuity in both the transverse and longitudinal directions eliminates reflective cracking over joints; 3) the NUDECK system exhibits improved fatigue resistance and crack control in the longitudinal direction over the girder lines; 4) construction speed is improved because of the elimination of field forming (Badie *et al*., 1998).

1.4.1.2 Full-Depth Precast Concrete Deck Panels

Full-depth precast concrete deck panels typically are 8 in. thick, 10 ft long, and span the full width of the bridge. A wearing course is not required for full-depth panels, but one may be applied to create a smooth driving surface. The transverse joint between panels is grouted to construct a shear key for transferring load between adjacent panels. Shear studs or reinforcing bars extend from the girders and connect the girders to the panels to develop composite action. This connection is made by grouting the open channel in the deck panel in which the steel lies (Hieber *et al*., 2005).

Panels are typically pretensioned in the transverse direction; however, mild reinforcement may also be present. If panels are not prestressed in the transverse direction, cracking may occur under service load conditions (Fallaha *et al*., 2004). Recent applications of full-depth panels include post-tensioning longitudinally. Longitudinal post-tensioning places the transverse joint in compression, thus improving durability and promoting monolithic behavior of the system (Hieber *et al*., 2005).

Full-depth deck panels have been used since the early 1960's. Currently, over 18 states, Japan, Great Britain, Canada, and Mexico use full-depth panels. The primary use for these panels is for replacing deteriorated CIP decks; however their use in new bridge construction is increasing (Hieber *et al*., 2005). The majority of applications using full-depth panels have

involved steel girder bridges. One explanation for this is that most older bridges requiring a deck replacement have steel girders (Slavis, 1982).

Full-depth precast concrete panels have been used in Japan in recent years because of the following benefits: improved durability, lower creep deformation, and fast construction time. The use of full-depth panels reduces construction time by eliminating the need for formwork and CIP concrete. In Japan, deck panels are not post-tensioned in the longitudinal direction (Russell *et al*., 2005).

Other countries, such as France, use a slightly modified design for full-depth deck panels. In France, deck panels are longitudinally post-tensioned together and contain screws used to adjust the elevation of the panel. Instead of match casting panels, a transverse CIP joint can be cast between the panels (Russell *et al*., 2005).

An advantage of using full-depth panels over CIP decks is the ability to use a wider girder spacing. Also, because the deck panels are connected to the girders by shear studs, a positive connection for lateral load is provided that was not included in the bridge design. Transverse continuity is accomplished through the use of overlapping hoop bars extending from the deck panels (Russell *et al*., 2005).

The full-depth, full width precast deck panel system could become a low cost solution for deck replacement projects if the panels are standardized. Use of the system needs to be widespread enough that contractors become familiar with the construction process. This system is very durable because all of the components are cast in a controlled environment, which alleviates the early age deck cracking and differential and restrained shrinkage cracking (Menkulasi and Carin, 2005).

1.4.1.3 Prestressed Concrete Multibeam Superstructures

Use of prestressed concrete multibeam superstructures has been extensive throughout the U.S. This system is common for bridges subjected to low traffic volumes and in remote areas where fresh concrete is difficult to obtain. Prestressed concrete multibeam superstructures consist of precast/prestressed concrete girders such as double tees, box beams, deck bulb-tees, and channels placed adjacently and spanning in the longitudinal direction of the bridge (Hieber *et al*, 2005).

Girders in multibeam superstructures serve as both the deck and support system for the superstructure. Adjacent girders are connected by one of or a combination of grout-filled shear keys, mechanical fasteners, or transverse post-tensioning. A non-composite wearing course is added to provide a smooth riding surface. In the state of Washington, poor performance of the longitudinal joint under heavy traffic has been observed (Hieber *et al.*, 2005).

Of the various multibeam superstructure shapes being used, the bulb tee is the most efficient. However, double tees and channels are more stable during handling and placing, and therefore are the preferred shape of contractors. Shapes such as the channel and box beam provide an additional advantage of having near-vertical flush sides; this allows adjacent members to be connected directly to each other and eliminates the need for intermediate diaphragms. Even though the box beam is less efficient than tees and channels, it is used extensively in many regions (Tokerud, 1979).

Precast prestressed concrete box girder bridges were widely used in Illinois state highways during the 1960s and 1970s. Use of these bridges was discontinued due to corrosion problems. Approximately 10 percent of prestressed box girder bridges inventoried on Illinois state highways had experienced significant corrosion, leading to a decreased bridge rating and

required load restrictions. Because these bridges are economical to build, they are still widely used on county roads throughout Illinois (Hawkins *et al*., 2002).

Illinois DOT box girders are either 36 in. or 48 in. wide and vary in depth. Shallower beams contain circular voids and welded wire fabric for the shear reinforcement. Deeper beams contain rectangular voids and the shear reinforcement consists of deformed bars. The deeper beams are limited to the 36 in. width to restrict the weight and size of the girders. This allows for easy transportation to the project site and placement with a mobile crane (Hawkins *et al*., 2002).

Differential deflections between adjacent girders allowed the development of reflective cracks along the longitudinal joint between girders. Corrosion of the prestressing strands resulted from salt laded water seeping through the cracked joint and into the girder. County engineers believe a lack of transverse load distribution between adjacent girders is the cause for the longitudinal cracking (Hawkins *et al*., 2003).

Two solutions used by the Illinois DOT to resolve this problem include transversely post-tensioning the girders together and providing a composite cast-in-place concrete deck. Both solutions have worked satisfactorily, but add considerably to the cost of construction, do not ensure that corrosion will be prevented, and make replacing damaged girders more difficult. Currently these are no reasonable solutions for retrofitting bridges in service (Hawkins *et al*., 2003).

The Ohio DOT requires 1 in. diameter steel tie bars spaced at distances no greater than 25 ft to be used in box girder bridges in the state. Tie bars are placed at midheight of the girder and pass through precast ducts. However, shear key failures and large relative deflections of adjacent girders were still observed. Suggestions to improve shear key performance in Ohio include

increasing the depth of the shear key and increasing the level of transverse post-tensioning (Huckelbridge *et al*., 1995).

1.4.1.4 Pre-Constructed Composite Units

Pre-constructed composite units (PCUs) are concrete or steel girders with a composite concrete bridge deck that are prefabricated. Fabrication takes place off-site and the PCUs are transported to the job by barge, truck, or rail. Once on-site, entire units are lifted into place, reducing construction time. After several units are set, the joints between units are grouted. Longitudinal and transverse post-tensioning is conducted to put the joints into compression (Hieber *et al*., 2005).

While on a scanning tour in April 2004, the Federal Highway Administration (FHWA) and the American Association of State Highway and Transportation Officials (AASHTO) observed the use of a partial depth panel system in Germany similar to the PCU system. The German system involved casting a partial depth panel on a beam prior to erecting the beam. Beams are then set into place so the panels almost touch. Because of the closeness of the panels, there is no need for additional formwork prior to placing the CIP concrete (Russell *et al*., 2005). A project using this system can be seen in Figure 1.3.

One advantage of PCUs is the ability to fabricate units with nonstructural elements such as barrier walls, light posts, and wearing surfaces. This helps reduce the construction time of the project. Use of PCUs has been limited mostly to large projects. The first applications of PCUs were large-scale superstructure replacement projects in the 1990's (Hieber *et al*., 2005).

Figure 1.3. Placement of partial depth panels cast on beams (Russell *et al.*, 2005).

1.4.2 Superstructure Element Connection Methods

The method used to connect the precast superstructure element varies with the type of element being used. Closure joints, shear keys, and cast-in-place concrete toppings are various methods used to connect precast elements and aid in load transfer.

1.4.2.1 Closure Joint

Closure joint details were observed by the FHWA and AASHTO while on the scanning tour in 2004. Prefabricated deck systems require longitudinal and transverse joints to provide continuity for live load distribution and seismic resistance. One method to accomplish this is by overlapping hoop bars that project from the edge of the slabs. The hoop bars are then overlapped by continuous loop bars, and straight bars pass through all the loops to provide continuity. This joint detail may provide better continuity between adjacent elements and better crack control along the joint than details used in the U.S (Russell *et al.*, 2005).

Details similar to those observed in other countries have been used in the state of New York and are being developed for use in Texas. However, issues concerning the amount of

concrete cover, loop bar bend radius, type of reinforcement to be used, properties of concrete used for the closure joint, sealing of the interface between the precast panels and CIP, and the need for an overlay need to be addressed. Several research projects sponsored by the National Cooperative Highway Research Program (NCHRP) are underway to evaluate the use of these joints (Russell *et al*., 2005).

A 1995 survey found the use of female to female joints was a common was to connect deck panels in the U.S. A variety of problems have been encountered with the use of these joints. Some of these problems are related to material quality, construction procedures, and maintenance. One problem frequently cited was leaking occurring at the joint (Issa *et al*., 1995).

1.4.2.2 Shear Key

The transverse joint must be able to resist vertical shear caused from wheel loads crossing the joint and bending induced by moving vehicular loads. The joint may be subjected to tension through drying shrinkage of the grouting material and transverse shortening of the precast concrete slabs. If the grouting material cannot resist the stresses induced during service, cracking will occur. Cracking will allow foreign materials to penetrate into the joint, gradually weakening the joint (Issa *et al*., 2003).

A visual inspection of various joint systems in bridges throughout the U.S. was conducted in 1995. From this inspection, the conclusion was drawn that the transverse joints between precast slabs should be female-to-female (shear key) with a minimum nominal width of 1 ¼ in. at the top and ½ in. at the bottom. Longitudinal post-tensioning should also be provided to compress all of the joints (Issa *et al*., 2003). If longitudinal post-tensioning is not done, a debonding of the transverse joint can occur (Issa *et al*., 1998).

A failure of the longitudinal shear key affects the strength and serviceability of the bridge. Failure compromises the lateral load distribution of the bridge, resulting in individual girders being exposed to greater live loads than designed for. Also, excessive relative displacements between adjacent girders can develop if the shear key fails. Excessive relative displacements occur because each girder acts individually with no load transfer between them (Bell III *et al*., 2006).

1.4.2.3 Cast-In-Place Topping

Use of a CIP concrete topping is another method to connect precast elements. A CIP topping will allow for production of a smooth riding surface. The topping will connect adjacent elements, allowing for continuity within the deck system and a means for transverse load transfer. CIP toppings can be made to act compositely with precast elements, improving the structural performance of the system. To achieve composite behavior, either shear reinforcement protruding from the precast sections or roughening of the contact surfaces of the elements or a combination of both are used (Bell III *et al*., 2006).

There are various drawbacks to using a CIP topping to achieve continuity between precast elements. Using CIP toppings leads to relatively slow construction speeds, the need for strict field quality control, and the possibility of cracking due to differential shrinkage between the CIP topping and the precast sections. Longitudinal reflective cracking often develops in the CIP topping about the joints formed between adjacent precast sections. Once cracking develop, water and deicing chemicals penetrate the cracks, leading to staining and spalling along with corrosion of the reinforcement (Bell III *et al*., 2006).

1.4.2.4 Post-tensioning

Providing post-tensioning is another method for connecting adjacent precast members to achieve continuity. Post-tensioning tendons are typically run perpendicular to the prestressing strands present in the member. Use of post-tensioning along with prestressing in full-depth panels eliminates concerns of cracking because the panel is compressed in both directions throughout its service life, resulting in a durable deck system (Fallaha *et al*., 2004).

The use of post-tensioning does have disadvantages. A large amount of post-tensioning is typically required for superstructures such as full-depth deck panels, which adds an additional cost and time in the field to the project (Badie *et al*., 1999). Use of post-tensioning requires the mobilization of a specialty contractor and increased construction monitoring, which increases the initial construction costs (Bell III *et al*., 2006).

One major problem associated with the use of post-tensioning is the possibility of corrosion. A walk-through inspection of 70 Florida bridges using post-tensioning revealed 44 with "indications of possible post-tensioning problems," 16 with "minor defects," and 10 with "no visible defects." However corrosion problems are not limited to Florida and not considered a problem specific to the environment of that state, as corrosion problems have been discovered in post-tensioned bridges in other states (Poston *et al*., 2003).

Corrosion problems found in the United States are the result of numerous factors, including deficient grouting specifications, possible deficiencies related to construction, and the effects of aggressive marine environments. Voids in the grout at the tendon anchorages have also been cited as a source of corrosion initiation. These problems have resulted in tendon failures within the bridges' first 10 years of service (Poston *et al*., 2003).

2. LABORATORY TESTING

Deck panels were fabricated at Andrews Prestressed Concrete, Inc. of Clear Lake, Iowa and delivered to ISU. ISU received three precast deck panels for testing. The project proposal called for the testing of two deck panels; however, ISU was able to purchase a third deck panel which had been rejected by the Iowa DOT due to the presence of a cold joint. Laboratory testing included concrete coring to determine the concrete compressive strength, determination of the compressive force in the #7 reinforcing bars due to prestressing, determination of strains in the panels while leveled and while lifted with a crane, service load testing, and ultimate load testing. A photograph of one of the precast deck panels used in this project is presented in Figure 2.1.

Figure 2.1. Full-depth precast concrete deck panel (courtesy of Iowa DOT).

2.1 Deck Panel Properties

Dimensions of the deck panels are given in Figure 2.2. As can be seen, the panels had a 60 degree skew; the dimension of the panels perpendicular to the centerline of the bridge was 16 ft - 1 in. This allowed each deck panel to span half the transverse width of the bridge. Each panel was 8 ft - 1 in. in the direction parallel to the centerline of the bridge; thus 36 panels were required to complete the bridge deck.

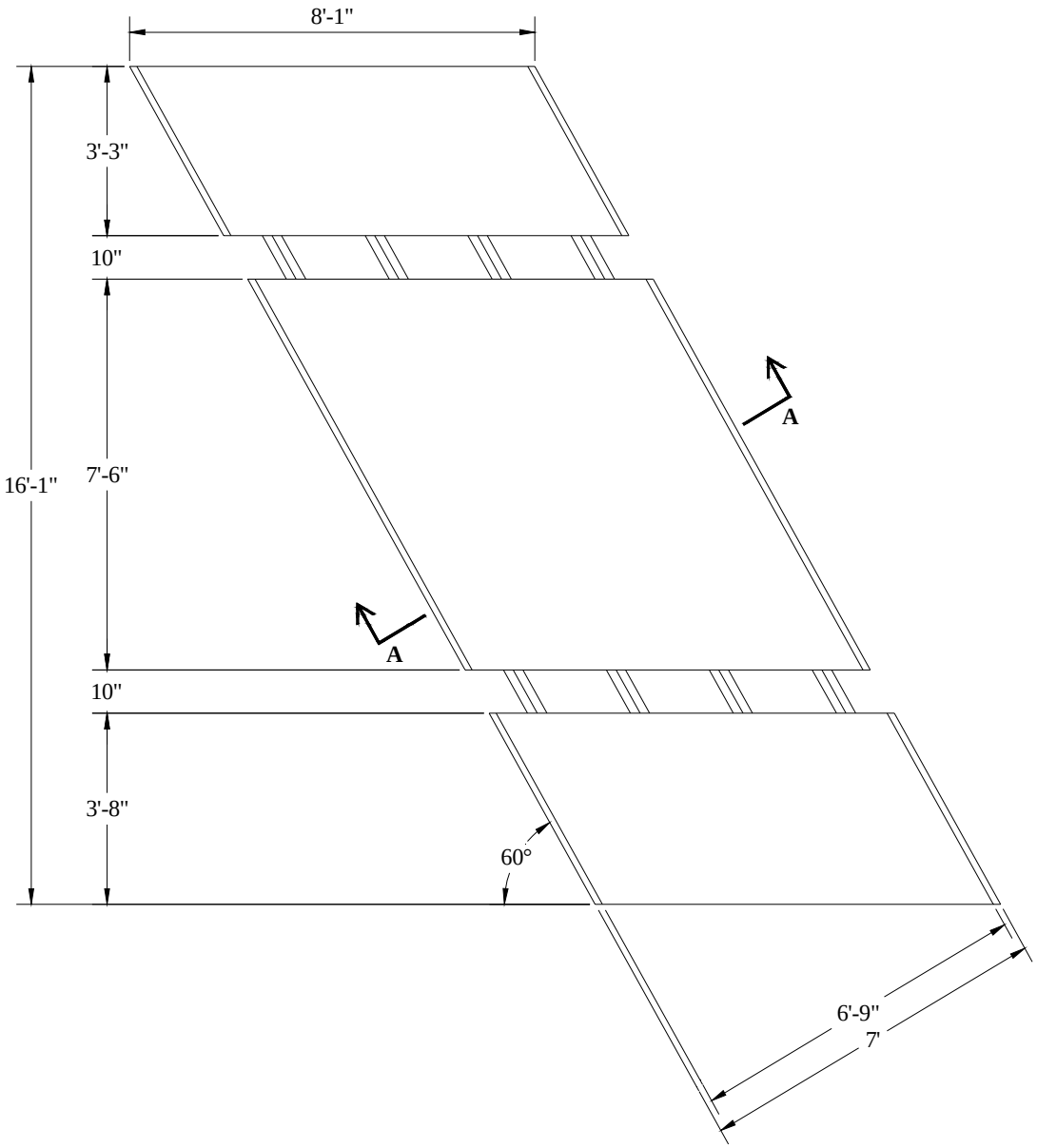

a) plan view of deck panel

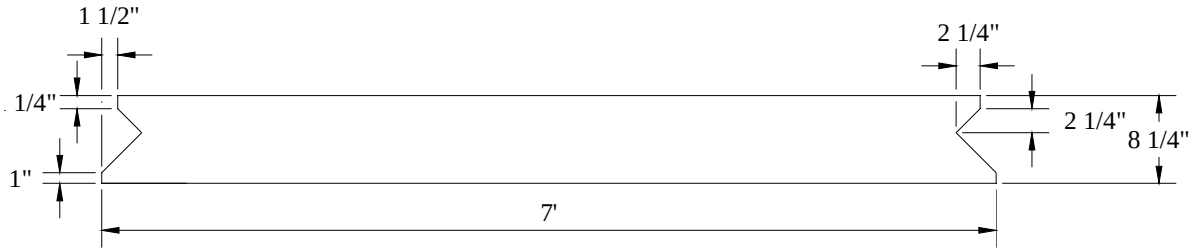

b) Section A-A

Figure 2.2. Deck panel dimensions.

Each panel consisted of three segments connected by prestressing strands and mild reinforcement. The purpose of the mild reinforcement was to "hold open" a channel between the segments for the post-tensioning strands which were placed in the field. Both 10 in. channels ran in the longitudinal direction of the bridge and were aligned over the prestressed concrete girders of the bridge.

Also of note in Figure 2.2 is that the bottom of the panels is 3 in. wider than the panel top. This provides an opening for placing the concrete for the shear key between the individual panels. The shear key runs transversely and provides continuity between the deck panels. As shown in Figure 2.3, the shear key surface had a diamond pattern to provide a better bond between the concrete in the panels and the concrete placed in the shear key.

Reinforcement in the deck panel is shown in Figure 2.4. All panels were reinforced the same, with the only difference among them being the presence of a cold joint in the third panel. The cold joint was a result of an equipment breakdown during casting. Grade 60 mild reinforcing bars were used for all the reinforcement; a modulus of elasticity equal to 29,000 ksi was assumed for the reinforcing steel as none of the reinforcing was tested. Number 7 and #6 reinforcing bars

Figure 2.3. Textured surface of transverse joint.

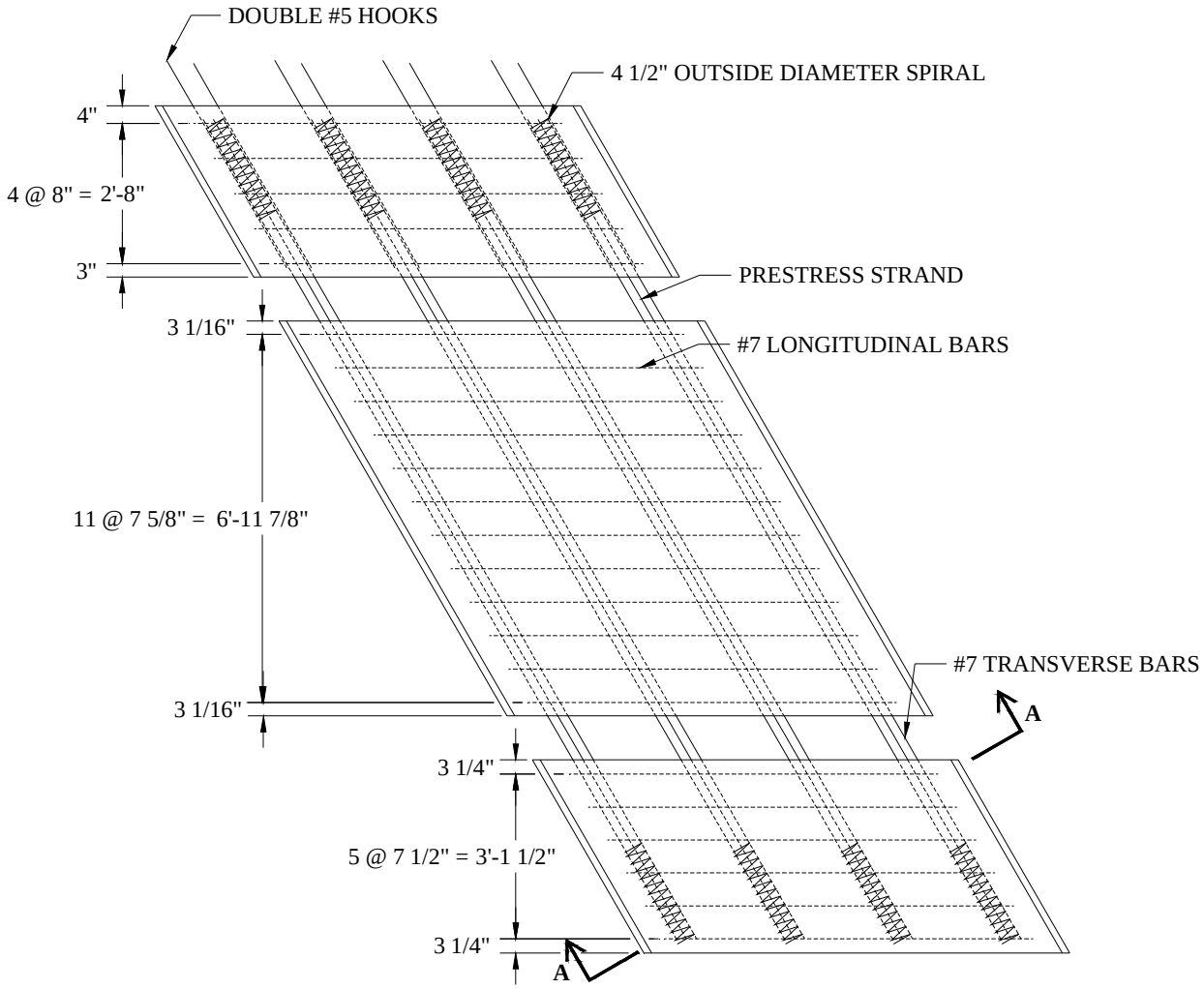

a) plan view of deck panel reinforcing

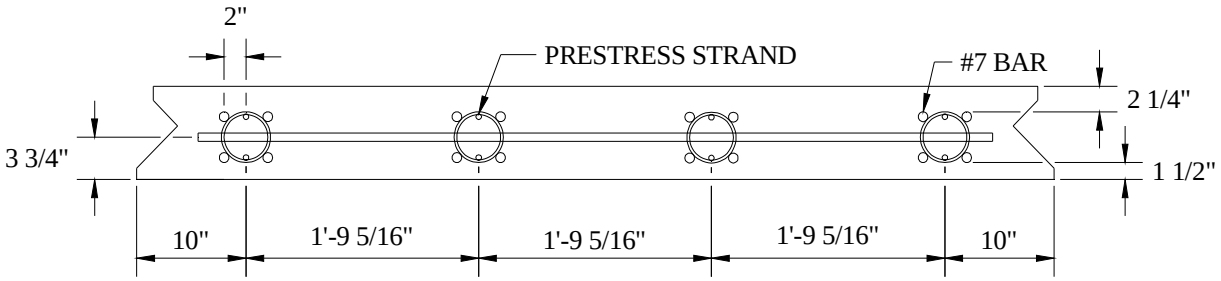

b) Section A-A

Figure 2.4. Reinforcing steel in deck panels.

were used in the transverse and longitudinal directions, respectively. Four #7 bars surrounded every two prestressing strands to carry the compressive force in the strands across the open longitudinal post-tensioning channels.

Eight prestressing strands were used in each of the deck panels. Prestressing strands were uncoated, seven-wire, low relaxation steel strand with a nominal diameter of ½ in.; a modulus of elasticity equal to 27,000 ksi was assumed by the Iowa DOT for the prestressing strands. Strands were to be tensioned to 31 kips prior to release, resulting in an initial stress of approximately 158 ksi in each strand. Deck panels were specified to have a concrete strength of 4,000 psi at stress transfer and a 28 day strength of 6,000 psi.

A 1 in. pitch spiral 2 ft in length with a 4.5 in. outer diameter and 4 in. inner diameter, ASTM A227 steel, is present at each end of the prestressing strands to help with confinement of the prestressing force. Eight pairs of #5 hook bars are shown at the top of the panel in Figure 2.4a. These bars are the reinforcing steel for the longitudinal closure pour located at the longitudinal center of the bridge for transferring load between adjacent transverse panels.

Shown in Figure 2.5 is the steel reinforcement in the deck panel casting beds. The four groups of prestressing steel and mild steel are visible in both figures, as well as the spirals encasing the ends of the prestressing strands. The additional steel seen in between the spirals in Figure 2.5a is the reinforcement for the barrier rail connections. Prestressing steel exiting the formwork and the double hooks are visible in Figure 2.5b.

2.2 Instrumentation

Instrumentation on the deck panels consisted of concrete strain gages, steel strain gages, and deflection transducers. In this section, the location of each type of gage installed as well as the numbering system for each type of strain measured will be presented. As will be detailed later, not every gage installed was used in every test. The specific gages used in a particular test will be presented during the discussion of the individual tests.

a) deck panel reinforcing steel

b) double hooks and prestressing strands

Figure 2.5. Deck panel reinforcing steel in formwork (courtesy of Iowa DOT).

A general numbering system was created for identifying concrete and steel strain measurements taken during testing; it follows the pattern PW-XYZ. The first letter, P, indicates the strain is in a deck panel and the second letter, W, is 1, 2, or 3 indicating the strain of interest

is in Panel 1, Panel 2, or Panel 3, respectively. The next letter, X, is either C or S and signifies the strain is in the concrete (C) or steel (S). The fourth variable, Y, is a number from 1 to 10 that identifies the location of the strain being discussed; figures displaying the locations of the strains are in the following sections. The final variable, Z, will be a T or B and denotes if the strain was measured in the top or bottom surface if it is a concrete strain, or in the bar closest to the top or bottom surface if it is a steel strain. All steel strains were measured in the top surfaces of the bars.

A similar numbering system is used for concrete and steel strains measured in the closure pour. For these strains, the general numbering system is CP-XYZ. In this system, CP designates the strain as in the closure pour. The variables X, Y, and Z have the same meaning as previously described for the deck panel strains.

Deflections are designated by PW-V. In this nomenclature, P signifies the deflection is that of a deck panel, W is either 1, 2, or 3 and designates the panel being discussed, and V varies from 1 to 10 and identifies the location of the deflection of interest. For closure pour deflections, the general naming system is CP-V. CP identifies the deflection as that of the closure pour, and V is a variable identifying the location of interest.

2.2.1 Concrete Strains

The location of the concrete strain gages used is shown in Figure 2.6a. Locations were the same for each deck panel and for both the bottom and top surfaces of the deck panel. In the longitudinal direction of the bridge, gages were placed along a line parallel to the skew. Strains were measured at the center of each panel segment and at the quarter points of the interior segment. In the transverse direction, strains were measured along two lines located in one-third of the panel width from the panel edge. A total of ten strain locations are shown in Figure 2.6a.

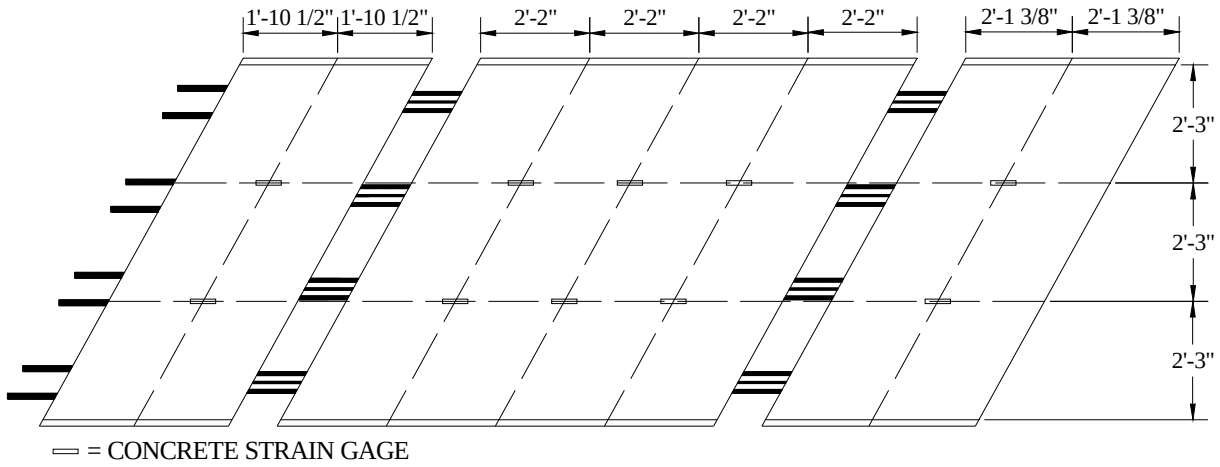

a) location of deck panel concrete strain gages

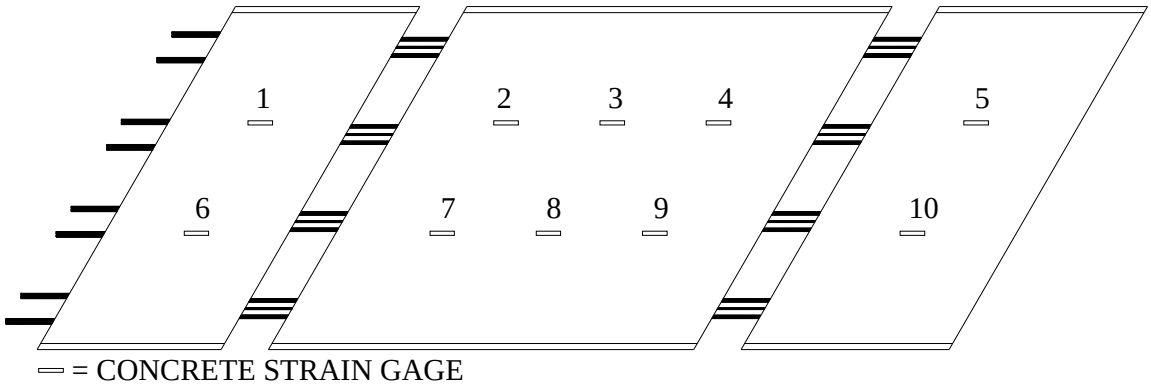

b) numbering of deck panel concrete strain locations

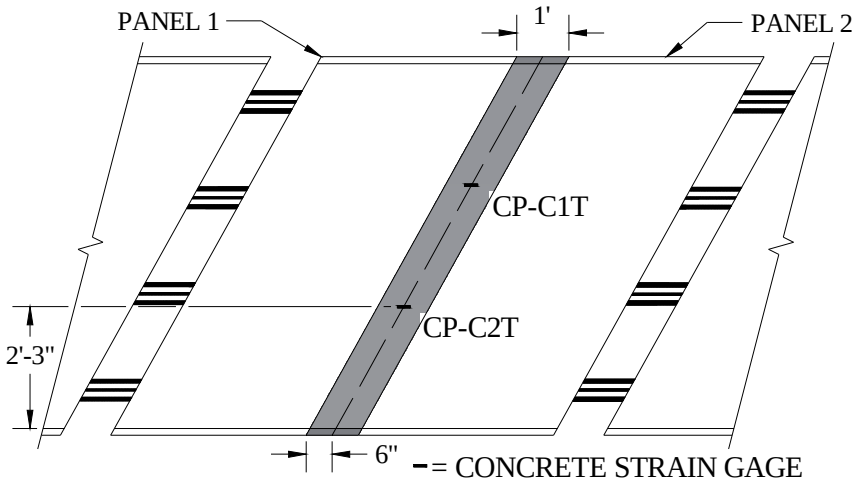

c) closure pour concrete strain location numbering system

Figure 2.6. Location and identification of concrete strains.

Strain locations are numbered in Figure 2.6b. An example of a strain designation is P2-C3T. This designation indicates the following: the strain is in deck panel (P) two (2); a concrete strain is being discussed (C); a strain at location number 3 in Figure 2.6b (3); and the strain is located on the top surface of the panel (T).

Shown in Figure 2.6c are the locations and numbering for the concrete strains in the closure pour connecting Panel 1 and Panel 2. Strains were measured 2 ft - 3 in. from the transverse edge of the panel and along the longitudinal center of the joint. Concrete strains were measured only on the top surface of the closure pour.

2.2.2 Steel Strains

Presented in Figure 2.7a and b are the numerical labels for the steel reinforcing bars for a deck panel. The number in Figure 2.7a refers to the vertical plane the measured strain is in. As illustrated in Figure 2.7b, T or B is used to indicate if a strain is in a top or bottom reinforcing bar in a particular vertical plane. An example of a number for a steel strain in a deck panel bar is P3-S3T; this strain would be in deck panel (P) three (3), is a steel strain (S) in Bar 3 (3), and in the top bar of the vertical plane (T).

Instrumentation of the closure pour hook bars is also shown in Figure 2.7; as illustrated, strains were measured for ten of the hook bars. The bar the strain was in can be seen in Figure 2.7c, and the locations of the strain measurements on the hook are shown in Figure 2.7d. As seen in Figure 2.7d, strains were only measured in the top surface of the bars, however strains in both the top and bottom bars of the hooks were measured. An example strain designation for the closure pour steel strains is CP-S7B, with CP meaning a closure pour strain, S for a steel strain, 7 being the bar number, and B meaning the bottom bar in the hook.

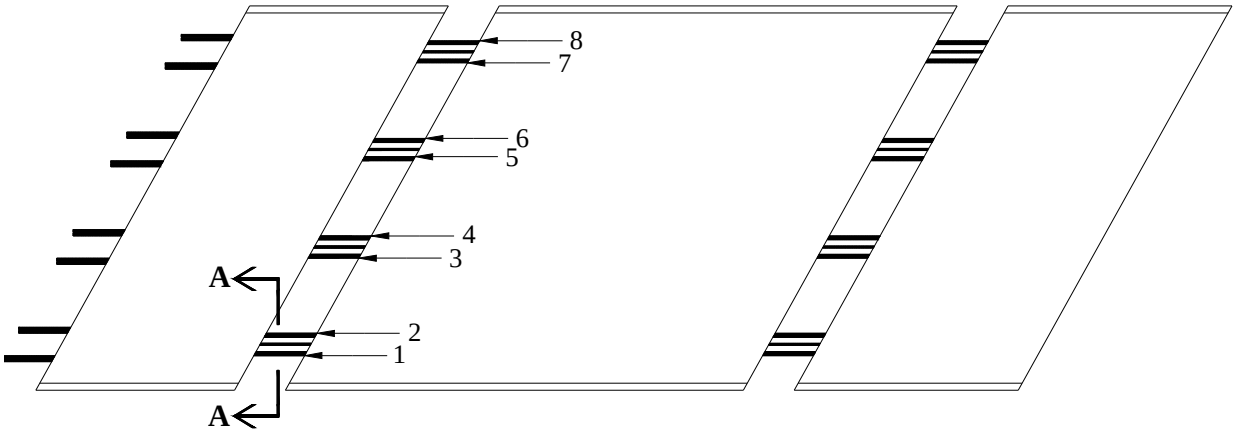

a) deck panel bar numbering

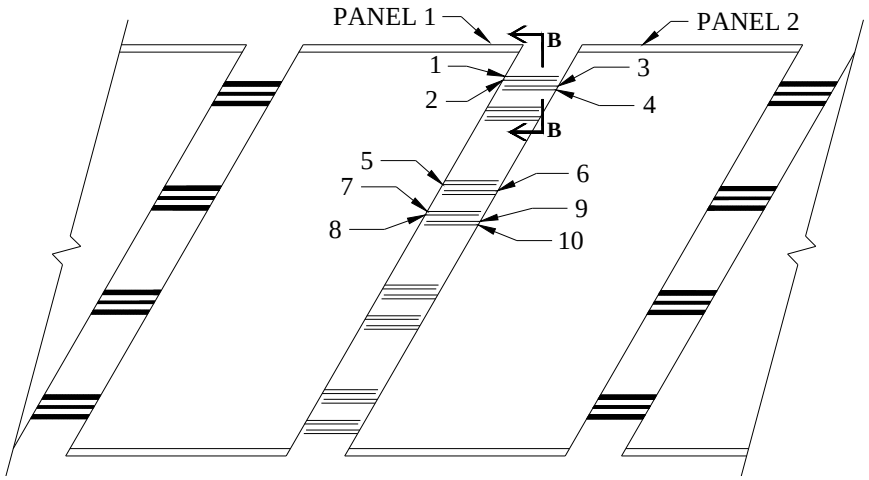

b) closure pour bar numbering

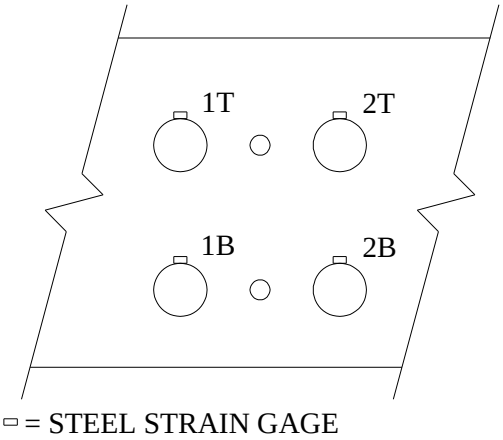

c) Section A-A

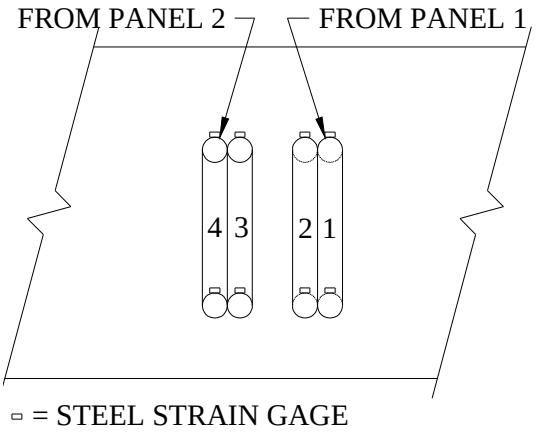

d) Section B-B

Figure 2.7. Location and identification of steel strains.

2.2.3 Deflections

Locations of deflections measured during testing are illustrated by black squares in Figure 2.8; deflection transducers were positioned at each location to measure the deflections. In a given test, a maximum of ten of the eleven deflection transducers were used. Deflection locations included: the four corners of the panel; the midpoints of the transverse edges; the center-point of the panel; and the midpoint between bar groups in the post-tensioning channel.

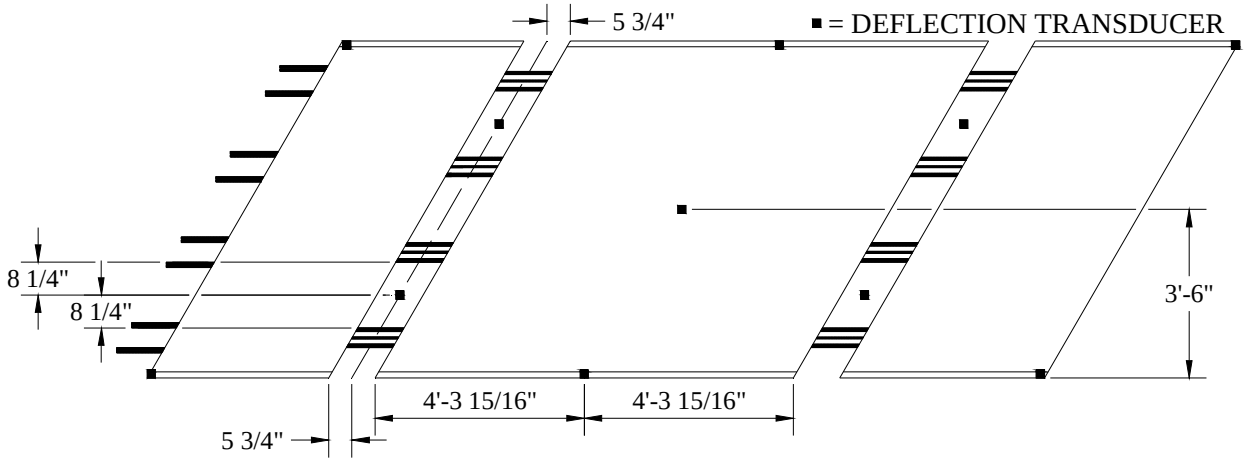

a) location of deflection measurements

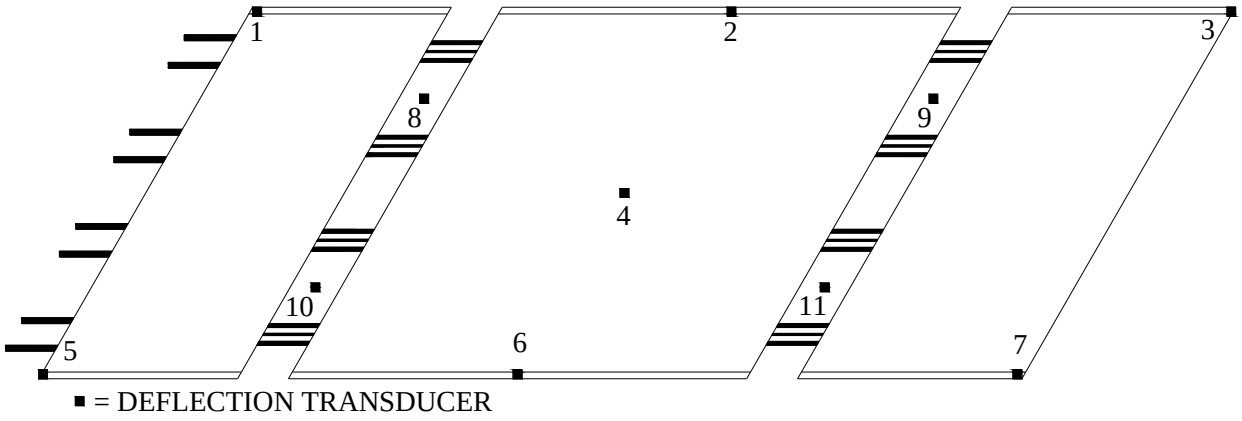

b) deck panel deflection numbering system

Figure 2.8. Location and identification of deflection measurements.

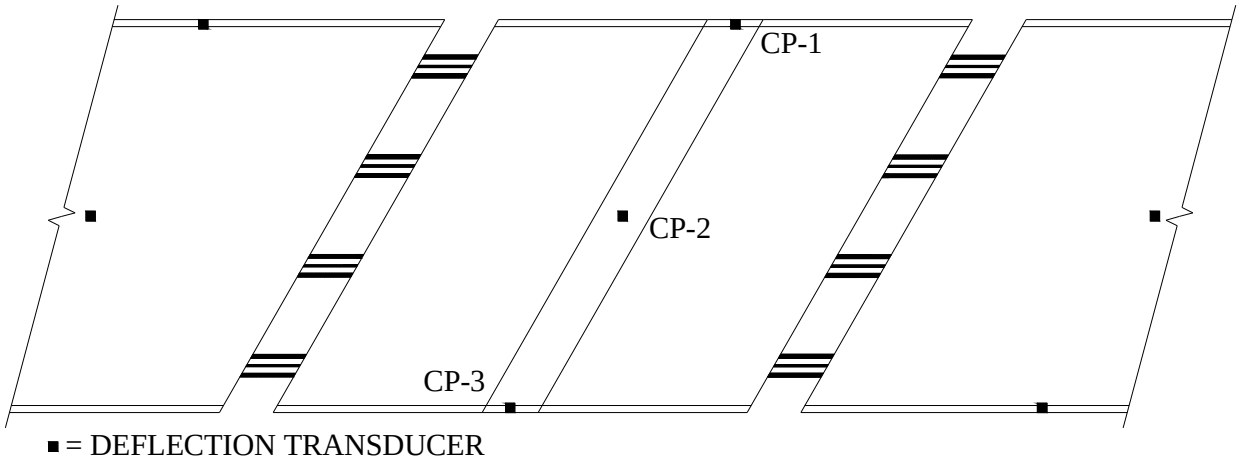

c) closure pour deflection numbering system

Figure 2.8. Continued

Presented in Figure 2.8b is the numbering system used for deck panel deflections. An example of the deflection numbering system is P2-3. This label is explained as follows: the deflection being analyzed is for deck panel (P) two (2); the deflection is for location 3 in Figure 2.8b.

A different configuration of deflection measurements was required once Panel 1 and Panel 2 were connected with the closure pour. Deflections measured at the deck panel corners near the closure pour were replaced with three measurements along the centerline of the closure pour. These deflections were labeled CP-1 through CP-3, as can be seen in Figure 2.8c.

2.3 Concrete Strength Testing

Concrete cores were taken to determine the actual concrete compressive strength of the deck panels at the time of testing. Cores were taken from Panel 1 after all testing on this panel was completed. Locations of the cores are shown in Figure 2.9. Panel 1 was selected for coring because this panel had sustained the least damage during loading. All cores were taken from the end span of the panel because this span was the only section that had not cracked during loading.

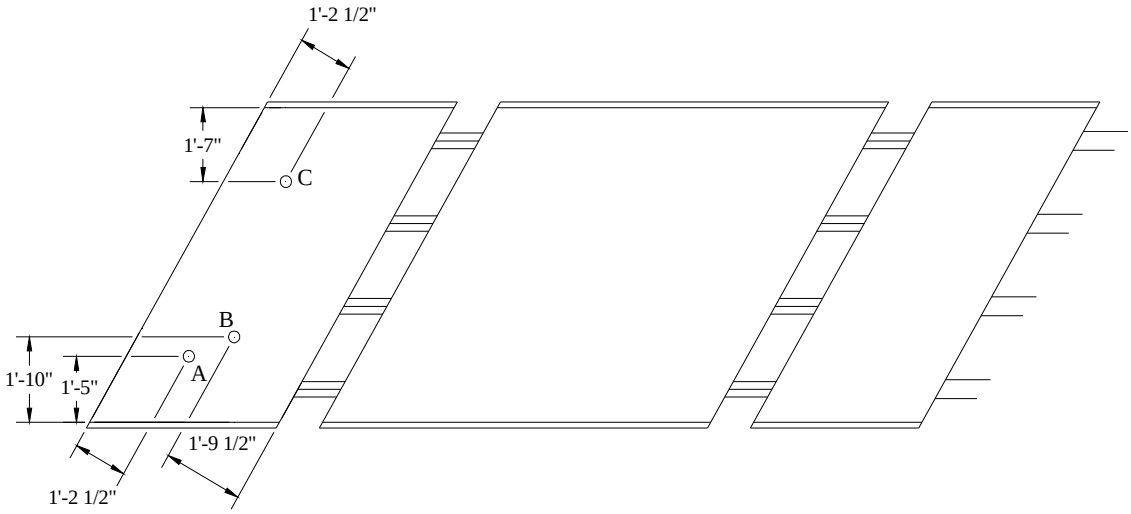

Figure 2.9. Core locations.

ASTM C 42 was followed to obtain three concrete cores from the deck panel. Cores had a diameter of 3 in. and a height of 8.25 in. Once removed from the deck panels, both ends of each core were cut resulting in a 6 in. specimen. The cores were cut to reduce the length to diameter ratio to two and also to provide a flat and smooth surface for testing. Cores were then tested in accordance to ASTM C 39 to determine the compressive strength of the concrete.

2.4 Stresses in Panel Mild Reinforcement Due to Prestressing

The eight prestressing strands present in one longitudinal channel of Panel 3 were cut to determine the compressive force in the mild reinforcement due to prestressing. Strains were measured while cutting the strands by installing strain gages on six of the twelve mild reinforcing bars. Bars 1T, 1B, 2T, 2B, 8T, and 8B (shown in Figure 2.7a) were instrumented; a photograph of these strain gages is shown in Figure 2.10.

An initial strain reading was taken prior to beginning the test in order to record the “zero” strain in the bars. After this, the top strand between Bars 1 and 2 was cut using a torch, as shown in Figure 2.11a. Once the strand was cut data readings were taken. Next the entire top

Figure 2.10. Reinforcing bars instrumented with steel strain gages.

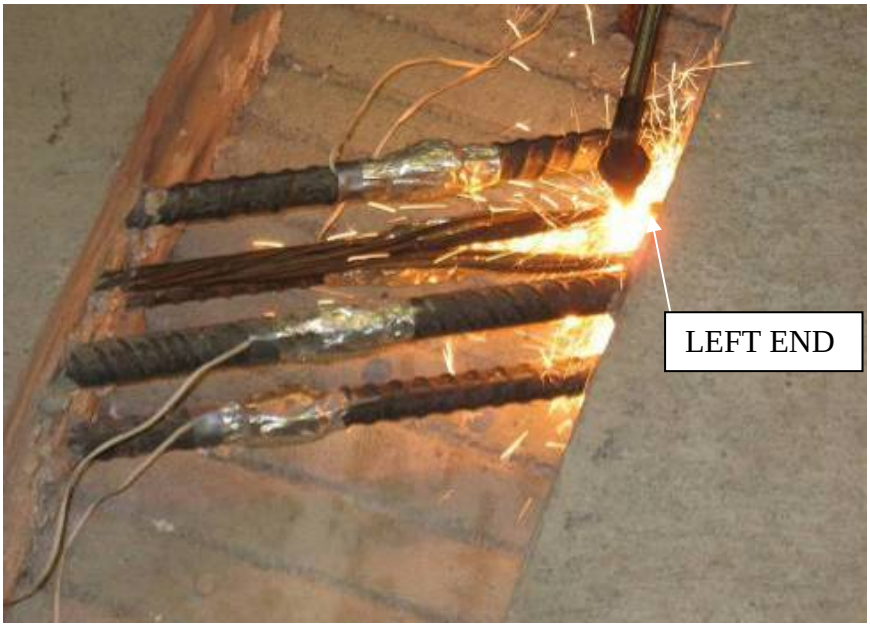

a) cutting the first prestress strand

Figure 2.11. Torch cutting of the prestress strands.

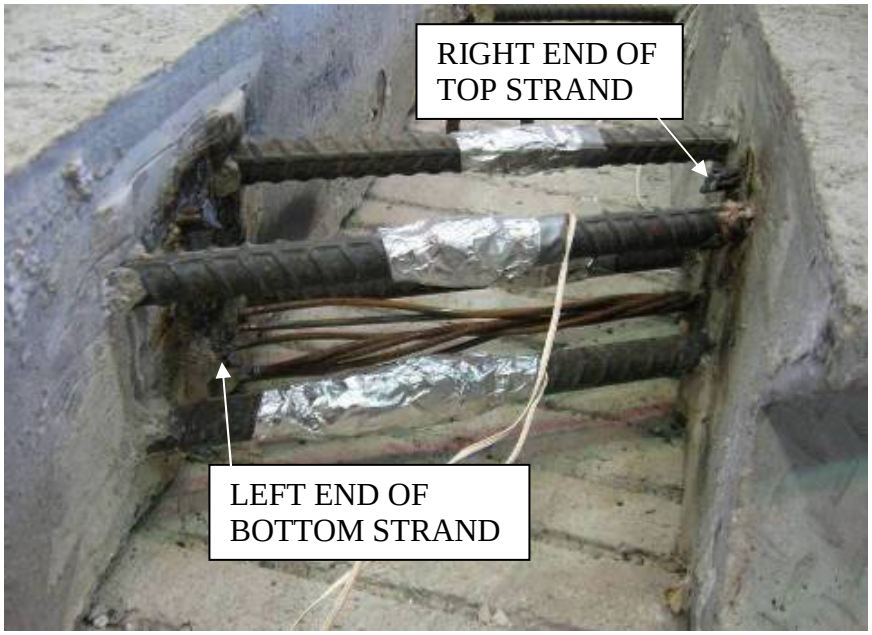

b) after removal of the prestress strands

Figure 2.11. Continued

prestressing strand was removed to provide better access to the lower strand, and then the lower strand was cut. The cut strands (top and bottom) are shown in Figure 2.11b.

Once the prestressing strands between Bars 1 and 2 were cut, the process was repeated to cut the strands between Bars 7 and 8, with data being recorded after each strand was cut. After these strands were cut, the strands between Bars 5 and 6 were cut, followed by the strands between Bars 3 and 4. The strands were cut in this order to reduce the extra compressive force in Bars 7 and 8 after the first two strands were cut.

2.5 Lifting Panel Strains

One concern about the deck panels was the additional stress exerted on the exposed mild reinforcing bars during lifting and transporting. Panel 2 and Panel 3 were instrumented and lifted with a crane in the laboratory to determine the additional stresses induced in the exposed

reinforcement. Straps were connected to the panels in two different configurations (four lifting straps and two lifting straps) and strain measurements were taken during lifting.

2.5.1 Four Lifting Straps

The first lifting configuration used four straps to lift the panel. Each strap was wrapped around two groups of reinforcing steel bars, after which the ends of two straps were paired together; the crane hook was then put through the ends of the straps to lift the panel. A photograph and sketch of the straps wrapped around the bar groups are shown in Figure 2.12. Straps had to be wrapped around the bar groups in different configurations in order to have a balanced pick of the panel. Panel 2 and Panel 3 were tested in this configuration. Eight gages on Bars 1, 2, 7 and 8 shown in Figure 2.7 were used to collect data in both panel tests. Each panel was lifted twice and the results compared.

a) photograph of lifting the deck panel with four straps

Figure 2.12. Setup of lifting test using four straps.

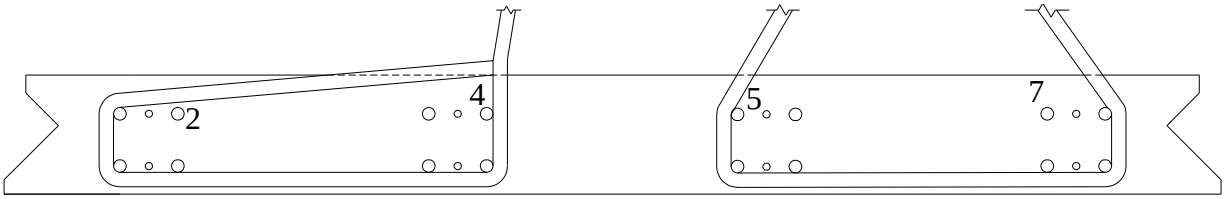

b) cross-section of strap setup

Figure 2.12. Continued

2.5.2 Two Lifting Straps

The second lifting configuration used two straps to lift the panel. Each strap was wrapped around the four bar groups in the longitudinal channel, as shown in Figure 2.13. Once both straps were in place, the panel was lifted and strain readings taken. Only Panel 3 was tested with this setup, and data were collected from four lifts. Steel strains using six strain gages on Bars 1, 2, and 8 were recorded during the tests.

a) photograph of two strap setup prior to lifting

Figure 2.13. Setup of lifting test using two straps.

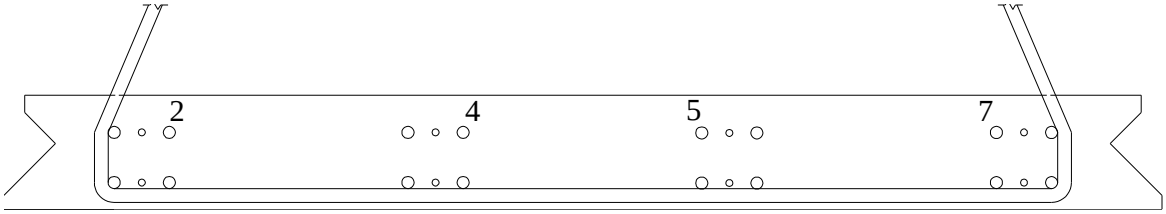

b) cross-section of strap setup

Figure 2.13. Continued

2.6 Leveling Test

In addition to during moving and transporting, there was concern about the stresses in the mild reinforcing steel during the leveling of the panels. Therefore, Panel 2 was tested in the laboratory to determine the magnitude of the stresses exerted on the mild reinforcing steel during panel leveling. For this test, two supports simulating the precast girders in the field were cast to support the panels; the simulated beams were 18 in. tall, 14 in. wide, and 10 ft long. Panel 2 supported by two simulated girders is shown in Figure 2.14.

Figure 2.14. Deck panel setup for leveling test.

For the field bridge, panels were leveled to a 2% transverse slope using a device designed by the contractor and approved by the Iowa DOT. Four devices were used to level each panel. Each device was placed under a group of exterior reinforcing bars, as shown in Figure 2.15. The leveling device consisted of a 3/4 in. coil nut welded to the bottom of a 3/4 in. plate that had a 13/16 in. hole. A 3/4 in. diameter coil bolt was then threaded through the nut, and the bolt was turned to adjust the height of the panel.

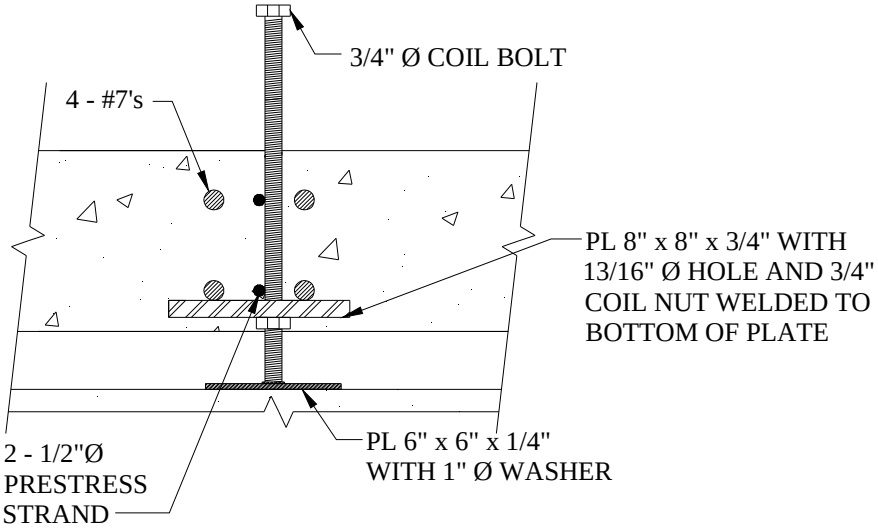

a) cross-section of leveling device

b) photograph of leveling device

Figure 2.15. Leveling device used to achieve correct elevation and 2% slope of the deck panels.

One variation made in the laboratory test setup was the addition of a 1/4 in. plate for the rod to bear on. A washer was welded to the plate to keep the rod from moving on the plate. The plate and washer were added because the test panel was not confined by other panels as would be

the situation in the field. In the field, these other panels would keep the panel and leveling devices from moving along the prestressed girder. The additional plate and washer used in the laboratory can be seen in Figure 2.15b.

To achieve the desired elevation of the panels, four leveling devices were used per panel. Using four devices allowed each corner of the deck panel to be adjusted separately until the required elevation and slope were achieved. A photograph of one leveling device and two deflection transducers in a simulated post-tensioning channel is shown in Figure 2.16. Through the use of the deflections measured at Points 8, 9, 10, and 11 shown in Figure 2.8, the slope of the panel was calculated and adjusted until a 2% slope was reached, as required in the field. The slope was calculated by dividing the difference in the height of the panels at Points 8 and 9 (and 10 and 11) and dividing by 8 ft – 4 in., which was the distance between deflection transducers.

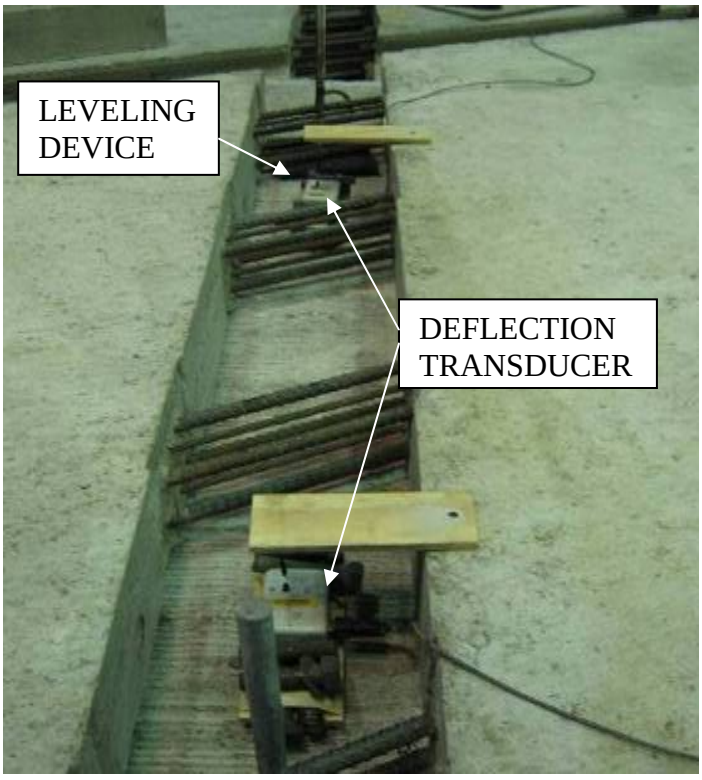

Figure 2.16. Leveling devices and transducers used in panel leveling tests.

In addition to leveling the panel to the desired field slope, various combinations of the four leveling devices were raised to a height of 1 in. to determine the panel response for different scenarios. These tests included the following: raising one corner of the panel, raising one side, raising opposite corners, and raising three panel corners. During each test, readings (strains and deflections) were taken for every 1/8 in. increment the leveling device was raised. Presented in Table 2.1 are the different tests conducted (i.e. adjusting the various leveling devices). The number in the table corresponds to the deflection closest to the leveling device being adjusted.

Table 2.1. Tests conducted with leveling devices.

Test Number	Leveling Device Adjusted
1	Pt 9 to 1 in.
2	Pts 9 and 11 to 1 in.
3	Pts 8, 9, and 11 to 1 in.
4	Pt 8 to 1 in.
5	Pts 8 and 9 to 1 in.
6	Pts 8 and 11 to 1 in.
7	Pt 10 to 1 in.
8	Pts 8 and 10 to 1 in.
9	"Field Leveling"

The panel was not lowered to the original position prior to each test listed in Table 2.1. For example, once the deflection at Point 9 reached 1 in. in Test 1, the leveling device next to deflection Point 11 was adjusted until the deflection at Point 11 reached 1 in. (Test 2 in Table 2.1). The leveling device next to deflection Point 9 was not adjusted during Test 2. Following Test 2, the leveling devices near Points 9 and 11 were untouched while the deflection at Point 8 was adjusted upward 1 in. (Test 3). Next, the panel was lowered to the zero position and Test 4 undertaken. This process was continued for all of the tests, with the panel only being lowered to the zero position after Tests 3 and 6.

The "Field Leveling" test was conducted to determine the stresses developed in the mild reinforcing steel during leveling of the panel to field requirements. For this test, the panel was to

be leveled to a 2% slope in the transverse direction. To achieve this, a difference of 3.86 in. was required between Points 1 and 3 and Points 5 and 7, located at the corners of the panel. This resulted in a difference of 2 in. between Points 8 and 9 and Points 10 and 11.

2.7 Longitudinal Post-Tensioning Channel Concrete Placement Test

One concern about the deck panel system was the placement of concrete in the post-tensioning channel (i.e. could concrete could flow around all of the steel in the post-tensioning channel?). Shown in Figure 2.17 is a photograph of one of the post-tensioning channels in the bridge prior to placement of concrete. In order to check this concern, a model of the channel was constructed in the laboratory and concrete was placed multiple times to determine if any void spaces were left around the steel.

Figure 2.17. Photograph of longitudinal post-tensioning channel prior to casting concrete in the field.

2.7.1 Channel Construction

The laboratory channel model was to have the same dimensions and all of the steel present in the field bridge channel. Therefore, the channel was 10 in. wide, 8 1/4 in. deep, and 6

ft long. A 6 ft channel length was chosen because this allowed construction of a channel where observations could be made on both the concrete flow around the leveling devices and through only the prestress strand. Figure 2.18 provides illustrations of the channel constructed.

a) constructed channel used in concrete placement tests (courtesy of Iowa DOT)

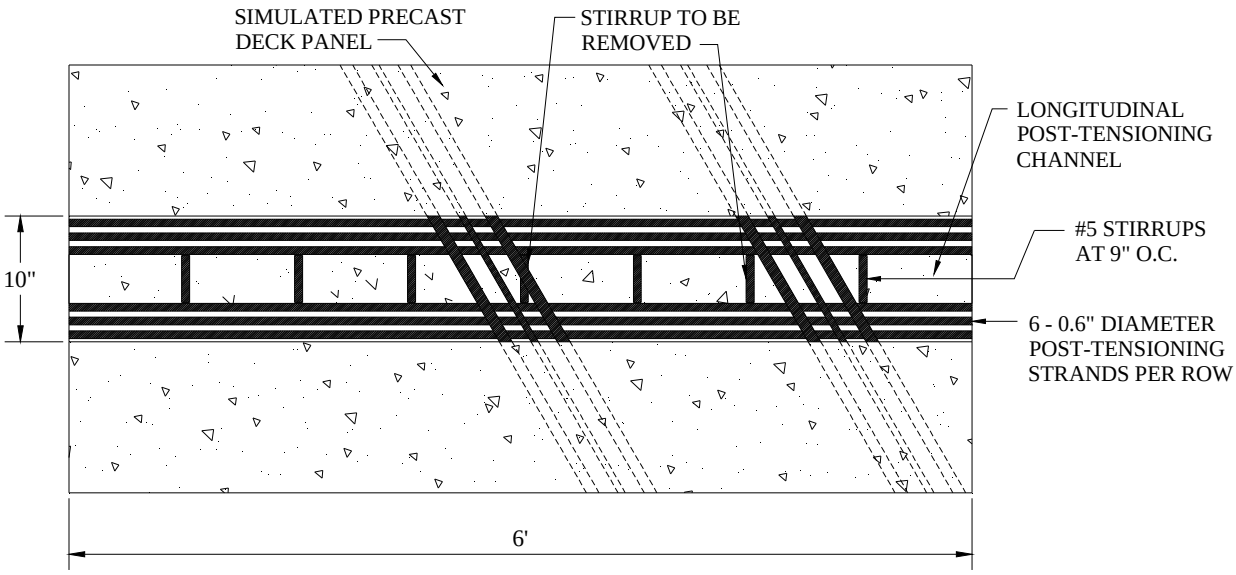

b) plan view of channel constructed

Figure 2.18. Channel constructed for longitudinal post-tensioning channel concrete placement test.

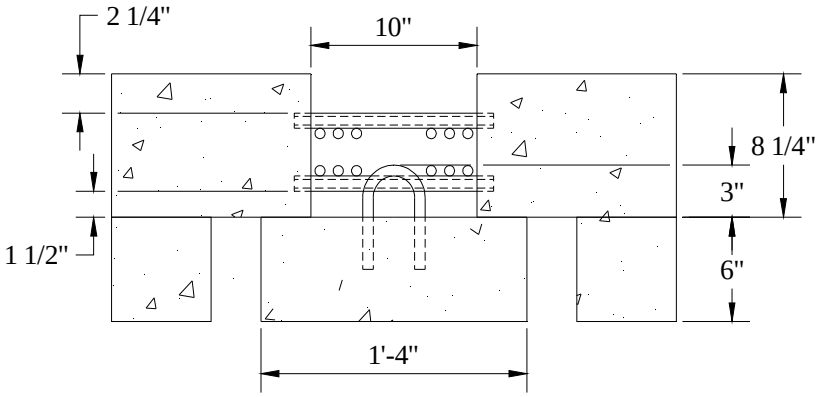

c) cross-section of channel constructed

Figure 2.18. Continued

Elements composing the completed model included a simulated deck panel with mild steel and prestress strands, a simulated girder, and concrete beams to support the simulated deck panel. Plywood was placed at the ends of the channel to close the channel and support the post-tensioning strands. The plywood could be removed between tests to allow for cleaning of the specimen before reuse. Presented in Figure 2.18a is a photograph of the constructed test specimen.

As can be seen in Figure 2.18c, a cross-section of the channel, the following are present in the channel: stirrups extending from the girder to provide composite action with the deck, two layers of prestressing strands, two layers of mild reinforcement, and 12 post-tensioning strands (6 in the top layer and 6 in the bottom layer) along the length of the channel. Excluded from the figure for simplicity is the leveling device.

Stirrups were spaced on 9 in. centers to simulate the worst-case spacing which occurred near the end of the girders. Two stirrups were removed from the beam prior to placing the simulated deck panel on the beam because the stirrups would interfere with either the mild steel

reinforcement or the leveling device. The specifications for the project also called for removal of any stirrups in the field that may interfere with installation of the deck panels.

Three inches of each stirrup were left exposed from the beam instead of the 4 1/2 in. specified in the plans, because in the field the panels would be raised and not resting on the girders once leveled. Leveling decreases the overlap of the stirrups with the post-tensioning strands and other bars. For this reason, the exposed length of the stirrups was reduced so the top of the stirrups would be located at a lower height on the model channel and closer simulate the field conditions.

Twelve post-tensioning strands ran the length of the channel. For the tests, the strands were not post-tensioned. In order to eliminate any sag in the strands, the strands were tied to the mild steel reinforcement and supported at the ends by plywood. The holes in the plywood were not oversized, allowing for a tight fit of the strands.

2.7.2 Concrete Placement

Placement testing was conducted on two days, November 9, 2006 and May 17, 2007. A total of three tests were conducted, two on the first test day and one on the second day. The third test will be the focus of this section. Unlike the first two tests, which took place inside the laboratory due to weather conditions, the third test was conducted outdoors. Photographs of the setup of the channel outside of the laboratory are presented in Figure 2.19.

Another change from the first two tests was the addition of the leveling devices to the channel. In the first two tests, the focus was to ensure the concrete left no void spaces among the mild reinforcement and post-tensioning strands; therefore the leveling devices were left out so this was easier to observe. Leveling devices were in-place during the third test, resulting in a worst-case scenario for obstructions in the channel and replicating field conditions. This test

setup provided a worse-case scenario for the opening between the leveling device plate and the girder because in the field, the plate would be raised higher due to leveling the deck panels. During this test, the space between the plate and the girder was 1 1/4 in. A photograph of a leveling device in the channel prior to testing is shown in Figure 2.19b.

a) outdoor test setup

b) steel in channel

Figure 2.19. Concrete placement test setup.

An O-4-S35 concrete mix was ordered from Iowa State Ready Mix for all three tests. This mix met the following requirements: a class O-4WR; maximum top size of aggregate of 3/8 in.; 35% replacement with ground granulated blast furnace slag (GGBFS); maximum water cement ratio of 0.38; maximum slump at the plant of 3 in.; maximum slump after addition of high range water reducer of 8 in.; and a minimum concrete temperature at time of placement of 70° F.

Testing began at 11:00 A.M. on May 17, 2007. Air temperature at the time of the test was 61°F. The temperature of the channel concrete was 45°F. Slump of the concrete at time of arrival was measured at 3 3/4 in. After the addition of 40 ounces of super plasticizer per cubic yard of concrete, the slump was 8 in. For comparison, the air temperature was 55°F and the slump at arrival was 2 in. for the first two tests. A 5 in. slump after the addition of super plasticizer was measured for the first test and the slump was 6 1/2 in. for the second test, after the addition of extra super plasticizer.

Concrete placement for the third test began near the mild steel, which is the right end of Figure 2.18. For this test, concrete from the concrete truck was placed into a wheel barrow, and then placed by the shovelful into the channel and vibrated. One location of the channel was filled at a time, and as the channel filled, placement continued until the channel was full.

2.8 Service Load Tests

A series of service load tests were conducted to determine the response of the deck panels to loads placed at various locations. Load magnitudes typically were 40 kips for interior spans and 20 kips on the cantilevered sections. Service load tests were first preformed on panels prior to the closure pour being cast, with concrete strains, steel strains, and deflection data recorded. Next, the closure pour was cast between two panels and service load testing repeated, with the

results between the series of tests compared to determine the effect of the closure pour on the system. All service loads were completed applying loads to a 9 in. square footprint.

2.8.1 Individual Panel Service Load Tests

Setup for the service load tests began with placing four simulated precast girders at the proper spacing on the laboratory floor. Once the girders were set in place, two deck panels were lowered into position. Leveling devices designed by the contractor were used to adjust the slope of the panels to 2%, matching the slope of the panels in the field bridge. Next, plywood formwork was attached to the beam below the deck panel and at both ends of the longitudinal post-tensioning channel, as shown in the photograph in Figure 2.20a.

Once the formwork was constructed, concrete could be placed in the post-tensioning channels. A C-4 mix with 3/8 in. chips and a 4 in. slump was used for the post-tensioning channel concrete. Concrete in the channels was placed on February 15, 2007; a photograph of the concrete placement in one of the channels is shown in Figure 2.20b.

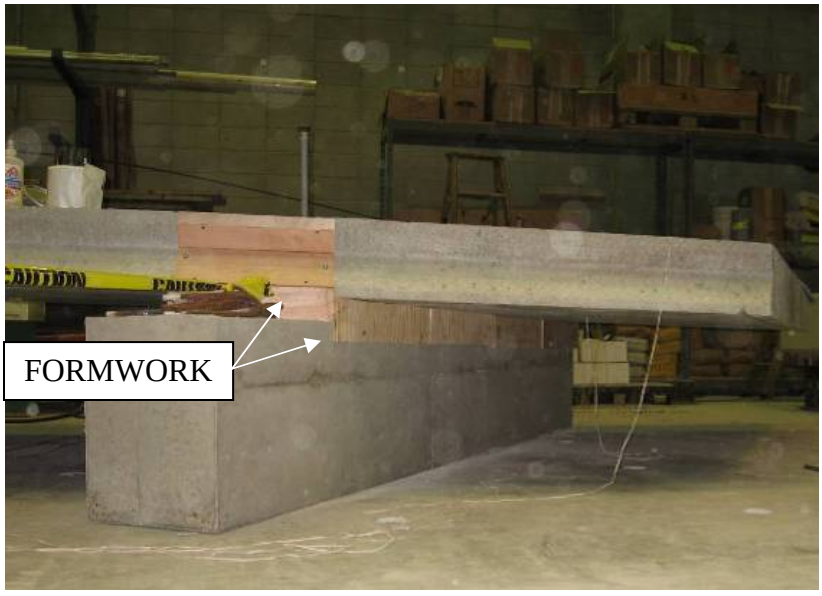

a) formwork along bottom of channel

Figure 2.20. Casting concrete in the post-tensioning channel.

b) placement of concrete in channel

Figure 2.20. Continued

Load locations used for the two panels are presented in Figure 2.21. Load locations were laid out along three lines in the transverse direction (A, B, and C) and fourteen lines in the longitudinal direction (1-14). Lines A, B, and C were equally spaced at 1 ft - 9 in., measured from the bottom of the transverse shear key. Lines 1 through 14 were spaced on 3 ft increments, with Line 1 approximately 2 in. from the corner of Panel 1. This was done so point B8 would be positioned over the center of the closure pour for the connected panel service load tests.

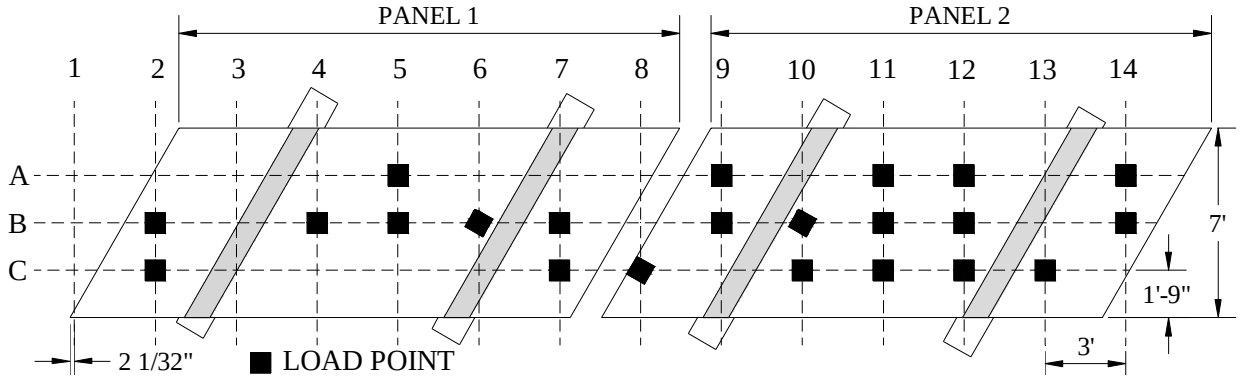

Figure 2.21. Load locations for service load tests on individual panels.

More instrumentation was installed on Panel 2 than on Panel 1, and therefore Panel 2 was tested more extensively, as illustrated in Figure 2.21. Each test point on Panel 1 was chosen to correspond to a point on Panel 2, allowing for a comparison of the data from the two panel tests. This it was possible to see how both panels responded to the same loading.

Also of note in Figure 2.21 are load locations B6 and B10. The footprint at these points is parallel to the support beams. This was done so the load would not be applied directly to the support, which would occur if the footprint was not rotated. Point C8 was also rotated so the load footprint would not overhang the deck panel.

Service load testing began on Panel 2 on February 22, 2007, seven days after the post-tensioning channel concrete was placed. The 7 day strength of the concrete in the channel was 4,650 psi. Loading of the panel began at Point B14, and shown in Figure 2.22 is the test setup for various load points. Each point was loaded twice to ensure consistent results. For Panel 2, loading varied from 32 kips for points on cantilevered sections to 40 kips for interior spans, with the load increased in 4 kip increments. All points on Panel 1 were loaded to 20 kips in 2 kip increments. A load cell was used to measure the applied load.

2.8.2 Connected Panels Service Load Tests

After the service load tests on the individual panels were completed, the closure pour was cast, connecting the two panels. Shown in Figure 2.23 is a photograph of the closure pour connection prior to concrete placement. Present in the joint are sixteen #5 double hooked bars and four #5 longitudinal bars.

Load points used for the connected panel service load tests are presented in Figure 2.24. Multiple goals were considered in determining these load points. These goals were to: determine

the panels' response as the load moved in the transverse direction; determine the response of the closure to loading; and determine the general effect the closure had on the system.

a) service load at Position B9

b) service load at Position C10

Figure 2.22. Individual panel service load test setup.

c) service load at Position B14

Figure 2.22. Continued

Figure 2.23. Longitudinal closure between panels prior to concrete placement.

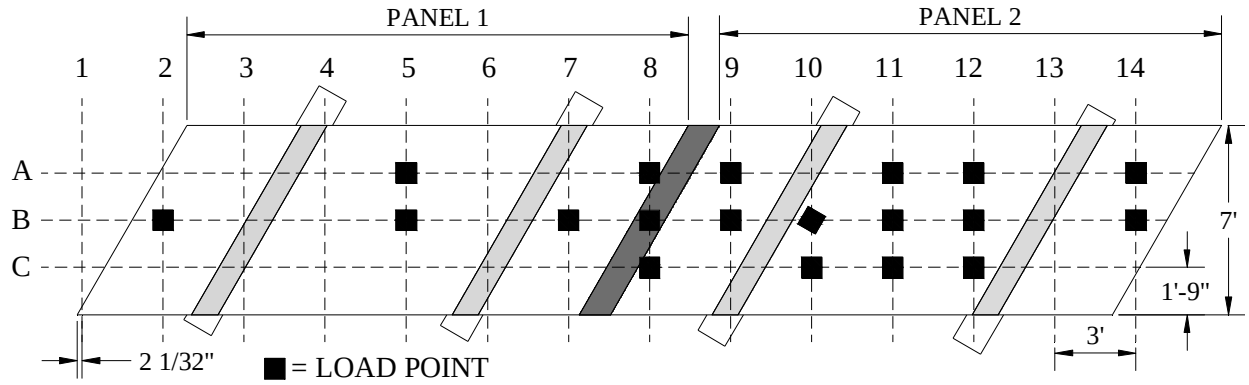

Figure 2.24. Load points used in connected panel service load tests.

The first test goal was to determine the panel response as a load moved transversely across the system. This was accomplished by applying load at multiple locations along Line B in Figure 2.24 and measuring the resulting concrete strains, steel strains, and deflections.

Another objective of the connected panel service load tests was to measure the response of the closure to loading. To do this, multiple load points were positioned in the vicinity of the closure, with concrete strains, steel strains, and deflections measured and recorded.

Finally, the general effect the closure had on the response of the system was to be determined. This was accomplished by comparing the response data between the individual panel tests and closure tests with the load in the same locations.

Review of Figure 2.24 reveals Panel 2 has the majority of the load points. There are two reasons for this. First, Panel 2 had the majority of the instrumentation; therefore by loading this panel, a better idea of the response would be obtained. Also, Panel 2 was subjected to more tests during the individual panel service load tests than Panel 1. Testing Panel 2 extensively again allowed for a better comparison of data between the two sets of service load tests.

The test setup in the laboratory for the connected panel tests is shown in Figure 2.25. Testing went from Column 14 to 1 and Row A to C in Figure 2.24. As previously noted, a 9 in. square footprint was used for each test, and each point was loaded twice to ensure consistent

results. Loading varied from 20 kips for points on Columns 2 and 14 (the cantilevered sections), to 40 kips for all the points in the interior spans. Instrument readings were taken ten times for each test, resulting in readings in 2 kip increments for the cantilevered spans and 4 kip increments for the interior spans. A load cell was used to measure the applied load. Instrumentation locations for this test were presented earlier in Section 2.2.

2.9 Ultimate Strength Tests

A series of ultimate load tests were conducted to determine flexural and punching shear capacities of the connected deck panels. Testing was done on both the single panel (Panel 3) and connected panels (Panels 1 and 2). Footprints used for the tests included a 9 in. square, tandem wheels, and line load.

a) service load at Position B2

Figure 2.25. Test setup for connected panel service load tests.

b) service load at Position B12

c) service load at Position A14

Figure 2.25. Continued

2.9.1 Test of a Single Panel

Panel 3 was tested to determine the flexural capacity of a single panel. This was accomplished by applying a line load at the midspan of the panel. As previously noted, Panel 3 also contained a cold joint, so this test would help determine if the cold joint affected the strength of the panel. The position of the line load is shown in Figure 2.26a.

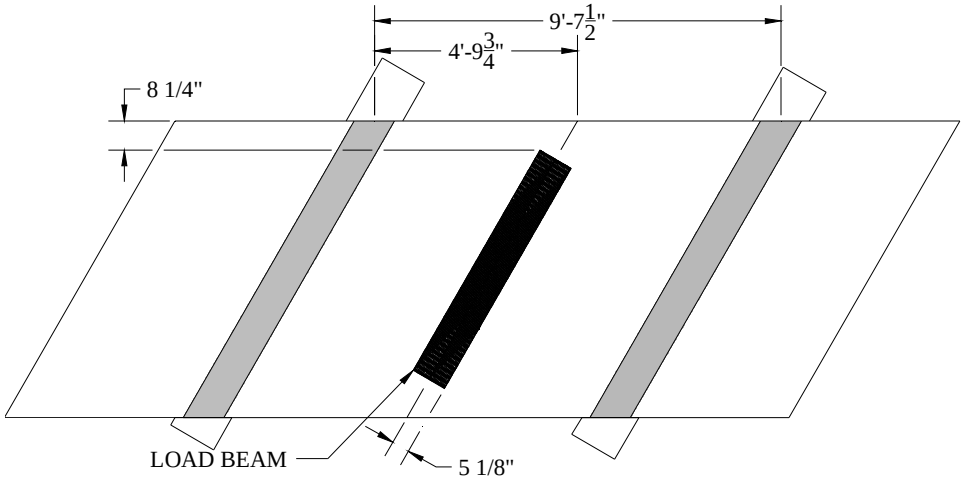

a) location of line load for Panel 3 test

b) Panel 3 setup prior to testing

Figure 2.26. Laboratory setup for Panel 3 ultimate load test.

Presented in Figure 2.26b is a photograph of the laboratory setup prior to the start of the test. The line load was applied by loading a 6 ft long HP10x42 section. Neoprene pads were placed between the load beam and deck panel to account for the roughness in the deck panel surface and to evenly distribute the load. A 300 kip load cell was placed between the load beam and the actuator. Deflection transducers were installed at the ends and midpoint of the load beam so the load distribution through the beam could be monitored. Data were collected for every 10 kip increment of load applied to the panel.

2.9.2 Test Using 9 in. Square Footprint

The goal of this ultimate strength test was to determine the strength of the longitudinal closure pour. Because of the anticipated strength of the closure pour and the capacities of the laboratory equipment, the decision was made to place a point load to one side of the joint for the test. This was done instead of placing one point load on each side of the joint and subjecting the joint to pure flexure. The reasoning for this was to expose the joint to both flexure and shear – a more severe loading condition.

A 9 in. square footprint was used to keep consistency between this test and the service tests to allow for data comparison. Location of the footprint relative to the closure joint can be seen in Figure 2.27a. The footprint was parallel to and 4 1/2 in. from the joint and 2 ft – 8 in. from the panel edge. Shown in Figure 2.27b is a photograph of the applied load relative to the closure joint and concrete strain gages on the specimen.

Steel beams were used to tie the specimen to the floor. This was done because of an anticipated uplift force at the exterior beams during loading. The locations of the restraining beams relative to the support beams can be seen in Figure 2.27a. Locations of the restraining

beams were controlled by the locations of the inserts in the tie down floor. The entire test setup with the two restraining beams is shown in the photograph in Figure 2.27c.

Loading was to continue during the test until either the specimen failed or the capacity of the actuator was reached, which was 400 kips. Instrumentation readings were collected at 10 kip increments until failure occurred. A load cell was used to measure the applied load.

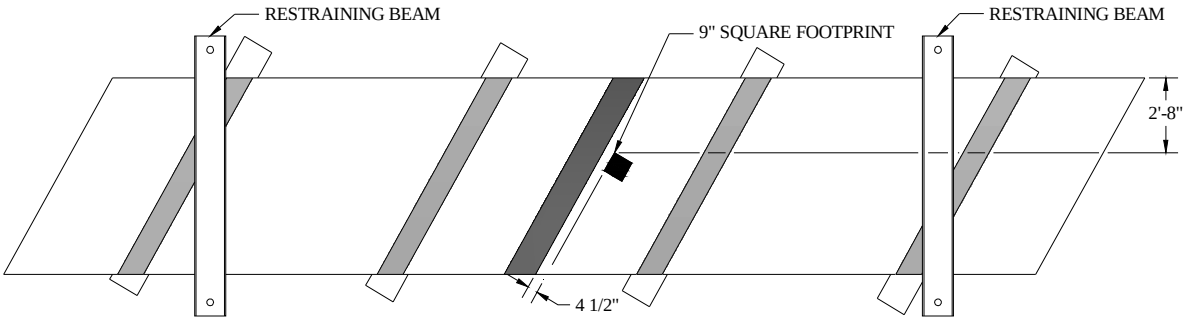

a) location of 9 in. square footprint

b) test setup for closure pour ultimate load test

Figure 2.27. Laboratory setup for closure joint ultimate load test.

c) restraining beams positioned for ultimate load test

Figure 2.27. Continued

2.9.3 Testing Using Tandem Wheel Footprint

A tandem wheel footprint was used for the third ultimate load test. The load was positioned as close to midspan of Panel 2 as possible based on the layout of the tie down floor. Shown in Figure 2.28a is the exact position of the load. A steel beam was positioned over one of the support beams to keep the panel from lifting during loading due to uplift forces. Presented in Figure 2.28b and c are photographs of the test setup.

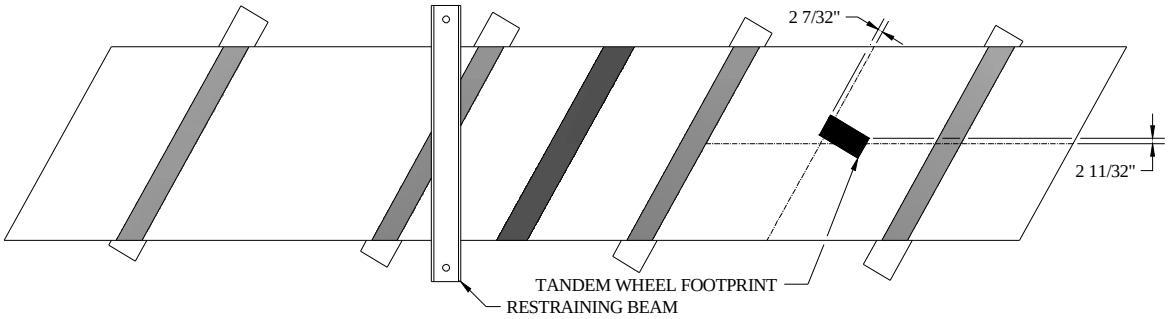

a) load position for tandem wheel footprint ultimate load test

Figure 2.28. Load position and laboratory setup for tandem wheel ultimate load test.

b) laboratory setup

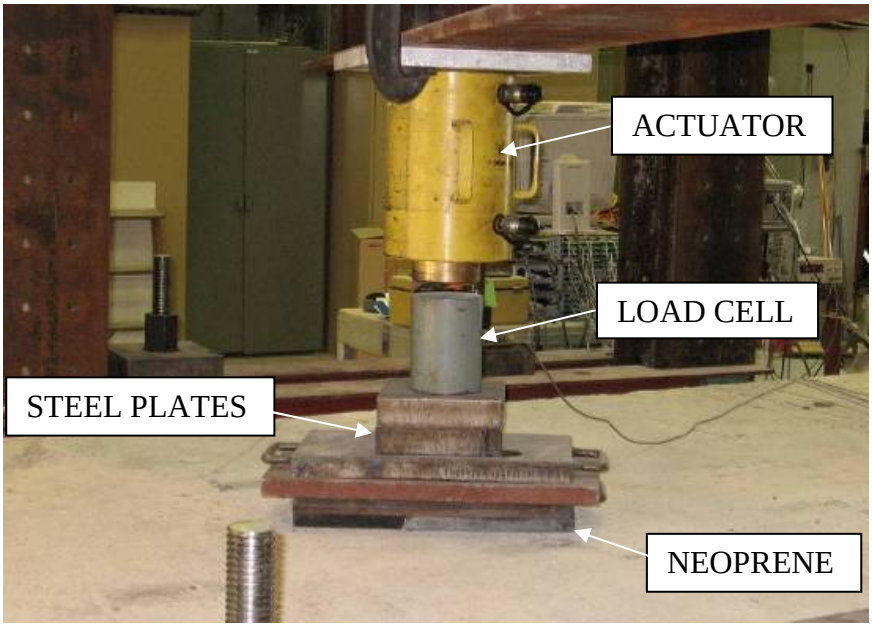

c) tandem wheel footprint

Figure 2.28. Continued

Shown in Figure 2.28c is a photograph of an overall view of the tandem wheel footprint. The following can be seen in this figure: two neoprene pads each with dimensions of 10 in. by 10 in., steel plates approximately 20 in. x 10 in., 9 in. square steel plates, a 300 kip load cell, and a

400 kip actuator. Load was applied until either a failure in the deck panel occurred or the capacity of the actuator was reached. Data were recorded for every 10 kip increments of load applied.

2.9.4 Line Load

A line load was applied to test a span of Panel 1 in flexure. The load was applied until a deck panel failure occurred. Data were recorded for every 10 kip increment of load applied to the panel; applied loads were measured with a load cell.

The line load was applied by loading a 6 ft long HP10x42 section. Neoprene pads were placed between the load beam and deck panel to account for the roughness in the deck panel surface and to evenly distribute the load. A 300 kip load cell was placed between the load beam and the actuator. Deflection transducers were installed at the ends and midpoint of the load beam so the load distribution through the beam could be monitored. A photograph of the setup in the laboratory prior to testing is shown in Figure 2.29a.

a) laboratory setup for line load ultimate load test

Figure 2.29. Laboratory setup for ultimate load test using a line load.

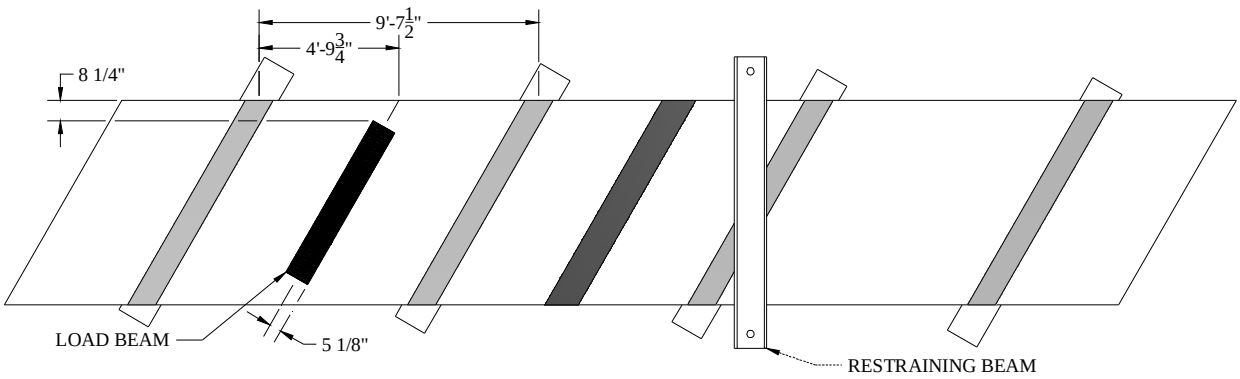

b) location of line load on Panel 1

Figure 2.29. Continued

Shown in Figure 2.29b is the position of the line load on Panel 1. The line load was placed at the midspan of the panel. Also shown is the location of the restraining beam used for this test. The restraining beam was needed to transfer the uplift forces developed in Panel 2 to the tie down floor.

3. LABORATORY TEST RESULTS

In this chapter, results for the various laboratory tests performed on the deck panels are presented. Test results presented include concrete compressive strengths, prestressing force measurements, strains measured in the deck panel during lifting, and strains measured during leveling. Observations made during placement of concrete in the longitudinal post-tensioning channel are discussed. Lastly, strain and deflection data from the service load tests and ultimate strength tests of the panels are presented.

3.1 Concrete Strength Test Results

Compressive strength results for the concrete cores taken from the Panel 1 are presented in Table 3.1. Results for this panel were assumed to be representative of the compressive strength of the concrete in all the deck panels tested. The compressive strengths ranged from 7,530 psi to 9,570 psi. Because the strength of Core A was significantly greater than Cores B and C, only the Core B and C strengths were used to calculate the average concrete compressive strength of 7,600 psi. By not using the high compressive strength of Core A, a conservative value was obtained. The average compressive strength exceeded the specified concrete strength of 5,000 psi by 27 percent.

Table 3.1. Deck panel concrete compressive strengths.

Core	Strength (psi)
A	9,570*
B	7,670
C	7,530
Average	7,600

*excluded from average

3.2 Stresses in Panel Mild Reinforcement Due to Prestressing

Presented in this section are the stresses calculated from strains measured in six reinforcing bars when the prestressing strands in one longitudinal channel were cut. Locations of

the instrumented bars can be seen in Figure 2.7. The experimental stress in each mild reinforcing bar was compared to the design stress for the mild bars. To determine the design stress in each bar, estimated losses were subtracted from one-half the initial stress in one prestressing strand. Estimated losses included losses due to creep, shrinkage, relaxation, and elastic shortening and were taken as a lump sum value of 40 ksi (Naaman, 2004). The design stress in each reinforcing bar without considering losses was 25.8 ksi and 20.7 ksi considering losses.

Calculated stresses for each instrumented bar are given in Table 3.2. Hooke's Law and an assumed steel modulus of elasticity equal to 29,000 ksi were used to determine stresses from the measured strains. Experimental stresses ranged from 13.0 ksi to 21.5 ksi. One of the six bars was stressed greater than the design stress less losses by 0.8 ksi. The average experimental stress was 16.1 ksi, which is 4.6 ksi less than the design stress less losses. Therefore losses in the prestressing force were greater than expected.

Table 3.2. Stress in each instrumented bar.

Bar	Stress (ksi)	Difference from Design Value Less Losses (%)
1T	13.8	-33
1B	17.2	-17
2T	13.0	-37
2B	21.5	+4
8T	15.8	-24
8B	15.1	-27

In Table 3.3 the average stress in the top and bottom bars is presented. The average stress in the bottom bars (17.9 ksi) was higher than that in the top bars (14.2 ksi); however both stresses were less than the design stress less losses. A reason for the difference in stresses could be that the bottom prestressing strands were stressed higher than the top strands; this is supported by comparing the values of 1T and 1B, or 2T and 2B. Both bottom strands were stressed higher than the corresponding top strands.

Table 3.3. Average stress in each bar layer.

Bar	Stress (ksi)	Difference from Design Value Less Losses (%)
Top	14.2	-31
Bottom	17.9	-14

3.3 Lifting Panel Strain Results

Presented in this section are the results for the crane lifting tests. A deck panel was lifted multiple times with two different strap configurations (see Figure 2.12 and Figure 2.13). Strains induced in the mild reinforcing bars were measured during each test to determine the state of stress in the bars.

3.3.1 Four Lifting Strap Test Results

Shown in Figure 3.1 is a plot of the strains experienced in each instrumented bar while the panel was lifted from the support beams. Locations of the instrumented bars are presented in Figure 2.7, and the configuration of the straps around the bars is shown in Figure 2.12. Strains measured in the test presented (the first test) agree with results from the other tests conducted with the same strap configuration. All strains plotted were temporary because they only occur during lifting; once lifting is completed and the panel is in place, the only strains present in the mild reinforcing bars are due to the prestressing force and bending of the cantilevered sections over the supports due to the self-weight of the panel.

As can be seen in the graph, half the bars experienced tension and half were in compression. However, not all the top bars experienced tension and not all the bottom bars experienced compression, as one would expect. Three of the top bars (1T, 7T, and 8T) and one bottom bar (8B) were in tension. The tension in the bottom bar, 8B, was due to a localized effect caused by bearing of the lifting strap directly on the bar near the strain gage. Bar 1T experienced

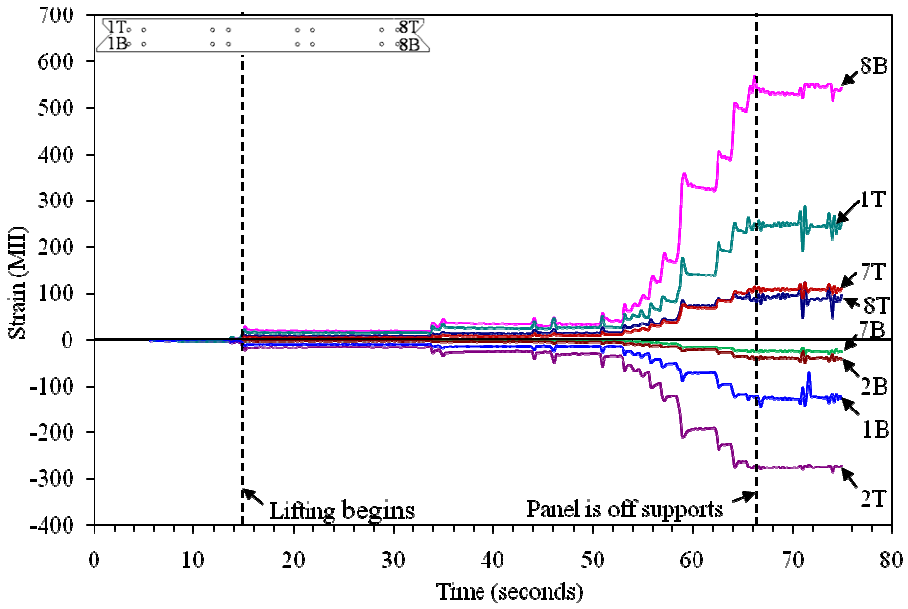

Figure 3.1. Strain results for first lift of Panel 2 with four straps.

the largest tensile strain (251 MII) if Bar 8B is neglected, and Bar 2T had the largest compressive strain (-278 MII).

Presented in Table 3.4 are the maximum strains measured for each instrumented bar during the four strap lifting tests. These strain values are only for the specific point where the strain gage was located; strains obviously will be different at other locations along the bar. Each strain was added to the strain induced in the bar due to prestressing, -1179 MII. This value was calculated using the following equation:

$$\varepsilon = \frac{P}{AE} \qquad (1)$$

Where P = prestressing force exerted on a #7 bar = -20.5 kips

A = area of a #7 bar = 0.60 in^2

E = steel modulus of elasticity = 29,000 ksi

Table 3.4. Strains and percent utilization of the #7 bar yield strain during four strap lifting.

Bar	Maximum Strain Measured (MII)	Total Strain (MII)	Utilization (%)
1T	251	-928	45
1B	-204	-1383	67
2T	-278	-1457	70
2B	79	-1100	53
7T	143	-1036	50
7B	-40	-1219	59
8T	93	-1086	52

Strains were then compared to the yield strain for 60 ksi steel, 2069 MII, to determine the percent utilization of the yield strain. Bars with utilization less than 100% have reserve strain capacity. Bar 2T had the highest percent utilization at 70%. All instrumented bars were utilized between 45% and 70%.

3.3.2 Two Lifting Strap Results

Six bars were instrumented when a deck panel was lifted with two straps; locations of each strain can be seen in Figure 2.7 and the layout of the straps can be seen in Figure 2.13. Strains induced while lifting a deck panel with two straps are plotted in Figure 3.2. Of the six bars instrumented, four experienced tension (1T, 8T, 2B, and 8B) and two were in compression (1B and 2T). As previously noted, these strains were temporary because they only occurred during lifting; once the panel was set in place, the only strains present in the mild reinforcing bars were due to the prestressing force and bending of the cantilevered sections over the supports due to the self-weight of the panel.

Bar 8B had the largest strain, stabilizing at a strain of 1780 MII. However, this strain was caused by a localized effect from the lifting strap bearing directly on the bar near the strain gage. Neglecting this strain, all the instrumented bars experienced strains less than 250 MII. The

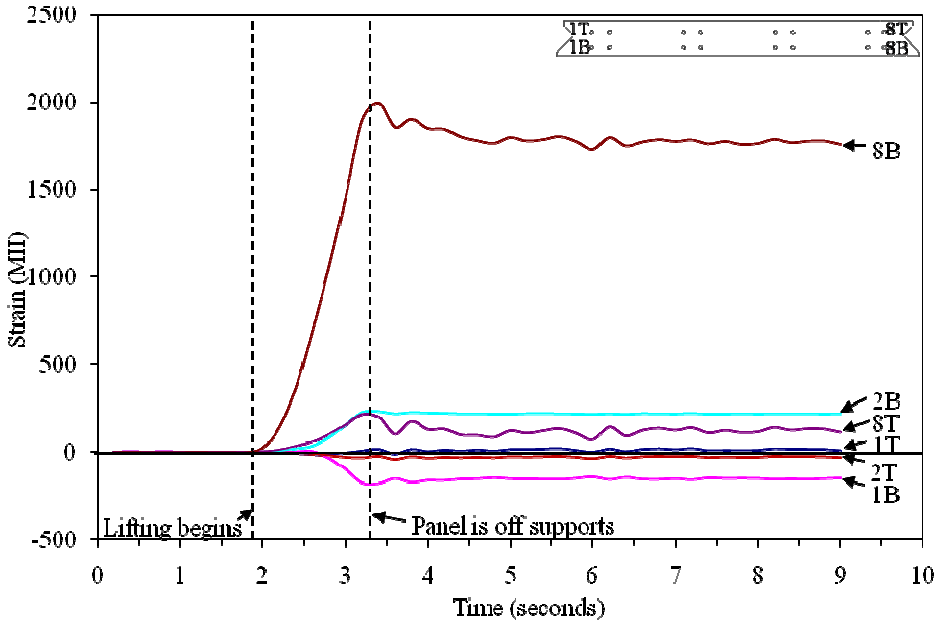

Figure 3.2. Strain results for fourth lift of Panel 3 with two straps.

strains measured during the two lifting strap tests were of a similar magnitude to those measured during the four lifting strap tests, even though the strap configuration was different. This shows that for the instrumented bars, the configuration of the lifting straps did not affect the strains in the bars.

In Table 3.5 the maximum strains in each instrumented bar during the two strap lifting tests are presented. These strain values are only for the specific point where the strain gage was located; strains obviously will be different at other locations along the bar. Each strain was added to the strain induced in the bar due to prestressing calculated using Equation 1. This total strain value was then compared to the yield strain for 60 ksi steel, 2069 MII, assuming linear behavior and a steel modulus of elasticity of 29,000 ksi. Values for percent of the yield strain utilized ranged from 46% to 66%.

Table 3.5. Strains and percent utilization of #7 bar yield strain during two strap lifting.

Bar	Maximum Strain Measured (MII)	Total Strain (MII)	Utilization (%)
1T	22	-1157	56
1B	-177	-1356	66
2T	-38	-1217	59
2B	231	-948	46
8T	217	-962	46

3.4 Leveling Test Results

Strains experienced during the various leveling tests conducted are presented in Figure 3.3. Tests conducted and the order leveling devices were raised were presented in Section 2.6; locations of the instrumented mild reinforcing bars were shown in Figure 2.7. Each event plotted on the horizontal axis in Figure 3.3 represents an increase of 1/8 in. in height of the leveling rod being adjusted.

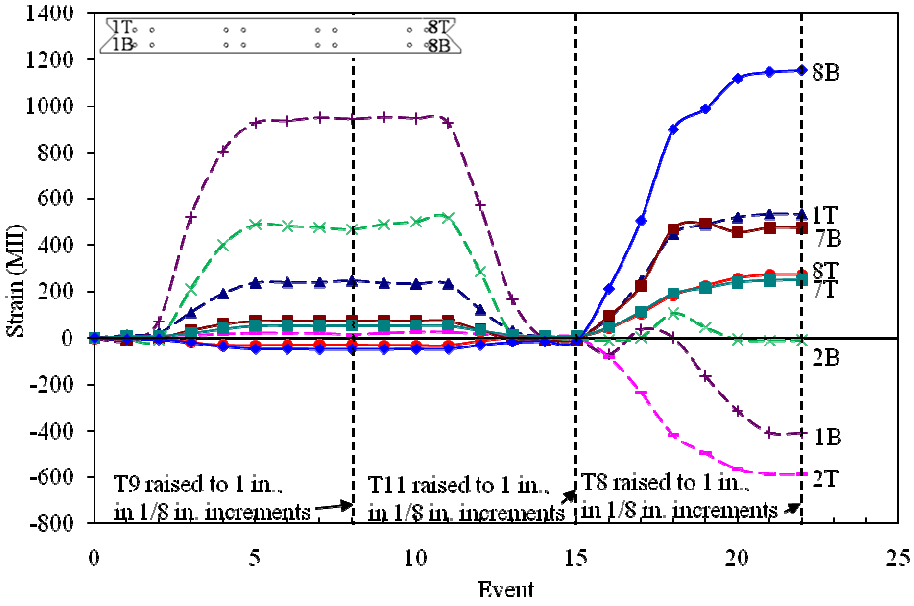

a) strains for all instrumented bars during Test 1

Figure 3.3. Measured steel strains in Panel 2 mild reinforcing bars during leveling tests.

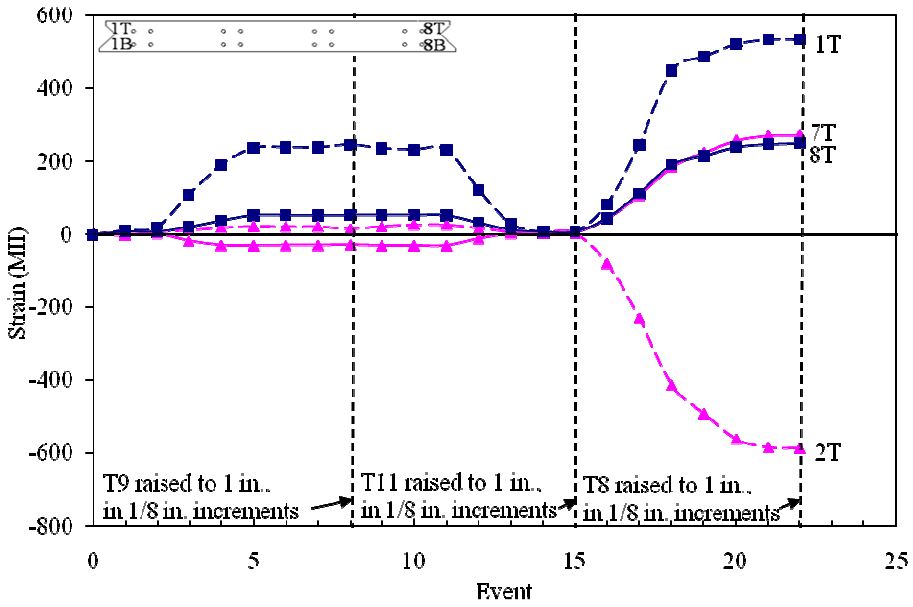

b) top bar strains in Tests 1, 2, and 3

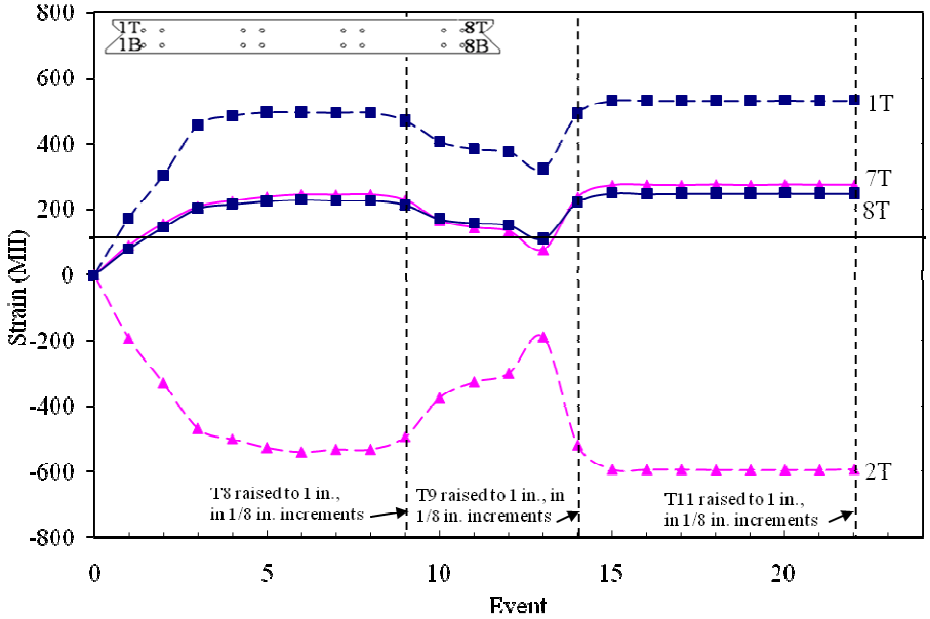

c) top bar strains in Tests 4, 5, and 6

Figure 3.3. Continued

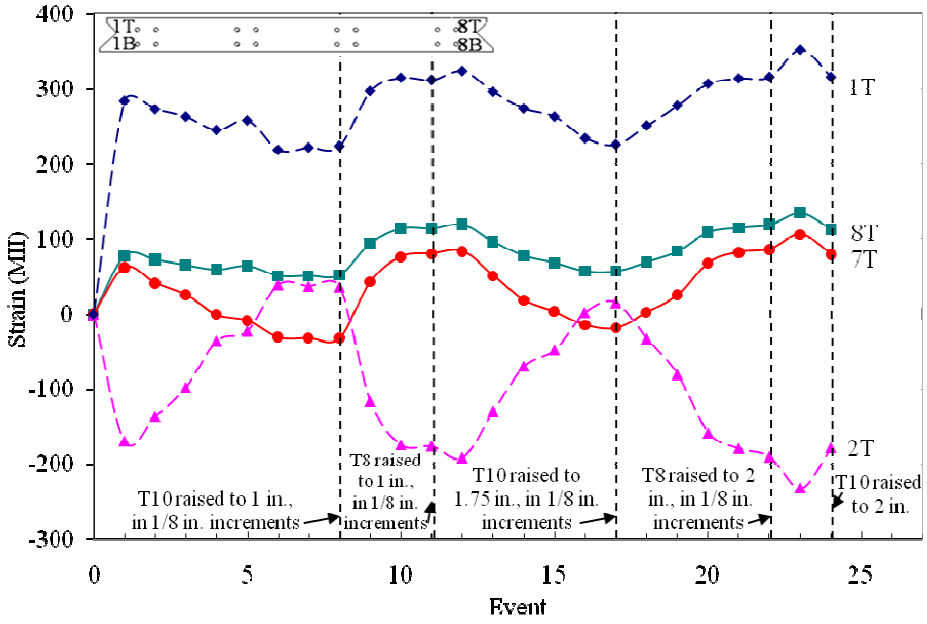

d) top bar strains in Test 7, 8, and 9

Figure 3.3. Continued

Shown in Figure 3.3a are the strains measured for each instrumented bar during Tests 1, 2, and 3. Bar 8B experienced the largest strain (1194 MII) during the test, with a strain twice that of the next largest strain. Strain data for all the bottom bars are disregarded in Figure 3.3b through d because these strains were the result of a localized effect caused by the bar bearing on the leveling plate.

Bar 2T and Bar 7T were the only bars to experience compressive strains during testing, and Bar 7T was the only bar that was always in compression. The maximum strain measured in the top bars during testing was approximately -600 MII. Another observation from the plots is that strains tended to change over the first 1/2 in. of adjusting a leveling device and then remained constant as the leveling device is raised the final 1/2 in. to a height of 1 in.

An observation that can be made from the results of the test replicating field leveling (Tests 7, 8, and 9) shown in Figure 3.3d is the maximum strain experienced by any of the bars

was independent of the height of the bar. Strains induced in bars were essentially the same when a leveling device was at 1 in. or when the same device reached 2 in.

Maximum strains measured for each instrumented bar during the leveling tests are presented in Table 3.6. These strain values are only for the specific point where the strain gage was located; strains obviously will be different at other locations along the bar. Each strain was added to the strain induced in the bar due to prestressing calculated using Equation 1. This total strain value was then compared to the yield strain for 60 ksi steel, 2069 MII, assuming linear behavior and a steel modulus of elasticity of 29,000 ksi. Values for percent of the yield strain utilized ranged from 31% to 86%.

Table 3.6. Strains and percent utilization during leveling tests.

Bar	Maximum Strain Measured (MII)	Total Strain (MII)	Utilization (%)
1T	533	-646	31
2T	-595	-1774	86
7T	273	-906	44
8T	249	-930	45

Values given in Table 3.6 were temporary because all strains went to zero once the deck panel was placed in a horizontal position on the support girders. However, because deck panels are left in a leveled position in the field, strains due to leveling may be permanent strains in the reinforcing bars.

3.5 Longitudinal Post-Tensioning Channel Concrete Placement Results

The photographs in Figure 3.4 address concerns the Iowa DOT had about the flow of concrete in the post-tensioning channel, specifically the flow around all of the steel present in the channel. In Figure 3.4a, one can see the concrete flowed through the channel in three layers, first under the prestress strand, then between and around the strands, and finally above the strands.

This was typical of all three tests conducted. Shown in Figure 3.4b is concrete flowing between the prestressing strands, addressing concerns of the Iowa DOT if concrete would leave void space between the strands.

a) concrete flowing in channel

b) concrete flowing between post-tensioning strands

Figure 3.4. Concrete flow during longitudinal post-tensioning channel concrete placement tests.

c) concrete below the leveling device

Figure 3.4. Continued

Concrete can be seen below the leveling device in Figure 3.4c, eliminating another concern of the Iowa DOT. Because concrete is beneath the leveling device, load is transferred from the deck panels by bearing on concrete and not through the leveling device rod. The leveling device was only present in the third test.

3.6 Service Load Tests Results

Presented in the following sections are results for the individual panel and connected panel service load tests. Concrete strains, steel strains, and deflection data are presented along with comparisons to service values where appropriate.

3.6.1 Individual Panel Service Test Results

The following section presents the results from the service load tests conducted prior to the closure pour being cast. A total of 22 load points were used; 8 points on Panel 1 and 14 points on Panel 2 (see Figure 2.21). In this section, results for loads positioned at B5, B11, and

B14 are presented. Load placed at B5 and B11 resulted in the largest strains and deflections for the cases of the load positioned between the support beams. A load at B14 resulted in the largest deflections in the deck panel. Results for these three load positions are representative of the results obtained from the other 19 load cases. Magnitude of loads applied varied however all were greater than the 16 kip wheel load of a HS 20-44 truck used in design.

Strains induced for a load varying from 0 to 48 kip positioned at B11 are plotted in Figure 3.5. Refer to Figure 2.7 for the location of each steel strain. All the steel strains for this load location resulted from bending of the cantilevered portion of the deck panel about the support beam.

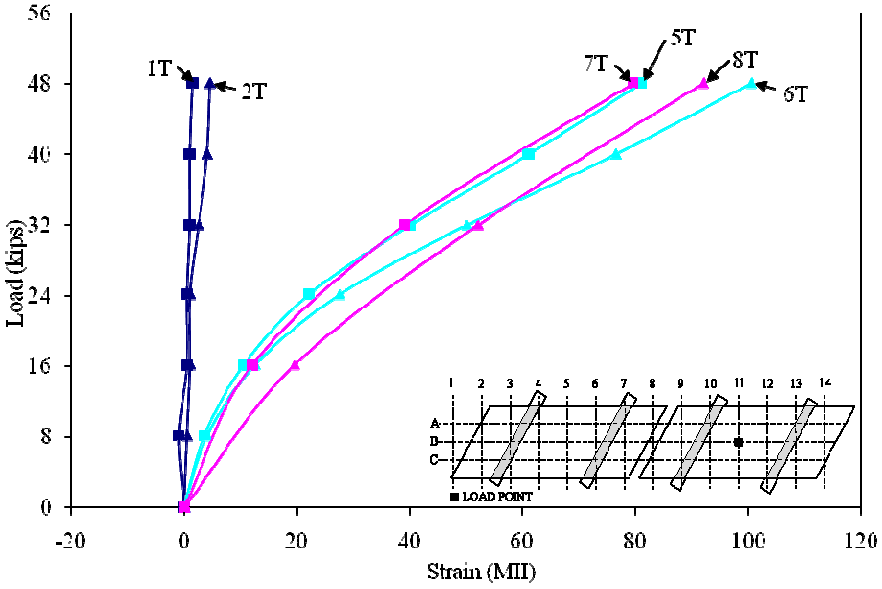

Figure 3.5. Steel strain versus load, load at B11, Panel 2.

Bottom bar strains were compressive and less than 20 MII and were not plotted for clarity. From Figure 3.5 one can see the top bars were in tension and the majority of the bending due to self weight occurred in Bars 5, 6, 7, and 8. The maximum steel strain measured during this test was 101 MII in Bar 6T.

Plotted in Figure 3.6 are deflections for a load varying from 0 to 48 kip at B11; locations of the deflections are shown in Figure 2.8. These deflection results are typical for tests with a load located between the support beams. For this load case, the cantilevered sections deflected upward (positive direction), and the loaded span deflected downward (negative direction). Each panel corner deflected a similar amount, with the deflections at P2-3 and P2-7 being slightly greater because these points were farther from the support than Points P2-1 and P2-5. The largest measured deflection (0.067 in.) was directly under the applied load.

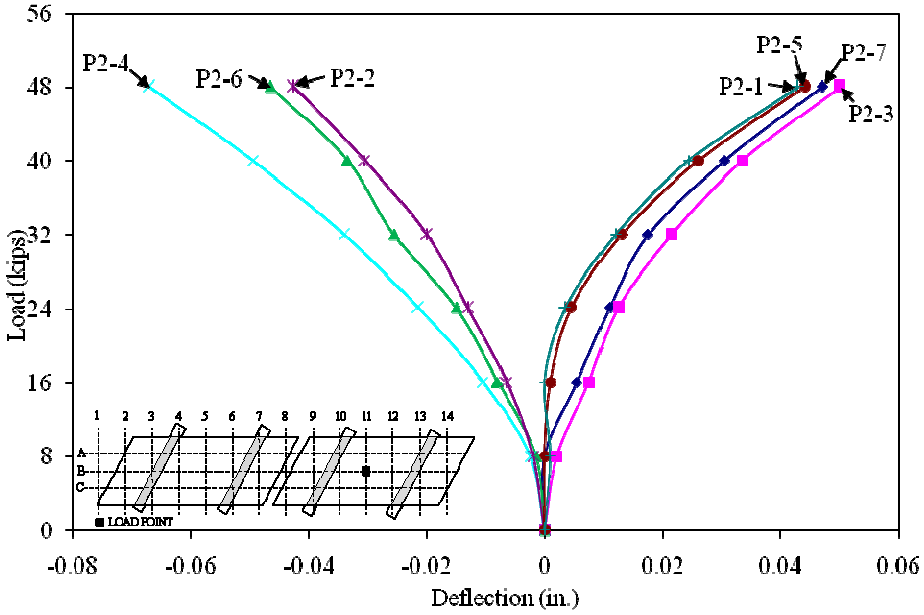

Figure 3.6. Deflection versus load, load at B11, no closure pour.

The largest concrete strain (-253 MII) for load varying from 0 to 48 kip at B11 occurred at P2-C8T. This strain was the closest to the applied load (1 ft - 9 ½ in. away). P2-C2T and P2-C3T are the second and third closest strains to the load, respectively, which agrees with the strains measured (-184 MII and -162 MII). P2-C4T was over 4 ft from the load, explaining why the strain was 2 MII. All concrete strains are presented in Figure 3.7 with locations of the strains shown in Figure 2.6. Concrete strains measured in the cantilever sections were less than 2 MII and therefore were not included in the figure for clarity.

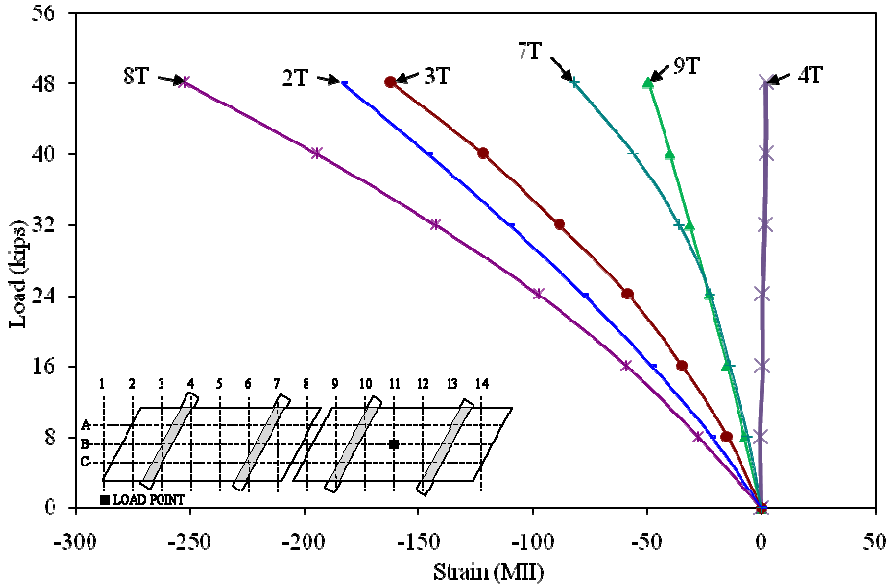

Figure 3.7. Concrete strains versus load, load at B11, Panel 2.

The largest changes in deflection for a single panel occurred with a load at B14. Deflections for a 0 kip to 32 kip load at this point are plotted in Figure 3.8. A 32 kip load was used for load at B14 because the panel began to rotate about the near support at loads greater than 32 kips. Point P2-3 deflected 0.433 in. under the 32 kip load.

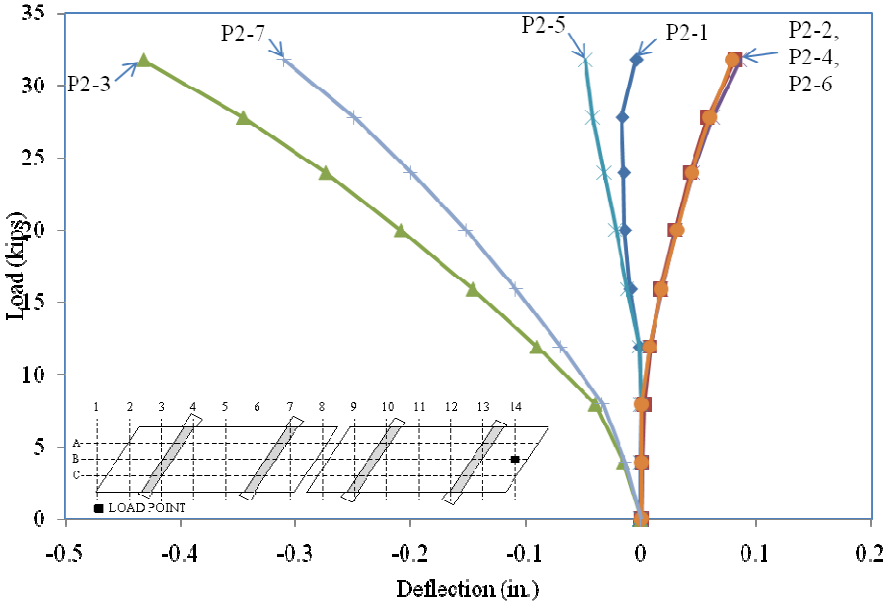

Figure 3.8. Deflection versus load, load at B14, no closure pour.

A comparison of the deflection of the individual panels with a load at B5 on Panel 1 and B11 on Panel 2 are plotted in Figure 3.9. Panel 1 was loaded 0 to 20 kips, while Panel 2 was loaded 0 to 24 kips. These load ranges were plotted because 20 kips was the maximum load applied at B5, whereas B11 was loaded to 48 kips in 8 kip increments. In order to plot the data over a similar load range and because data were not recorded at 20 kips, 24 kips was chosen as the maximum load to plot for B11. Locations of each measured deflection are presented in Figure 2.8. These results are presented to show that the two deck panels when loaded similarly responded essentially the same way; the deflections for the two panels are within 0.005 in.

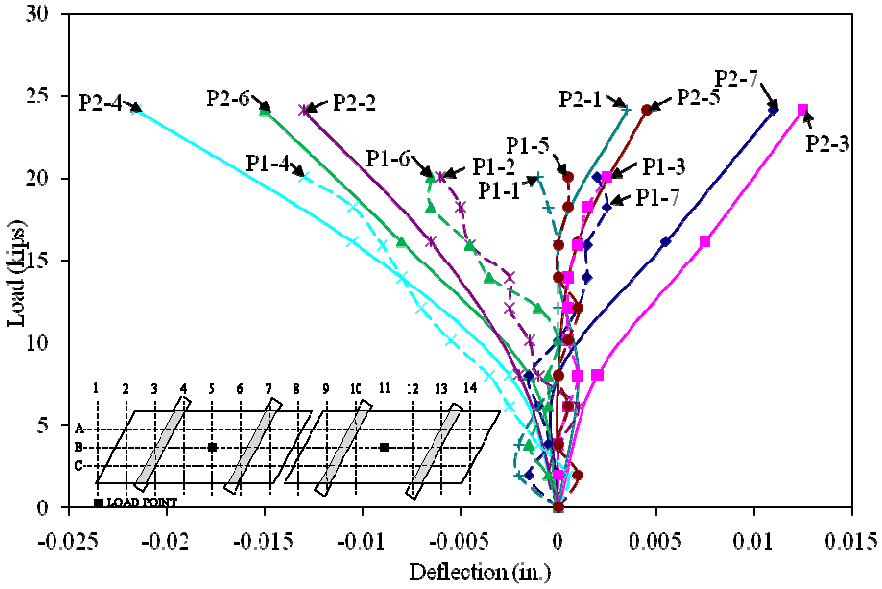

Figure 3.9. Comparison of deflection versus load results, for loads at B5 (on Panel 1) and B11 (on Panel 2).

3.6.2 Connected Panel Service Load Test Results

Nineteen points on the deck panels were loaded after the closure pour was cast (see Figure 2.24). These points were chosen to meet the test objectives stated in Section 2.8.2. The results for a load at B8 are presented to show the response of the closure pour to load. Plots illustrating the response of the system as a load moves longitudinally or transversely are also

shown, along with a plot showing deflections of the deck panels with and without the closure pour in place.

Steel strains measured for the closure pour hooked bars for a load 0 to 40 kips at B8 are plotted in Figure 3.10, and the locations of the strains are shown in Figure 2.7. Strain gages on Bars CP-S3T and CP-S5B were damaged when the closure pour was cast and no strain in these bars are shown in the plot. Bottom bars in a hook were in tension and top bars in compression during loading at B8. Bars experienced greater tensile strains than compressive strains because the bars were at different depths in the cross-section; bottom bars had 1 1/2 in. of clear cover and top bars had 2 1/4 in. of clear cover. The largest strain measured was 307 MII in Bar CP-S8B, which was located at the location of the load and is less than the yielding strain of 2069 MII.

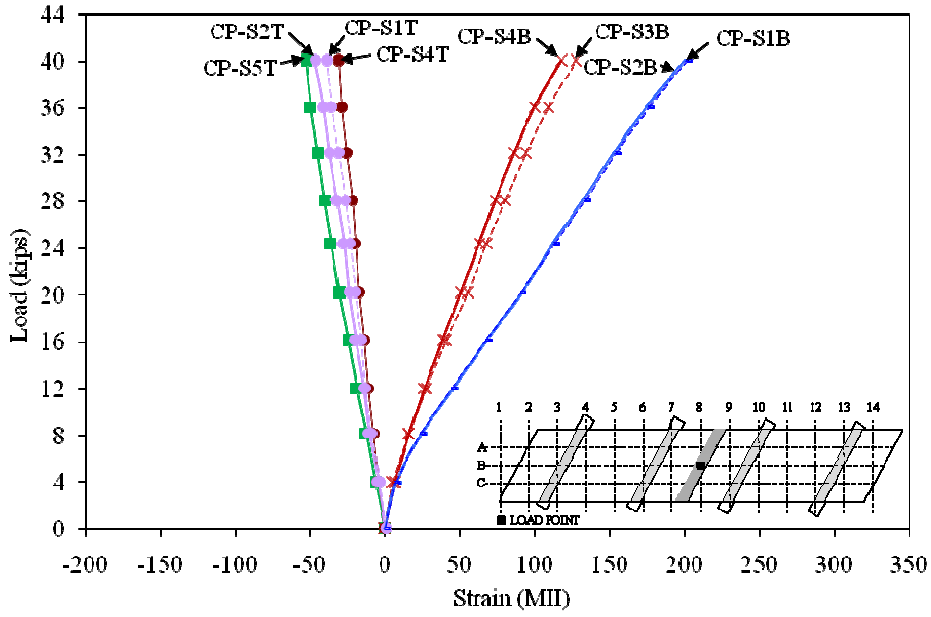

a) strains CP-S1 through CP-S5, top and bottom bars

Figure 3.10. Closure pour steel strains versus load, load at B8, closure pour in place.

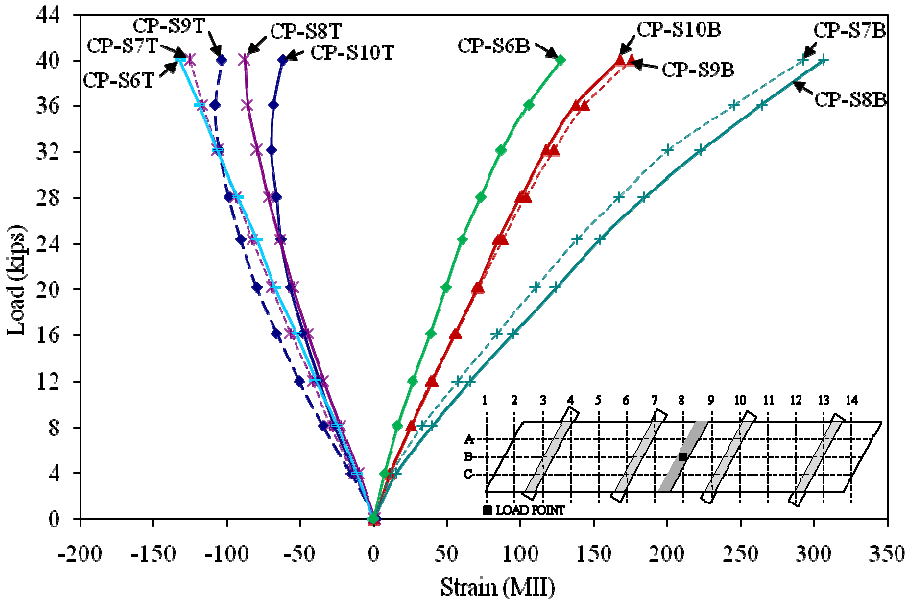

b) strains CP-S6 through CP-S10, top and bottom bars

Figure 3.10. Continued

Adjacent bars comprising a double hook had tensile strains within 15 MII, and bars in compression were within 45 MII of each other. One reason as to why the compressive strains varied more than the tensile strains is because the gages were wrapped in foil to protect them prior to placing concrete (see Figure 2.23) , the concrete may not have bonded as well to some of the bars. Therefore some bars had to carry a larger compressive force than other bars.

Bar P1-S8T was the only bar to experience a compressive strain for a 40 kip load at B8, and the strain was -20 MII. Reinforcing bars with strains greater than 20 MII are plotted in Figure 3.11; bars with strains less than 20 MII are not shown for clarity. Refer to Figure 2.7 for the locations of the bars. The largest strain was 278 MII and occurred in Bar P2-S2T, a top bar. Top bars experienced larger strains than bottom bars because the panel had negative bending over the support beam, therefore subjecting the top bars to larger strains than the bottom bars; top bars were at a different depth in the cross-section than bottom bars due to panel leveling. All of the reinforcing steel strains were less than the yielding strain of 2069 MII.

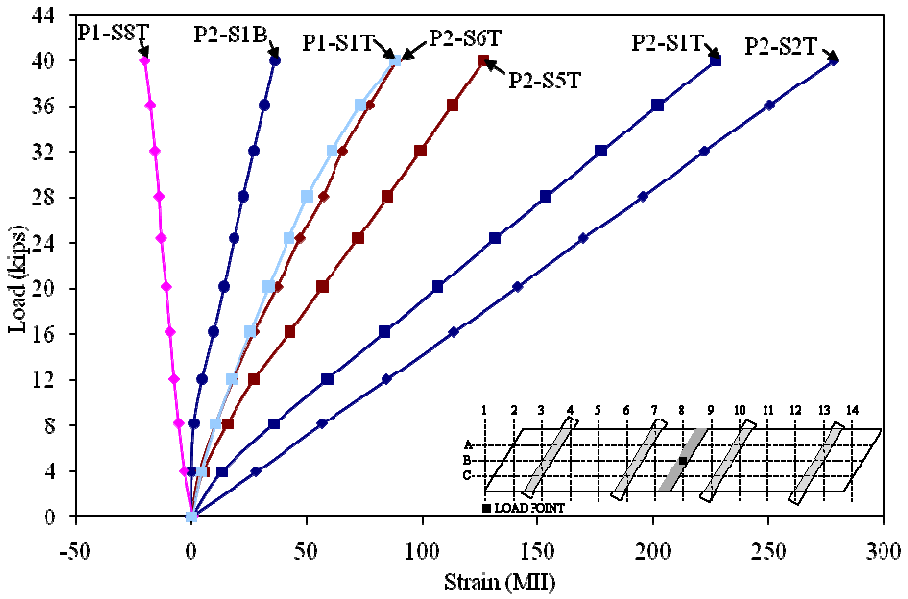

Figure 3.11. Steel strain versus load, load at B8, closure pour in place.

A plot of concrete strains versus load for a 40 kip load applied at B8 is shown in Figure 3.12. Locations of each strain can be seen in Figure 2.6. The largest strains occurred in the closure pour concrete; strains in the top surface of the closure pour were compressive and strains in the top surface of the deck panels were tensile. Deck panel strains were less than 16 MII. Location CP-C2T experienced the largest strain (286 MII). All of the strains were less than 3000 MII, which is the maximum useable strain at the extreme concrete compression fiber specified by the American Concrete Institute (ACI) Building Code Requirements for Structural Concrete (2005). Greater strains were experienced at CP-C2T than CP-C1T even though the gages were the same distance from the load because of the skew of the deck panels.

Deflections due to a 40 kip load at B8 are plotted in Figure 3.13; the locations of the deflections are given in Figure 2.8. Deck panel deflections were less than 0.002 in. and not included in the plot for clarity. CP-2 was at the applied load and underwent the largest deflection, 0.051 in.

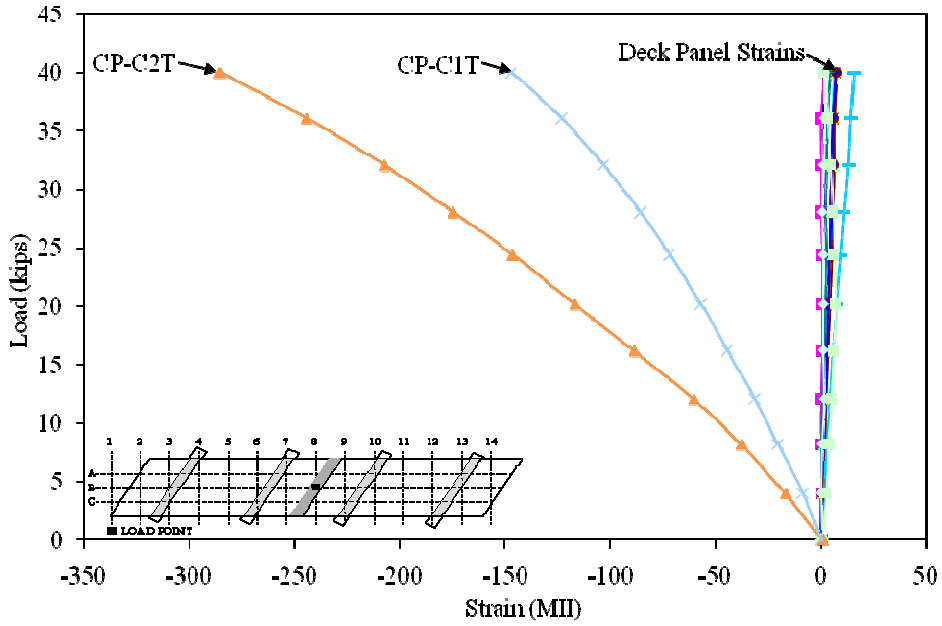

Figure 3.12. Concrete strains versus load, load at B8, closure pour in place.

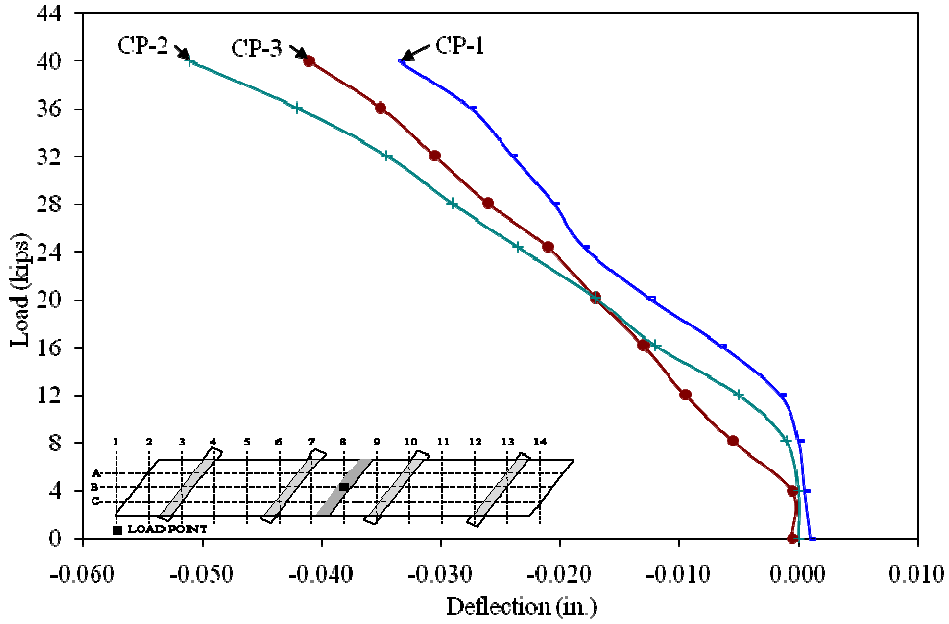

Figure 3.13. Deflection versus load, load at B8, closure pour in place.

Graphs of the change in deflection as a 16 kip load moved along Line B are presented in Figure 3.14. Results for a 16 kip load are plotted because this load is equivalent to a HS 20-44 wheel load. Changes in deflection near the load were the largest; deflection changes of unloaded

spans were less than 0.005 in. For example, from Figure 3.14a one can see that as the load moved from Panel 1 to Panel 2 (B1 to B14) the deflection of points on Panel 1 changed 0.002 in. or less.

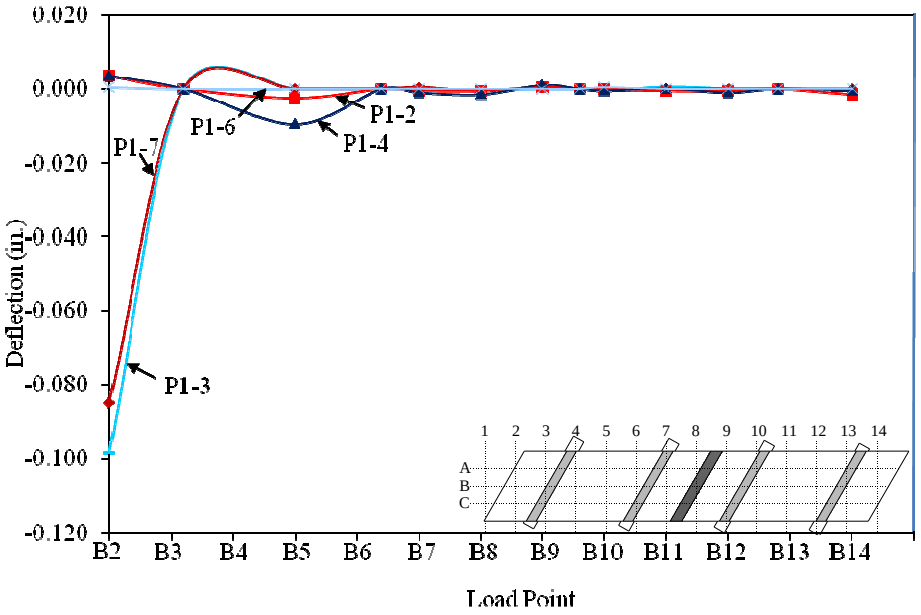

a) Panel 1 deflections

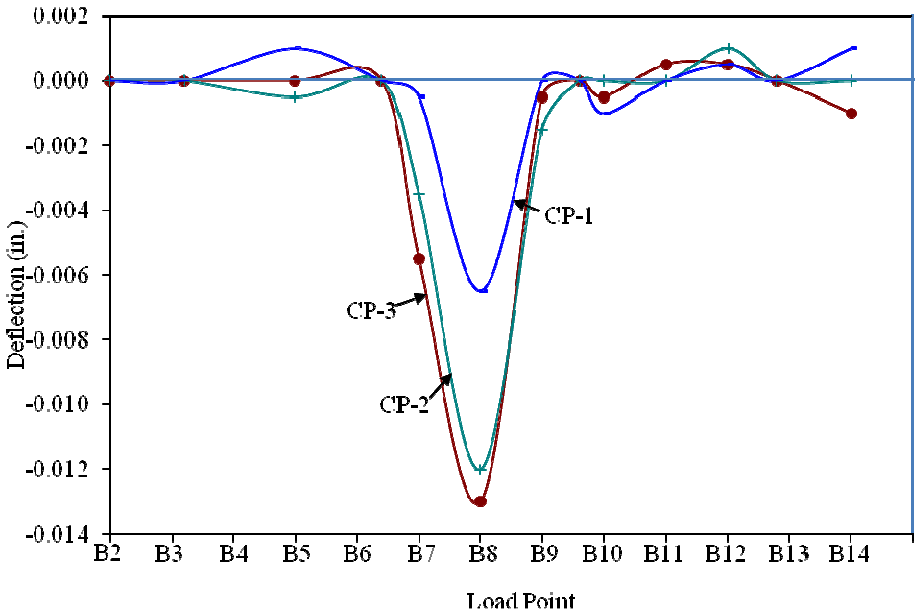

b) closure pour deflections

Figure 3.14. Deflection of the deck panels as a 16 kip load moved across grid Line B.

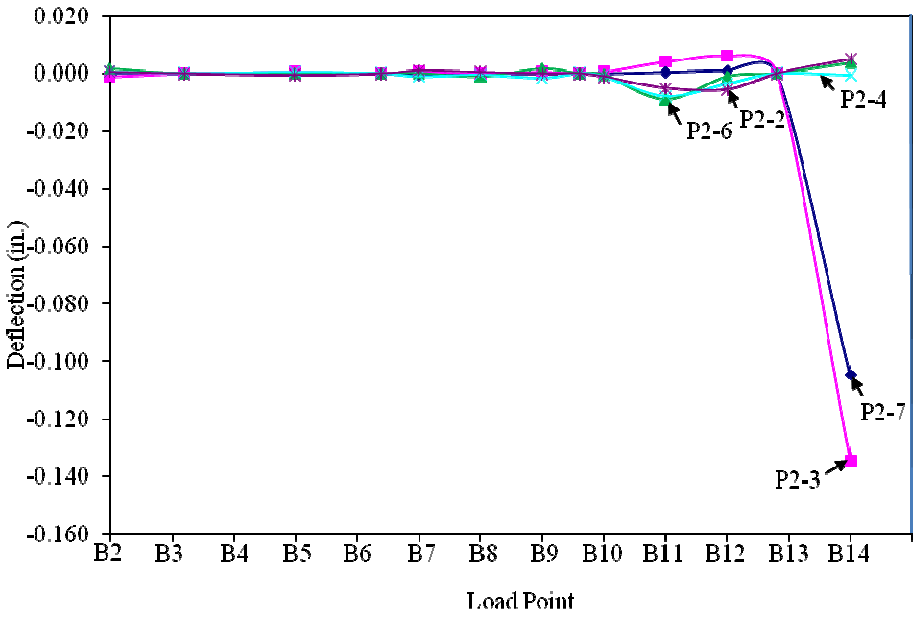

c) Panel 2 deflections

Figure 3.14. Continued

The largest change in deflection occurred when the cantilever section was loaded. These are load points B2 and B14. Point P2-3 underwent the largest deflection change, 0.135 in. (see Figure 3.14c). Deflections for the deck panel spanning between the support beams had a maximum value of 0.017 in.

Presented in Figure 3.15 are the deflection changes experienced as a 40 kip load moved from load point A11 to C11 along grid Line 11. Locations of load points can be seen in Figure 2.24 and locations of deflection are shown in Figure 2.8. Changes in deflection of Panel 1 were less than 0.002 in. and excluded from the plot for clarity. As one would expect, the cantilevered section of the deck panel (P2-3 and P2-7) deflected upward (positive) and the loaded portion of the deck panel (P2-2, P2-4, P2-6) deflected downward (negative). Deflections for the cantilevered section were independent of the location of the load, as the deflection changed 0.002 in. among the three load points. The stiffness of the closure pour was apparent in this test, as deflection changes of the closure pour were a maximum of 0.002 in.

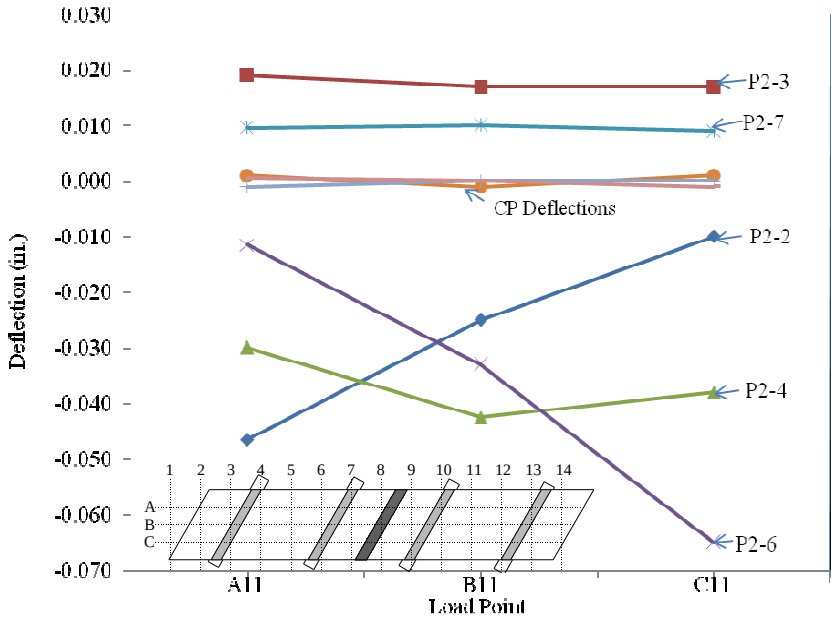

Figure 3.15. Deflection of the deck panels as a 40 kip load moved along grid line 11.

Another observation from Figure 3.15 is the loaded span responded as expected. When the load was at A11, P2-2 experienced the greatest deflection, and the deflection at this point decreased as the load moved to C11. P2-4 deflected the most when the load was above this point (at B11) and deflected approximately the average of the P2-2 and P2-6 deflections for load points A11 and C11. Point P2-6 deflected the least of P2-2, P2-4, and P2-6 when the load was at A11, and the deflection increased as the load moved along Line 11.

A plot of deflections for a load at point B11 for the individual and connected panels is shown in Figure 3.16. From these plots, one can see the effect the closure pour had on the system. Every deflection decreased after the closure pour was cast, with the greatest changes occurring at the cantilevered sections of the deck panel. Deflections at P2-7, located at a corner of the cantilevered deck panel, decreased by 0.02 in. after the closure pour was cast. In Figure 3.16, deflections CP-1 and P2-5, along with CP-3 and P2-7, are at approximately the same location and can be compared. Casting the closure pour resulted in a decrease of 0.025 in. in deflections at the locations.

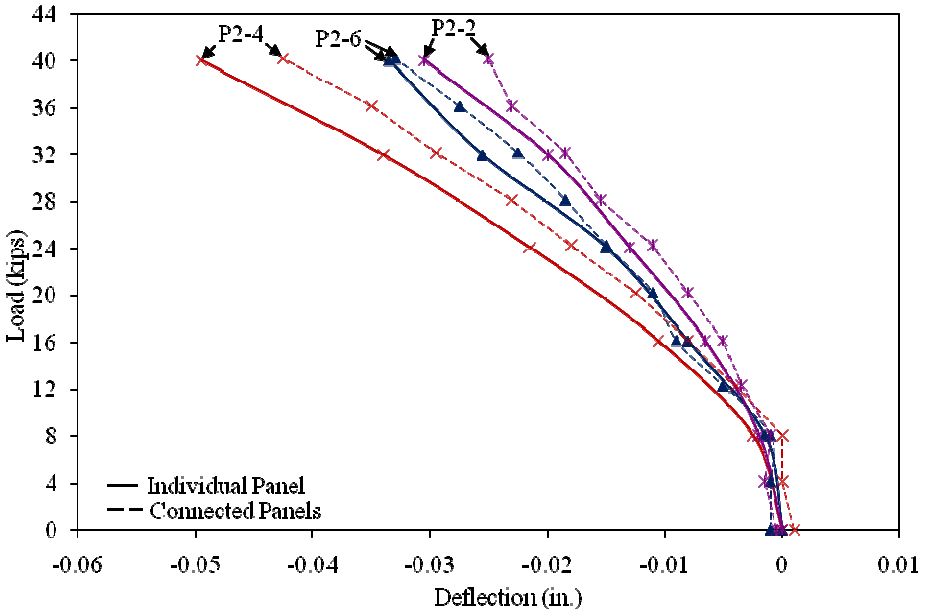

a) deflections P2-2, P2-4, and P2-6

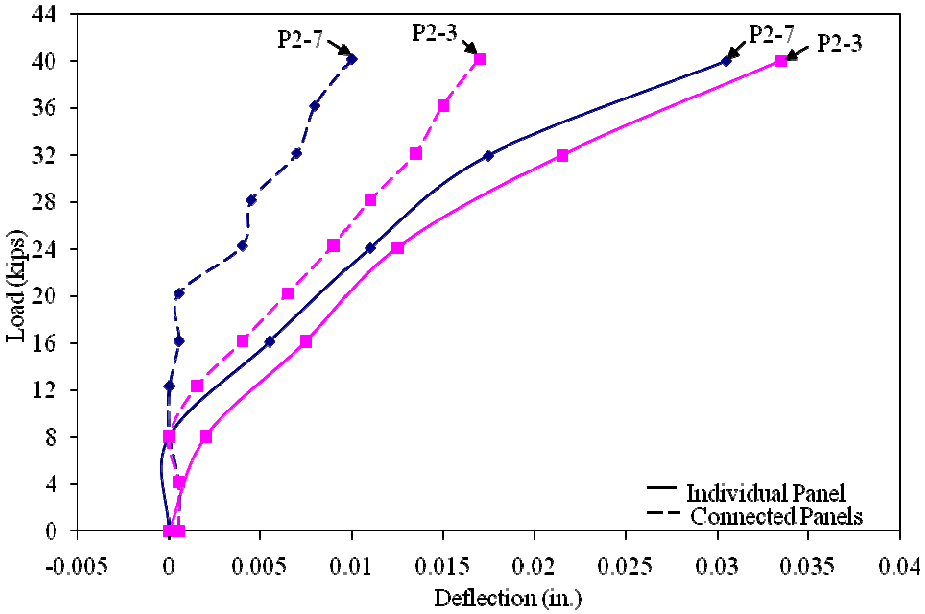

b) deflections P2-3 and P2-7

Figure 3.16. Deflections for load point B11 before and after casting the closure pour.

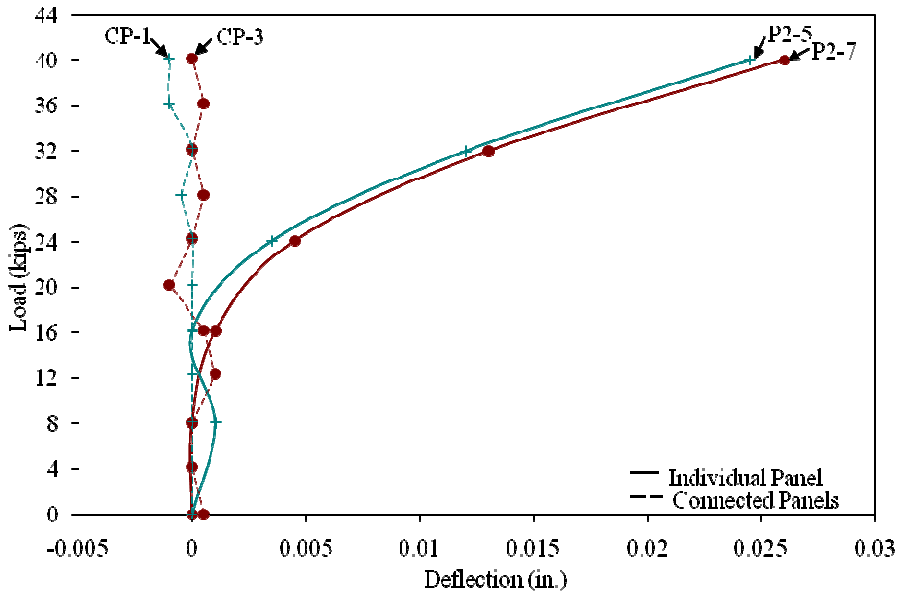

c) deflections P2-5, P2-7, CP-1, and CP-3

Figure 3.16. Continued

3.7 Ultimate Strength Results

Results for the ultimate strength tests are presented in the following sections. A single panel was tested to its ultimate flexural strength. Strength testing on connected panels included testing to the following failures: punching shear; combined punching shear and flexure; and flexure.

3.7.1 Single Panel Ultimate Test Results

Photographs of a single panel tested to failure are presented in Figure 3.17. A line load was applied to the deck panel, and a flexural failure occurred at a load of 153 kips. Concrete that spalled from the deck panel surface is visible in Figure 3.17a. In Figure 3.17b one can see flexure cracks propagating up the side of the deck panel.

Two values for the experimental moment due to the line load were calculated; this was done because the fixity provided by the supports was unknown. The first value assumes the support beams acted as pinned supports and the second value assumes fixed supports. The

a) deck panel after loading

b) flexure cracks

Figure 3.17. Flexural failure of the single deck panel tested.

experimental moment was 368 ft-kips when the supports were treated as pinned and 184 ft-kips when fixed. These values bracket the theoretical strength of 263 ft-kips, calculated using strain compatibility equations. Because the theoretical strength lies between the pinned moment and fixed moment, the support beams provided a fixity between pinned and fully fixed. Theoretical and experimental flexural strengths for a single deck panel are presented in Table 3.7.

Table 3.7. Single panel flexural strengths.

Flexural Capacity	Capacity (ft-kips)
Theoretical	263
Experimental (for pinned supports)	368
Experimental (for fixed supports)	184

The largest concrete strains occurred along the axis of bending. Concrete strains are plotted in Figure 3.18 for a load to 150 kips, and the location of each strain is shown in Figure 2.6. Point P3-C8T experienced the largest strain (-3919 MII). This strain exceeds the strain value of -3000 MII specified by ACI as the maximum useable strain at the extreme concrete compression fiber. P3-C3T experienced -2969 MII of strain, and all other strains were less than -700 MII.

Deflections experienced during the test for a load up to 150 kips are plotted in Figure 3.19, and locations of each deflection are shown in Figure 2.8. Deflections of the loaded span of the panel were downward (negative), and deflections of the cantilevered sections were upward (positive). P3-4 was at midspan at the location of the applied load and therefore experienced the largest deflection, 0.95 in. at failure. Location P3-6 had a greater deflection change than P3-2 because of the skew of the deck panel. Point P3-3 deflected 1.24 in. upward and experienced the largest deflection during the test.

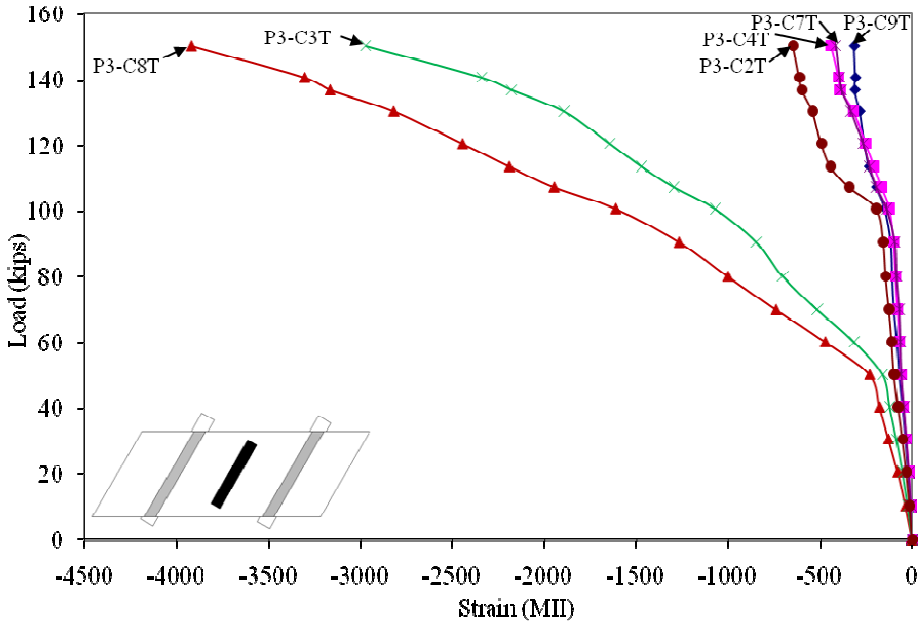

Figure 3.18. Concrete strain versus load for single panel ultimate load test.

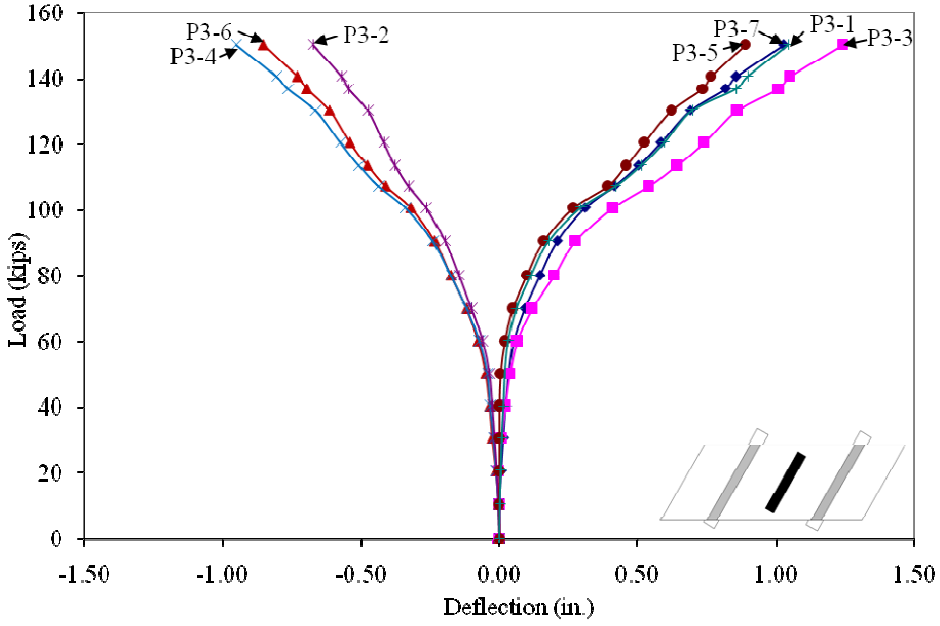

Figure 3.19. Deflection versus load for single panel ultimate load test.

3.7.2 Nine Inch Square Footprint Results

A punching shear failure of the deck panel occurred at a load of 150 kips; photographs of the deck panel from above after failing in punching shear are presented in Figure 3.20. The failed concrete has been removed to show the reinforcing steel in Figure 3.20b. Inspection of the deck panel after failure occurred showed the reinforcing steel had been pushed downward and caused strips of the concrete to spall from the underside of the deck panel (Figure 3.20c).

The theoretical punching shear was calculated using concrete shear strength equations published by ACI (2005). A concrete compressive strength equal to 7,600 psi (from the concrete strength testing) was used to determine the theoretical punching shear strength. The experimental shear force was 146 kips, which exceeded the theoretical strength of 135 kips by 8%. Theoretical and experimental punching shear capacities are presented in Table 3.8.

a) top view of punching shear failure footprint

Figure 3.20. Photographs of the deck panel after a punching shear failure.

b) top view after concrete removal

c) underside of the deck panel

Figure 3.20. Continued

Table 3.8. Punching shear capacity.

Capacity	Shear Force (kips)
Theoretical	135
Experimental	146

Concrete strains experienced during loading were measured for loading up to 140 kips and are plotted in Figure 3.21; locations for each strain are shown in Figure 2.6. Strains were recorded only to 140 kips because failure occurred prior to the next automated reading by the DAS. Strain gages at concrete strain locations on Panel 1 did not measure the strain accurately and are excluded from the plot. Strains were the largest in the closure pour, reaching -1101 MII prior to failure. This value was less than -3000 MII, which is specified by ACI as the maximum useable strain at the extreme concrete compression fiber. The maximum strain measured in Panel 2 was 118 MII.

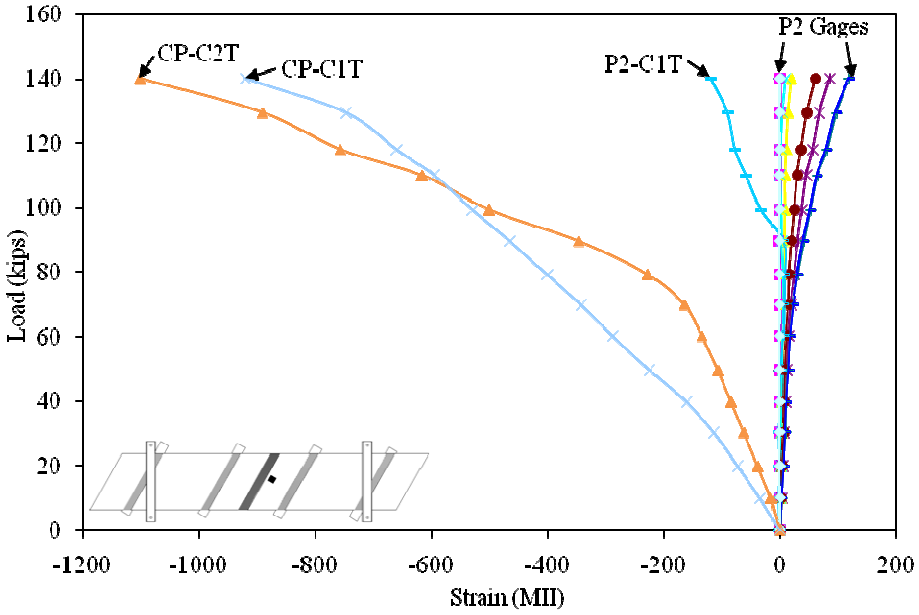

Figure 3.21. Concrete strain versus load for 9 in. square footprint loading.

A maximum steel strain experienced during testing was a tensile strain of 1740 MII. This strain is equivalent to a stress of 50 ksi, which is less than the bar yield stress of 60 ksi. Steel

strains for the closure pour hooked bars are presented in Figure 3.22 for loading to 140 kips. Locations for each strain are shown in Figure 2.7. As expected, the bottom bars of each hook were in tension throughout the test. Half of the top bars started as compression reinforcement and carried tension by the end of the test as a result of the concrete cracking and the depth of the compression zone in the concrete decreasing.

Strains in the reinforcing steel of the longitudinal channels are plotted in Figure 3.23 for loading to 140 kips. Strains less than 140 MII were excluded from the graph for clarity, and the location of each plotted strain is shown in Figure 2.7. From the figure, one can see the Panel 2 reinforcement carried more load than the Panel 1 reinforcement, as only one instrumented bar on Panel 1 experienced over 140 MII. This load distribution would be expected because the load was closer to the Panel 2 bars. All of the bars were in tension as the panel underwent negative bending about the support, and the top bars experienced the largest strains. The largest strain was 1158 MII in Bar P2-S2T.

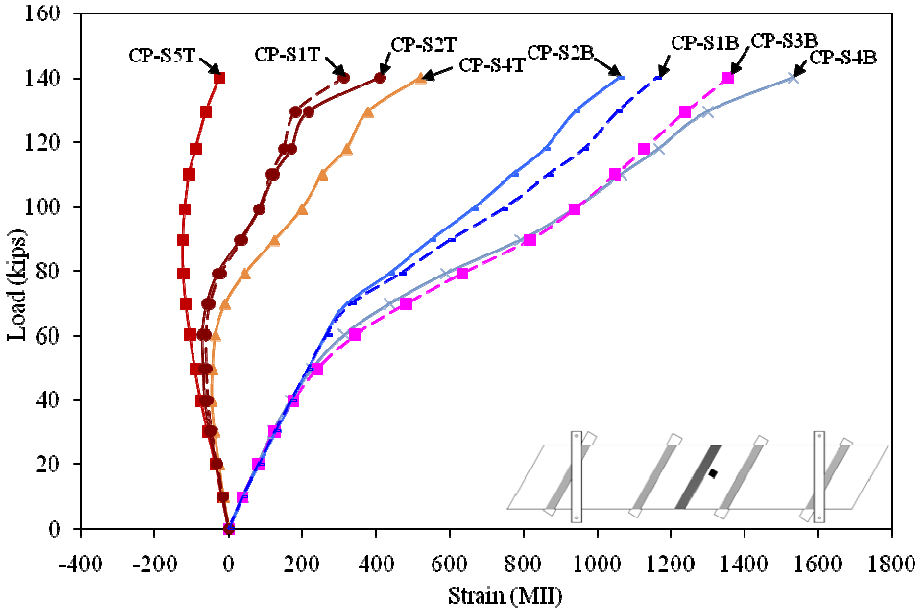

a) strains CP-S1 through CP-S5, top and bottom bars

Figure 3.22. Closure pour steel strain versus load for 9 in. square footprint loading.

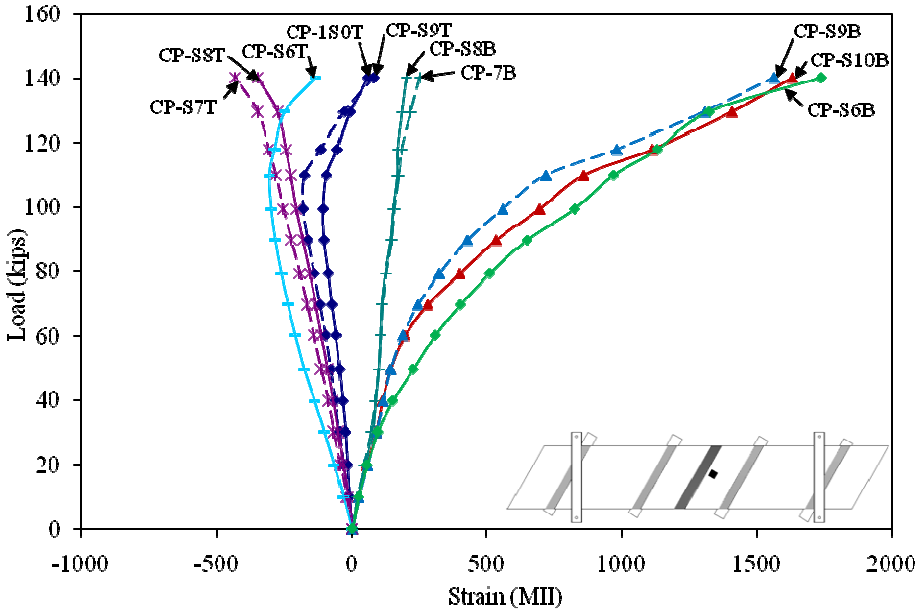

b) strains CP-S6 through CP-S10, top and bottom bars

Figure 3.22. Continued

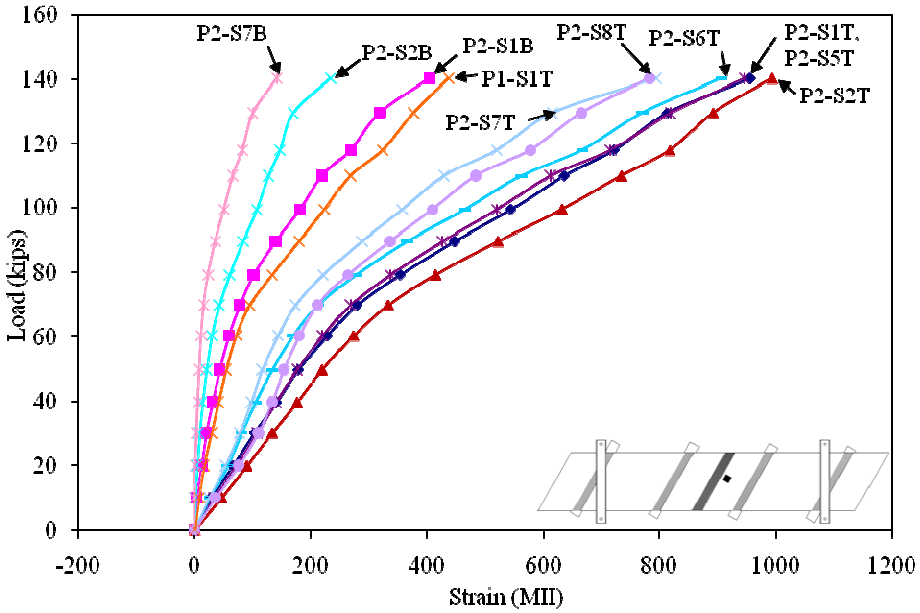

Figure 3.23. Steel strain versus load for 9 in. square footprint loading.

Deflections for the 9 in. square footprint test show the closure pour was stiffer than the rest of the deck panels. The maximum deflection measured for the closure pour was 0.02 in. and was 0.032 in. for a non-cantilevered section of the deck panels, even though the load was applied

next to the closure pour. Plotted in Figure 3.24 are deflections experienced for loading up to 140 kips at the locations shown in Figure 2.8. Changes in deflection at P1-2 and P2-2 were less than 0.002 in. and were not plotted for clarity. These deflections were less than anticipated due to the nearby restraining beam limiting the positive deflection of the deck panels. When observing the data, one will notice the deflections had a sudden increase in the positive direction for loads between 80 kips and 100 kips. This sudden change in the deflections could not be explained by the researchers, as nothing abnormal was observed during testing and the strain data for the concrete and reinforcing bars does not exhibit a similar response.

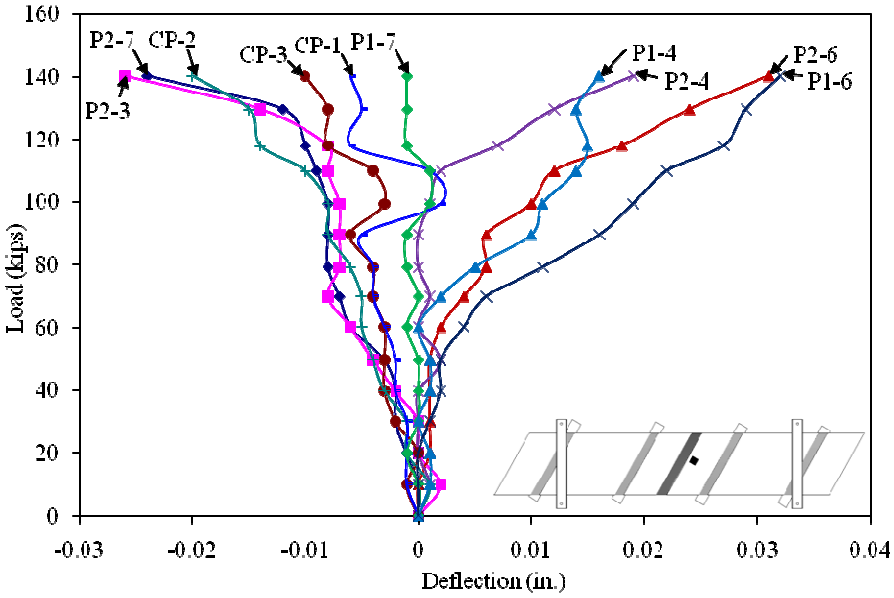

Figure 3.24. Deflection versus load for 9 in. square footprint loading.

3.7.3 Tandem Wheel Footprint Results

Failure occurred at a load of 157 kips do to a combination of punching shear and flexure. Figure 3.25 is a photograph of the deck panel failure caused by the tandem wheel footprint. In this figure, the concrete that failed around the footprint due to punching shear can be seen, along with the concrete that spalled from the surface due to bending.

Figure 3.25. Punching shear and flexure failure due to tandem wheel footprint.

Provided in Table 3.9 are the theoretical and experimental flexure and shear capacities of a deck panel for loading by a tandem wheel footprint. Experimental values were calculated with statics, theoretical flexure strength from strain compatibility equations, and punching shear strength from equations in ACI Building Code Requirements for Structural Concrete (2005). A comparison of the values shows the applied moment (298 ft-kips) exceeded the theoretical flexural strength (263 ft-kips) by 14%. One reason for this is the support beams provided some restraint, reducing the applied moment by providing additional fixity. Also of note is the applied shear (150 kips) was 80% of the theoretical punching shear capacity (188 kips), yet a punching shear failure occurred. The punching shear capacity may have been reduced because of the flexural cracks reduced the depth of concrete available to resist punching shear.

Table 3.9. Theoretical and experimental capacities for the tandem wheel footprint test.

Failure Mode	Strength
Theoretical Punching Shear	188 kips
Applied Punching Shear	150 kips
Theoretical Flexural	263 ft-kips
Applied Moment	298 ft-kips

Closure pour hooked bar steel strain values were low, with the maximum strain being 342 MII. This strain is equivalent to a stress of 10 ksi, which is significantly below the yielding stress of 60 ksi for the hooked bars. Steel strains experienced in the closure pour hooked bars are plotted in Figure 3.26 for loads up to 149 kips; refer to Figure 2.7 for the location of each strain. Strains are only plotted to a load of 149 kips because failure occurred prior to the next automated DAS recording. Any strain less than 30 MII was excluded from the plot for clarity. The plot also shows the top bars were in tension and the bottom bars in compression, meaning negative bending occurred at the closure pour.

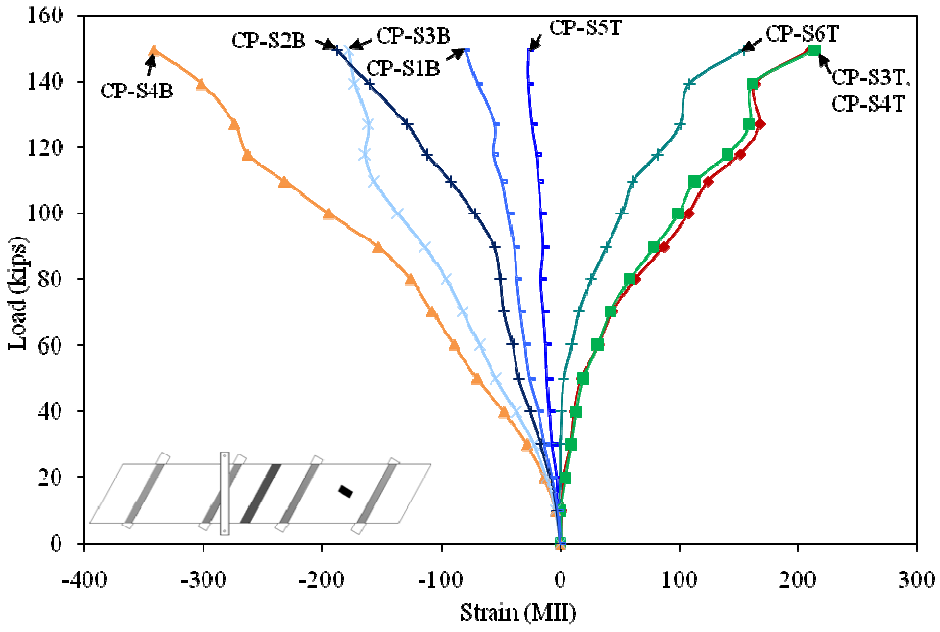

Figure 3.26. Closure pour steel strain versus load for tandem wheel footprint.

Mild reinforcement bar strains for loading to 149 kips are shown in Figure 3.27, and the locations of each strain are presented in Figure 2.7. Excluded from the figure for clarity were the strains in the Panel 1 bars, which all were less than -100 MII. Panel 2 strains were tensile, with the top bar strains greater than the bottom bar strains by 800 MII on average. The strain in the

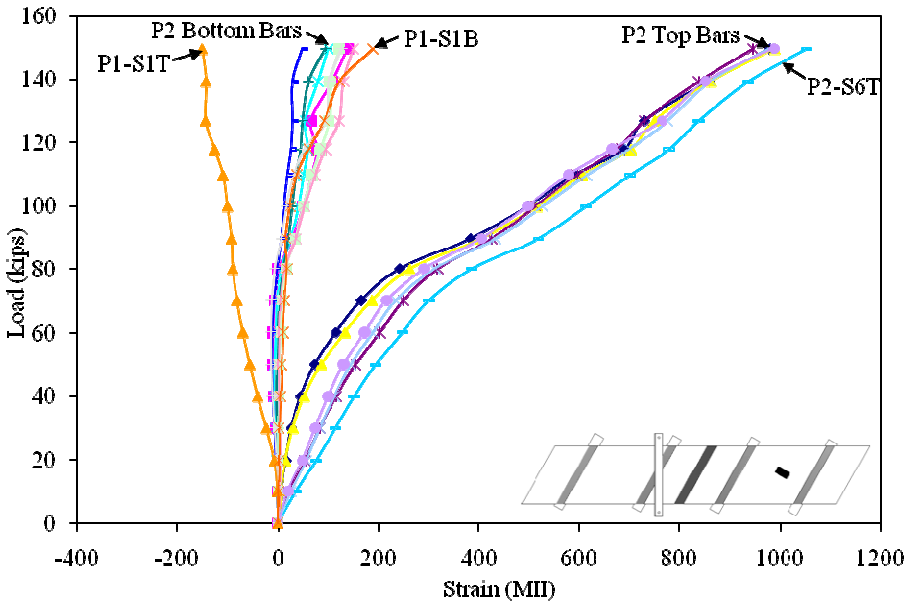

Figure 3.27. Steel strain versus load for tandem wheel footprint test.

top bars of Panel 2 was similar in magnitude, showing load was distributed equally throughout the deck panel. Bottom bar strains were less than 200 MII of strain. Point P2-S6T experienced the largest strain (1054 MII) which is equivalent to a stress of 31 ksi.

The highest concrete strain (-2163 MII) was at P2-C3T, which was closest to the applied load. P2C8T was located on the axis of bending for the deck panel, which explains why the strain experienced at this point was the second largest even though P2-C9T was located closer to the load. The low strains in the closure pour verify the steel strains previously discussed and that a low portion of the load was transferred to that section of the deck panel system. All the concrete strains experienced during the tandem wheel footprint test for loading to 149 kips are plotted in Figure 3.28, and locations for each strain plotted are given in Figure 2.6. Strains in Panel 1 were not plotted because the gages malfunctioned, and strains in Panel 2 and the closure pour that were less than -165 MII were excluded for clarity.

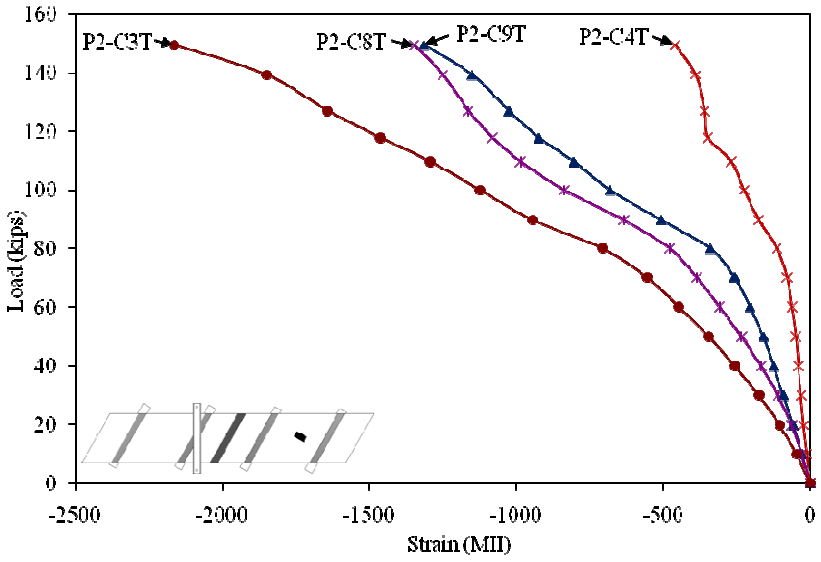

Figure 3.28. Concrete strain versus load for tandem wheel footprint loading.

Deflections at the locations shown in Figure 2.8 are plotted versus loading to 149 kips in Figure 3.29. Panel 1 deflections were less than 0.007 in. and were not included in the plot for clarity, along with the deflection at CP-2, which had the transducer removed after the 9 in. footprint test. The cantilevered section adjacent to the loaded span deflected upward 1.11 in., and the loaded span deflected downward 0.078 in. Point P2-2 had a greater deflection change than P2-6, a result due to the skew of the deck panels.

3.7.4 Line Load Results

A photograph of the deck panel failure due to an applied line load is shown in Figure 3.30; Figure 2.29 presents the location of the applied load. The deck panel failed due to flexure at an applied load of 196 kips. This load is equivalent to a moment of 372 ft-kips, which exceeds the theoretical flexural strength of 263 ft-kips. These values are given in Table 3.10. The applied moment value was calculated by using statics and treating the deck panel system as a simply supported continuous beam. However, the support beams supply some restraint against rotation, which was shown in the single panel test. Strain compatibility was used to calculate the theoretical flexural strength of the deck panel.

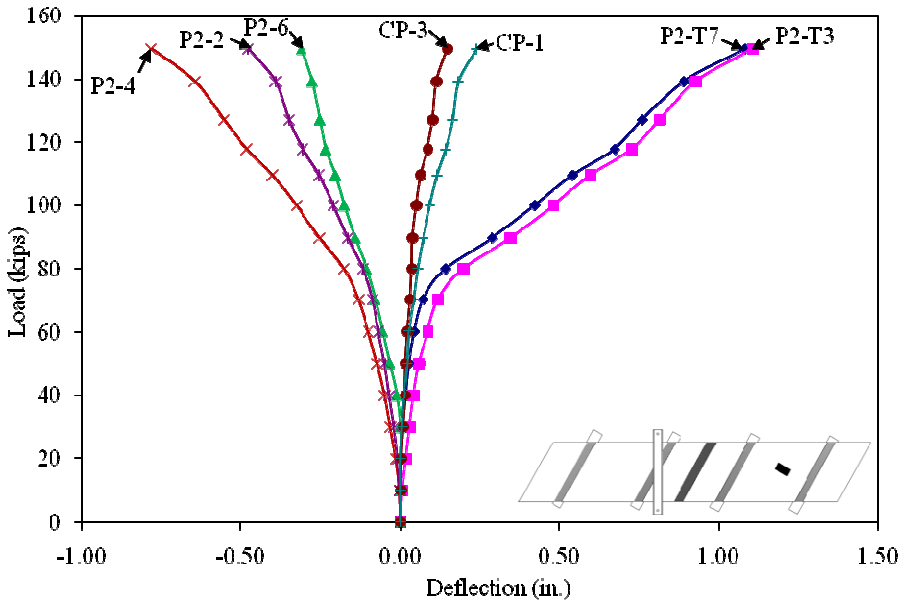

Figure 3.29. Deflection versus load for tandem wheel footprint loading.

Figure 3.30. Flexural cracking in deck panel due to applied line load.

Table 3.10. Deck panel moment capacities.

Failure Type	Capacity (ft-kips)
Theoretical Flexure	263
Applied Moment	372

Tensile strains in the closure pour steel were less than 310 MII, and compressive strains were less than -100 MII. Every top bar was in tension, while half the bottom bars were in compression and half in tension. The maximum strain experienced was 303 MII, which is equivalent to a stress of 9 ksi. Closure pour steel strains are plotted in Figure 3.31 for loading to 189 kips, and locations for each strain are shown in Figure 2.7.

Plots of concrete strains and steel strains for the post-tensioning channel reinforcement are not provided for this test. Concrete strain gages on Panel 1 malfunctioned, and strains for Panel 2 and the closure pour were less than 100 MII. Panel 1 steel strains also were not measured correctly, so these strains were discarded.

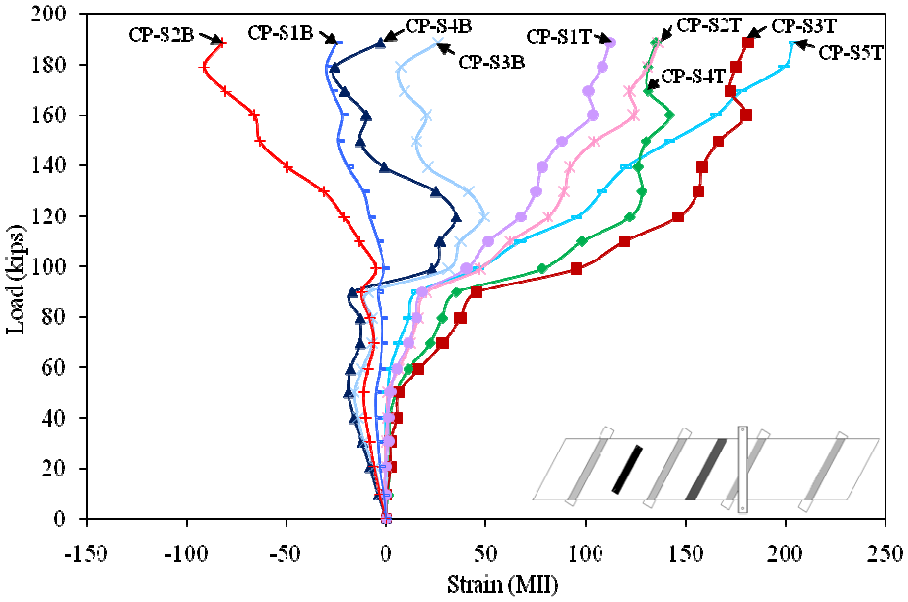

a) CP-S1 through CP-S5, top and bottom bars

Figure 3.31. Closure pour steel strain versus load for applied line load.

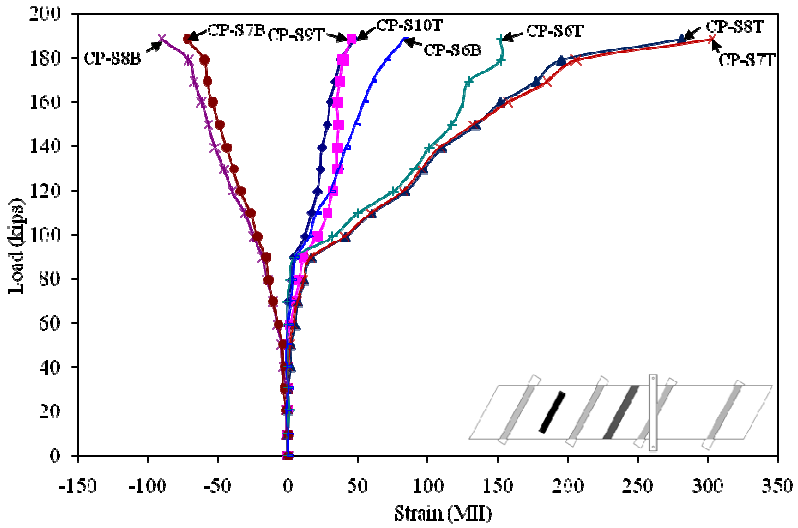

b) CP-S6 throught CP-S10, top and bottom bars

Figure 3.31. Continued

Deflections experienced during this test are plotted for loading up to 189 kips in Figure 3.32, and locations of each deflection are given in Figure 2.8. Deflections along the closure pour and Panel 2 were less than 0.08 in. and were excluded from the plot for clarity. As one would expect, the loaded span deflected the most, with the panel deflecting 0.808 in. at midspan. Points P1-2 and P1-6 deflected different amounts because of the skew of the deck panels. The cantilevered portion of the deck panel deflected upward, with P1-3 deflecting 0.139 in.

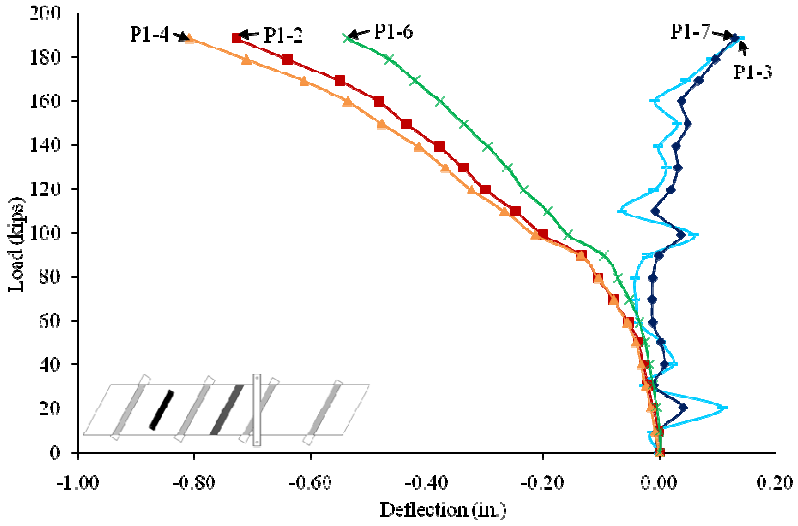

Figure 3.32. Deflection versus load for applied line load.

4. SUMMARY, CONCLUSIONS, AND RECOMMENDATIONS

4.1 Summary

Three deck panels were obtained from Andrews Prestressed Concrete, Inc. for laboratory testing. Testing included determining the concrete strength of the deck panels, determination of the stress in the mild reinforcing due to the prestressing force, determining strains in the panels while lifting them with a crane, determining the strains in the panels while leveling them, observation of the concrete flow through a model of the longitudinal post-tensioning channel, service load testing of individual panels and two panels with the closure pour in place, and ultimate strength testing of a single panel and connected panels.

4.1.1 Concrete Strength Testing Summary

Three concrete cores were removed from one deck panel after the conclusion of testing and tested to determine the compressive strength of the concrete. The strength of the cores was assumed to be representative of the three deck panels. Cores were found to have an average strength of 7,600 psi, which exceeds the specified compressive strength of 5,000 psi by 27%.

4.1.2 Stresses in Mild Reinforcing Due to Prestressing

Strains in six mild reinforcing bars were measured while the prestressing strands in one longitudinal channel were cut. Stresses in five of the six bars were less than the theoretical compressive stress with prestressing losses considered of 20.7 ksi. Bar 2B had the largest stress (21.5 ksi), exceeding the theoretical compressive stress minus losses by 4%. The lowest stress was found in Bar 2T (13.0 ksi), 37% less than the theoretical compressive stress considering losses.

The average stress in the top and bottom bars was calculated and compared. Top bars were found to be under an average compressive stress of 14.2 ksi. Bottom bars experienced an

average compressive stress of 17.9 ksi. Both of these values were less than the theoretical compressive stress minus prestressing force losses which was 20.7 ksi.

4.1.3 Lifting Panel Strain Summary

Temporary strains induced in the mild reinforcement in the longitudinal post-tensioning channels were measured during the crane lifting tests. Two different strap configurations were used to lift a deck panel, and the panel was lifted twice for each setup. The first configuration used four straps, with each strap wrapped around two groups of bars (see Figure 2.12). Bar 2T experienced a strain of -278 MII, the largest strain during this test. When added to the strain induced in the bar due to prestressing, the total strain at a point was -1457 MII. If this strain is compared to the yield strain of the bar, 70% of the bar strain is utilized.

Lifting configuration two used two straps to lift a deck panel, with one strap wrapped around all the bars in the bottom layer of a post-tensioning channel (see Figure 2.13). Bar 2B experienced the largest strain during this test, 231 MII. Bar 1B experienced the largest compressive strain, and therefore was under the largest total strain when strains due to the prestressing force are included. The total strain for this bar at the point the strain gage was applied was -1356 MII. When compared to the yield strain for 60 ksi steel, 66% of the total strain was utilized.

The utilization of bars for the four lifting strap test ranged from 45% to 70%; utilization for the two lifting strap configuration ranged from 46% to 66%. These results show the strains in the bars essentially did not vary with the two strap configurations tested.

4.1.4 Leveling Test Summary

A deck panel was leveled in the laboratory to the slope required in the field bridge. Eight additional tests were conducted to determine the deck panel’s response to various slopes, with

strains experienced in the mild reinforcing bars recorded during the testing. A strain of -595 MII was experienced in Bar 2T, and was the largest strain in any bar during testing. If axial strains due to the prestressing force are included, 86% of the bar strain was utilized.

4.1.5 Longitudinal Post-Tensioning Channel Concrete Placement Test Summary

A model of the post-tensioning channel was created to observe the flow of concrete through the channel in a laboratory setting. The model provided a worse-case scenario for flow, as the stirrups and mild reinforcement were at a lower height than would be encountered in the field due to panel leveling. Concrete was observed to flow around all of the steel in the channel and leave no void spaces.

4.1.6 Service Load Test Summary

Service load testing was conducted on an individual panel and on two connected panels. Loads on the individual panels ranged from 20 kips on cantilevered portions to 48 kips on the interior span. A 9 in. square footprint was used to apply the load. Load was applied at eight points on Panel 1 and 14 points on Panel 2 (see Figure 2.21). Application of load to eight of the same points on the two panels allowed for comparison of results. Deflections at the same locations for the same load points on the two panels were found to be within 0.005 in.

Concrete strains, steel strains, and deflection data were recorded during testing. Steel strains induced by the cantilevered portions of the deck panel bending over the support girders resulted in a maximum strain of 101 MII. Concrete strains were less than -253 MII. The maximum deflection for an interior span was 0.067 in., and the maximum deflection for a cantilever was 0.146 in. Load was applied at 19 different location in the connected panel service load tests; applied loads were limited to 20 kips on cantilevers and 40 kips on interior spans. Steel strains for the closure pour hooked bars reached a maximum strain of 307 MII during

service load testing, which is significantly less than the yield strain of 2069 MII for Grade 60 reinforcement. The maximum strain experienced in a mild reinforcing bar was a tensile strain of 278 MII. Concrete strains did not approach ACI limits for the maximum useable compressive strain of -3000 MII, having a maximum value of -286 MII. As one would expect, deck panel deflections decreased after casting the closure pour. Changes in deflection decreased 0.025 in. for a 40 kip load at B11 after the closure pour was cast.

4.1.7 Ultimate Strength Test Summary.

Four ultimate strength tests were conducted on the deck panels. An individual panel was tested to flexural failure, and three tests were conducted on two connected deck panels. The single panel failed in flexure at a load of 153 kips, or a moment equal to 368 ft-kips for pinned supports and 184 ft-kips for fixed supports. These values bracket the theoretical strength of 263 ft-kips, indicating that the laboratory support girders provided a fixity between pinned and fully fixed.

The second ultimate strength test was an attempt to fail the closure pour connecting the panels; however, the deck panel next to the closure pour failed in punching shear instead. A 9 in. square footprint was used in this test, and failure occurred at an applied shear force of 146 kips. The theoretical punching shear capacity for a 9 in. square footprint is 135 kips, which was 8% less than the applied shear.

A tandem wheel footprint was used for the second ultimate strength test conducted on the connected panels. This footprint resulted in a combinations punching shear and flexure failure at a load of 157 kips. For this load, the applied shear was 150 kips and the moment was 298 ft-kips. The theoretical punching shear was 188 kips, and the theoretical flexure strength was 263 ft-kips. Reasons for the discrepancies in the loading are: the restraining beams used to resist the

uplift forces caused by loading provided fixity to the system and decreased the applied moment; punching shear capacity was reduced because flexure cracks in the deck panel reduced the depth of concrete available to resist shear stresses.

For the final ultimate strength test, the connected panels were tested to flexure failure. A beam was used to apply a 196 kip load to the panel as a line load. The applied moment of 372 ft-kips exceeded the theoretical flexural strength of 263 ft-kips by 41%; however the restraining beams used to resist the uplift force provided some fixity to the system, reducing the applied moment to a value less than that given.

4.2 Conclusions

4.2.1 Concrete Strength Testing Conclusions

The following conclusions can be drawn from the concrete strength tests:

- The average compressive strength of the concrete cores was 7,600 psi.
- The average strength exceeded the specified strength of 5,000 psi by 27%

4.2.2 Stresses in Mild Reinforcing Due to Prestressing

The following can be concluded about the stresses in the mild reinforcing due to prestressing:

- Stresses in five of the six instrumented bars were less than the theoretical stress minus prestress losses (20.7 ksi).
- Top bars had an average stress of 14.2 ksi.
- Bottom bars had an average stress of 17.9 ksi.

4.2.3 Lifting Panel Strain Conclusions

The following conclusions can be drawn from the crane lifting tests conducted on the deck panels:

- The maximum compressive strain measured when lifting a deck panel with four lifting straps was 251 MII.
- The utilization of the reinforcing bar yield strain when lifted with four straps ranged from 45% to 70%.
- The maximum compressive strain measured when lifting a deck panel with two lifting straps was 177 MII.
- The utilization of the reinforcing bar when lifted with two straps ranged from 46% to 66% of the yield strain.
- Because bar utilization ranged from 45% to 70% for four strap lifting and 46% to 66% for two strap lifting, the strap configuration used did not have a significant effect on the reinforcing bars.
- Bars were less than 100% utilized for both lifting configurations, showing both are acceptable for use.

4.2.4 Leveling Test Conclusions

The following conclusions can be drawn from the leveling tests conducted on the deck panels:

- The maximum strain measured during the leveling tests was -595 MII.
- The utilization of the reinforcing bar due to combined bending and axial stresses ranged from 31% to 86% of the yield strain.
- Mild reinforcing bars did not exceed the yield strain during any of the leveling tests.

4.2.5 Longitudinal Post-Tensioning Channel Concrete Placement Test Conclusions

The following can be concluded from the longitudinal post-tensioning channel concrete placement test results:

- Concrete was observed flowing below the leveling device.

- Concrete was observed flowing between the post-tensioning strands.
- No void spaces were observed in the channel during the tests.

4.2.6 Service Load Test Conclusions

The following conclusions can be drawn from the service load test results:

- Strains induced in the reinforcing bars during tests without the closure pour cast were less than yielding, with 101 MII (a stress of 2.9 ksi) the maximum strain experienced.
- Deflections of the deck panel between the supports reached 0.067 in. prior to casting the closure pour.
- Strains in the concrete before casting the closure pour reached -253 MII, which is less than the value of -3000 MII recommended by ACI as the maximum useable compressive strain.
- The deflection of the cantilever portion of the deck panel reached 0.146 in. for a 16 kip load prior to casting the closure pour.
- Reinforcing steel experienced 278 MII of strain (a stress of 8.1 ksi) in tests after the closure pour was cast.
- Strains in the hooked bars in the closure pour reached 307 MII (a stress of 8.9 ksi), which is less than the yielding strain of 2069 MII.
- The maximum strain measured in the concrete after the closure pour was cast was -286 MII, which is less than the -3000 MII recommended by ACI as the maximum usable compressive strain.
- The maximum deflection of a portion of the deck panels spanning between two support beams after the closure pour was cast was 0.051 in.

- Deflections of the deck panel spanning between support beams decreased by 18% after the closure pour was cast.
- Cantilever deflections decreased 49% or more after the closure pour was cast.

4.2.7 Ultimate Strength Test Conclusions

The following conclusions can be made from the ultimate strength test results:

- The support beams provided a fixity between pinned and fully fixed. A single panel failed under an applied moment of 368 ft-kips if the supports are pinned or 184 ft-kips if the supports are fixed. The theoretical moment capacity was 263 ft-kips.
- The experimental punching shear capacity of the deck panels for a 9 in. square footprint was 146 kips, which was 8% greater than the theoretical strength of 135 kips.
- A deck panel failed under combined flexure and punching shear for a load applied by a tandem wheel footprint. The applied moment at failure was 298 ft-kips, 13% greater than the theoretical flexural capacity of 263 ft-kips. The shear force at failure was 150 kips, 80% of the theoretical punching shear of 188 kips.
- The moment applied to the two deck panel system was 372 ft-kips, exceeding the theoretical capacity of 263 ft-kips by 41%. The difference in values was due to the fixity provided by the support beams.
- Deck panel failures occurred at loads much greater than those the panels would be exposed to in the actual field bridge.

4.3 Recommendations

The following actions are recommended based on the laboratory testing of the deck panels:

- The mild reinforcement and prestressing force should be evaluated to produce a more efficient deck panel section.

- Additional testing should be conducted if panel lifting configurations other than those tested are to be used.
- Testing should be conducted to determine the strength benefit of having adjacent panels in the longitudinal direction.
- Strains should be measured during panel leveling and subsequent placement of concrete in the longitudinal channels to determine if concrete placement has an effect on the strains in the bars (i.e. if strains are permanent or temporary).

REFERENCES

AASHTO. 2002. *Standard Specifications for Highway Bridges.* Washington, DC: American Association of State Highway and Transportation Officials.

American Concrete Institute. 2005. *ACI 318-05 Building Code Requirements for Structural Concrete*. American Concrete Institute.

American Institute of Steel Construction. 2005. *Steel Construction Manual*. Thirteenth Edition. American Institute of Steel Construction Inc.

Badie, Sameh S., Mantu C. Baishya, Maher K. Tadros. 1998. *NUDECK-An Efficient and Economical Precast Prestressed Bridge Deck System.* PCI Journal, Vol. 43, No. 5: 56-71.

Badie, Sameh S., Mounir R. Kamel, and Maher K. Tadros. 1999. *Precast Pretensioned Trapezoidal Box Beam for Short Span Bridges*. PCI Journal, Vol. 44, No. 1: 48-59.

Bell III, Charles, Carol K. Shield, and Catherine French. 2006. *Application of Precast Decks and Other Elements to Bridge Structures*. Report No. 2006-37. Minnesota Department of Transportation.

Ehmke, Forrest Gregory. 2006. Analysis of a Bridge Deck Built on Interstate Highway 39/90 with Full-Depth, Precast, Prestressed Concrete Deck Panels. Master's thesis, University of Wisconsin-Madison.

Fallaha, Sam, Chuanbing Sun, Mark D. Lafferty, and Maher K. Tadros. 2004. *High Performance Precast Concrete NUDECK Panel System for Nebraska's Skyline Bridge*. PCI Journal, Vol. 49, No. 5: 40-50.

Hawkins, N. M., and J. B. Fuentes. 2002. *Test to Failure of a 54 ft. Deteriorated Pretensioned Precast Concrete Deck Beam.* Illinois Cooperative Highway and Transportation Series No. 281. University of Illinois: Urbana-Champaign.

Hawkins, N. M., and J. B. Fuentes. 2003. *Structural Condition Assessment and Service Load Performance of Deteriorated Pretensioned Deck Beam Bridges.* Illinois Cooperative Highway and Transportation Series No. 285. University of Illinois: Urbana-Champaign.

Hieber, D.G., J.M. Wacker, M.O. Eberhard, and J.F. Stanton. 2005. *State-of-the-Art Report on Precast Concrete Systems for Rapid Construction of Bridges*. Final Technical Report, Contract T2695, Task 53. Washington State Department of Transportation and Federal Highway Administration.

Huckelbridge Jr., Arthur A., Hassan El-Esnawi, and Fred Moses. 1995. *Shear Key Performance in Multibeam Box Girder Bridges*. Journal of Performance of Constructed Facilities, Vol. 9, No. 4: 271-285.

Issa, Mohsen A., Ahmad-Talal Idriss, Iraj I. Kaspar, and Salah Y. Khayyat. 1995. *Full Depth Precast and Precast, Prestressed Concrete Bridge Deck Panels*. PCI Journal, Vol. 40, No. 1: 59-69.

Issa, Mohsen A., Alfred A. Yousif, Mahmoud A. Issa, Iraj I. Kaspar, and Salah Y. Khayyat. 1998. *Analysis of Full Depth Precast Concrete Bridge Deck Panels*. PCI Journal, Vol. 43, No. 1: 74-85.

Issa, Mohsen A., Cyro L. Ribeiro do Valle, Hiba A. Abdalla, Shahid Islam, Mahmoud A. Issa. 2003. *Performance of Transverse Joint Grout Materials in Full-Depth Precast Concrete Bridge Deck Systems*. PCI Journal Vol. 48, No. 4: 92-103.

Menkulasi, Fatmir, and Carin L. Roberts-Wollman. 2005. *Behavior of Horizontal Shear Connections for Full-Depth Precast Concrete Bridge Decks on Prestressed I-Girders*. PCI Journal, Vol. 50, No. 3: 60-73.

Naaman, Antoine E. 2004. *Prestressed Concrete Analysis and Design: Fundamentals*. Second Edition. Techno Press.

Poston, Randall W., Karl H. Frank, and Jeffery S. West. 2003. *Enduring Strength*. Civil Engineering, Vol. 73, No. 9: 58-63.

Russell, Henry G., Mary Lou Ralls, and Benjamin M. Tang. 2005. *Prefabricated Bridge Elements and Systems in Japan and Europe*. Transportation Research Record: Journal of the Transportation Research Board, No. 1928: 103-109.

Slavis, C. 1982. *Precast Concrete Deck Modules for Bridge Deck Reconstruction*. Transportation Research Record 871, Transportation Research Board: 30-33.

Tokerud, Roy. 1979. *Precast Prestressed Concrete Bridges for Low-Volume Roads*. PCI Journal, Vol. 24, No. 4: 42-55.

VanGeem, Martha. 2006. *Achieving Sustainability with Precast Concrete*. PCI Journal, Vol. 51, No. 1: 42-55.

APPENDIX

Moment Capacity of Panel

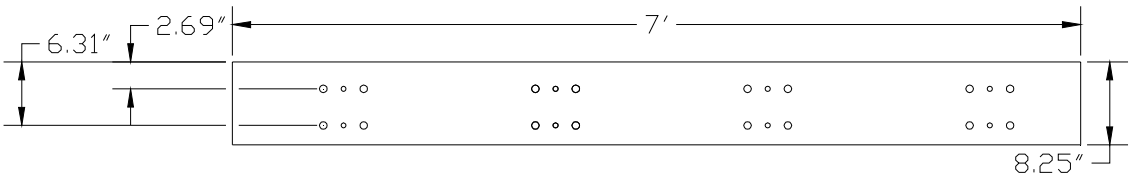

$f_c^{'} = 6ksi$

$f_y = 60ksi$

$f_{pu} = 270ksi$

$pretensioning\ \ force = 31\frac{kips}{strand}$

$A_{ps1} = A_{ps2} = 0.153in^2 * 4 = 0.612in^2$

$A_{s1} = A_{s2} = 4.8in^2$

$\beta_1 = 0.75$

$f_{si} = \frac{31kip}{0.153in^2} = 202.6ksi$

$E_{ps} = 29000ksi$

$E_c = 57{,}000\sqrt{6000\,psi} = 4{,}415ksi$

Lower pretensioning strands

$\varepsilon_{s1} = \frac{f_{se}}{E_{ps}} = \frac{162.1ksi}{29{,}000ksi} = 0.00559\frac{in}{in}$

$P_e = (4strands)(0.153in)(162.1ksi) = 99.2kips$

$e = \left|\frac{8.25in}{2} - 6.3125in\right| = 2.1875in$

$r = \sqrt{\frac{bh^3}{12A}} = \sqrt{\frac{(84in)(8.25in)^3}{12(84in)(8.25in)}} = 2.38in$

$r^2 = 5.67in^2$

$|\varepsilon_{s2}| = \frac{-P_e}{AE}\left(1 + \frac{e^2}{r^2}\right) = \frac{-99.2kip}{(84in)(8.25in)(4.415x10^3 ksi)}\left[1 + \frac{(2.1875in)^2}{5.67in^2}\right] = 5.98x10^{-5}\frac{in}{in}$

Try c = 2.05 in.

$$\varepsilon_{s2} = 0.003\left(\frac{6.3125in - 2.05in}{2.05in}\right) = 0.00624\frac{in}{in}$$

$$f_{s2} = 60ksi$$

$$\varepsilon_{ps2} = 0.00559 + 5.98x10^{-5} + 0.00624 = 0.0119\frac{in}{in}$$

$$f_{ps2} = 235ksi$$

$$\varepsilon_{s1} = 0.003\left(\frac{2.6875in - 2.05in}{2.05in}\right) = 0.000933\frac{in}{in}$$

$$f_{s1} = 27.1ksi$$

$$\varepsilon_{ps1} = 0.000933 + 5.98x10^{-5} + 0.00559 = 0.0066\frac{in}{in}$$

$$f_{ps1} = 165ksi$$

$$T_{ps} = 0.612in^2(165ksi + 235ksi) = 244.8kips$$

$$T_s = 4.8in^2(60ksi + 27.1ksi) = 418.1kips$$

$$C = 0.85(6ksi)(84in)(0.75)(2.05in) = 658.7kips$$

$$T = 662.9kips$$

$$C \approx T$$

Determine M_n

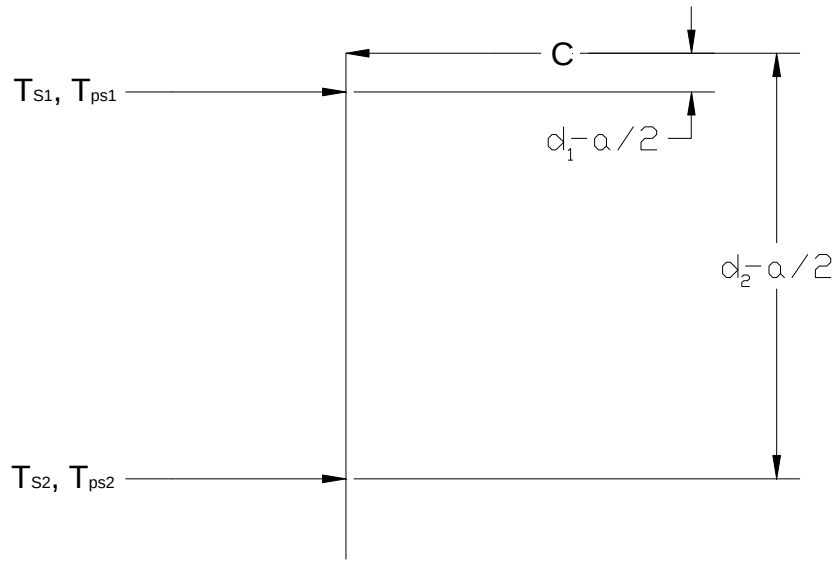

$$a = 0.75(2.05in) = 1.5375in$$

$$\sum M_c = M_n$$

$$M_n = (0.612in^2)(165ksi)\left(2.6875in - \frac{1.5375in}{2}\right) + (4.8in^2)(27.1ksi)\left(2.6875in - \frac{1.5375in}{2}\right)$$

$$+ (0.612in^2)(235ksi)\left(6.3125in - \frac{1.5375in}{2}\right) + (4.8in^2)(60ksi)\left(6.3125in - \frac{1.5375in}{2}\right)$$

$$= 193.8in*k + 249.6in*k + 797.3in*k + 1596.6in*k$$

$$= 2{,}837in*k$$

$$= 236\,ft*k$$

Punching Shear Strength, 9 in. x 9 in. footprint

$$b_o = 4(6.31in + 9in) = 61.25in$$

$$V_{c1} = \left(2 + \frac{4}{1}\right)\sqrt{7600\,psi}\,(61.25in)(6.31in) = 202kips$$

$$V_{c2} = \left[\frac{30(6.31in)}{61.25in} + 2\right]\sqrt{7600\,psi}\,(61.25in)(6.31in) = 172kips$$

$$V_{c3} = 4\sqrt{7600\,psi}\,(61.25in)(6.31in) = 135kips$$

$$V_c = 135kips$$

Punching Shear Strength, Tandem Wheel Footprint

$$b_o = 2(6.31in + 20in) + 2(10in + 6.31in) = 85.24in$$

$$\beta = \frac{20in}{10in} = 2$$

$$\alpha_s = 40$$

$$V_{c1} = \left(2 + \frac{4}{2}\right)\sqrt{7600\,psi}\,(85.24in)(6.31in) = 188kips$$

$$V_{c2} = \left[\frac{40(6.31in)}{85.24in} + 2\right]\sqrt{7600\,psi}\,(85.24in)(6.31in) = 233kips$$

$$V_{c3} = 4\sqrt{7600\,psi}\,(85.24in)(6.31in) = 188kips$$

$$V_c = 188kips$$

Shear Force, 9 in. x 9 in. Footprint

$$P = 150kip$$

$$\omega = \frac{150kip}{\left(3.25\,ft + 3.25\,ft + 1\,ft + \frac{10in}{12in/\,ft}\right)(8\,ft)} = 2.25ksf$$

$$V_u = 2.25ksf\left[66.67\,ft^2 - \left(\frac{6.31in + 9in}{12in/\,ft}\right)^2\right] = 146kips$$

Shear Force, Tandem Wheel Footprint

$$P = 157kip$$

$$\omega = \frac{157kip}{(8\,ft)(8.33\,ft)} = 2.36ksf$$

$$V_u = 2.36ksf\left[66.67\,ft^2 - \left(\frac{6.31in + 10in}{12in/\,ft}\right)\left(\frac{20in + 6.31in}{12in/\,ft}\right)\right] = 150kips$$